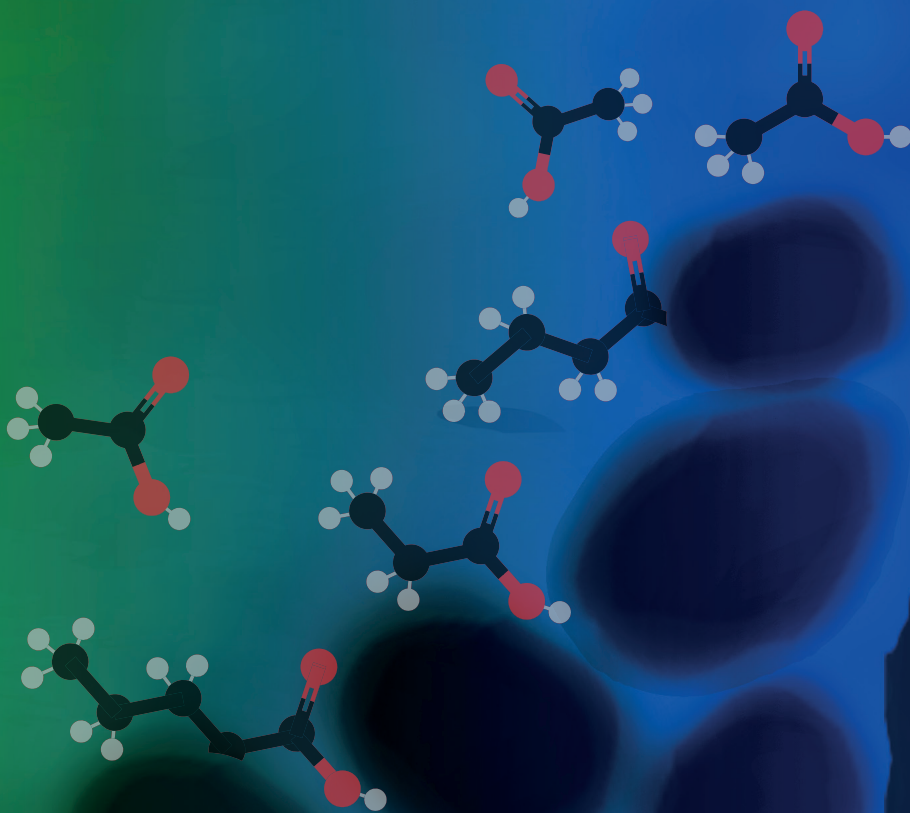


Bioelectrochemical chain elongation



Sanne M.T. Raes

Propositions

- 1 An electrode can serve as electron donor for microbial metabolism in continuous bioelectrochemical chain elongation systems.
(this thesis)
- 2 The biological conversion with which an ionic liquid (IL) is microbially regenerated, determines the added value of using an IL as in situ extractant.
(this thesis)
- 3 The use of the word 'believe' (meaning 'having faith in') in science, is a direct undermining of the questioning nature of science.
- 4 The contemporary Dutch human education system hinders the innate desire to explore.
(based on the socio-cognitive model, Francesco de Giorgio – Learning Animals)
- 5 The current livestock system will in the foreseeable future be perceived with the same moral indignation as slavery nowadays is perceived with.
- 6 Conceiving a child in this resource limited world should be a conscious action.
- 7 Gender-based quota are not the solution for unequal appreciation based on gender.

Propositions belonging to the thesis, entitled
Bioelectrochemical chain elongation

Sanne M.T. Raes

Wageningen, 29 May 2019

Bioelectrochemical chain elongation

Sanne M.T. Raes

Thesis committee

Promotor

Prof. Dr C.J.N. Buisman

Professor of Biological Recovery and Re-use Technology

Wageningen University & Research

Co-promotor

Dr D.P.B.T.B. Strik

Assistant professor, Department of Agrotechnology and Food Sciences

Wageningen University & Research

Other members

Prof. Dr G. Eggink, Wageningen University & Research

Prof. Dr J. Keller, Advanced Water Management Centre, The University of Queensland, Australia

Dr K.J.J. Steinbusch, Delft Advanced Biorenewables

Dr E. Croese, Bioclear – Microbial Analysis, Groningen

This research was conducted under the auspices of the Graduate School for Socio-Economic and Natural Sciences of the Environment (SENSE)

Bioelectrochemical chain elongation

Sanne M.T. Raes

Thesis

Submitted in fulfilment of the requirements for the degree of doctor

at Wageningen University

by the authority of Rector Magnificus,

Prof. Dr A.P.J. Mol,

in the presence of the

Thesis committee appointed by the Academic Board

to be defended in public

on Wednesday 29 May 2019

at 1:30 pm in the Aula.

Sanne M.T. Raes

Bioelectrochemical Chain Elongation

175 pages

PhD thesis, Wageningen University, Wageningen, the Netherlands (2019)

With references, with summary in English

ISBN: 978-94-6343-916-9

DOI: <https://doi.org/10.18174/472842>

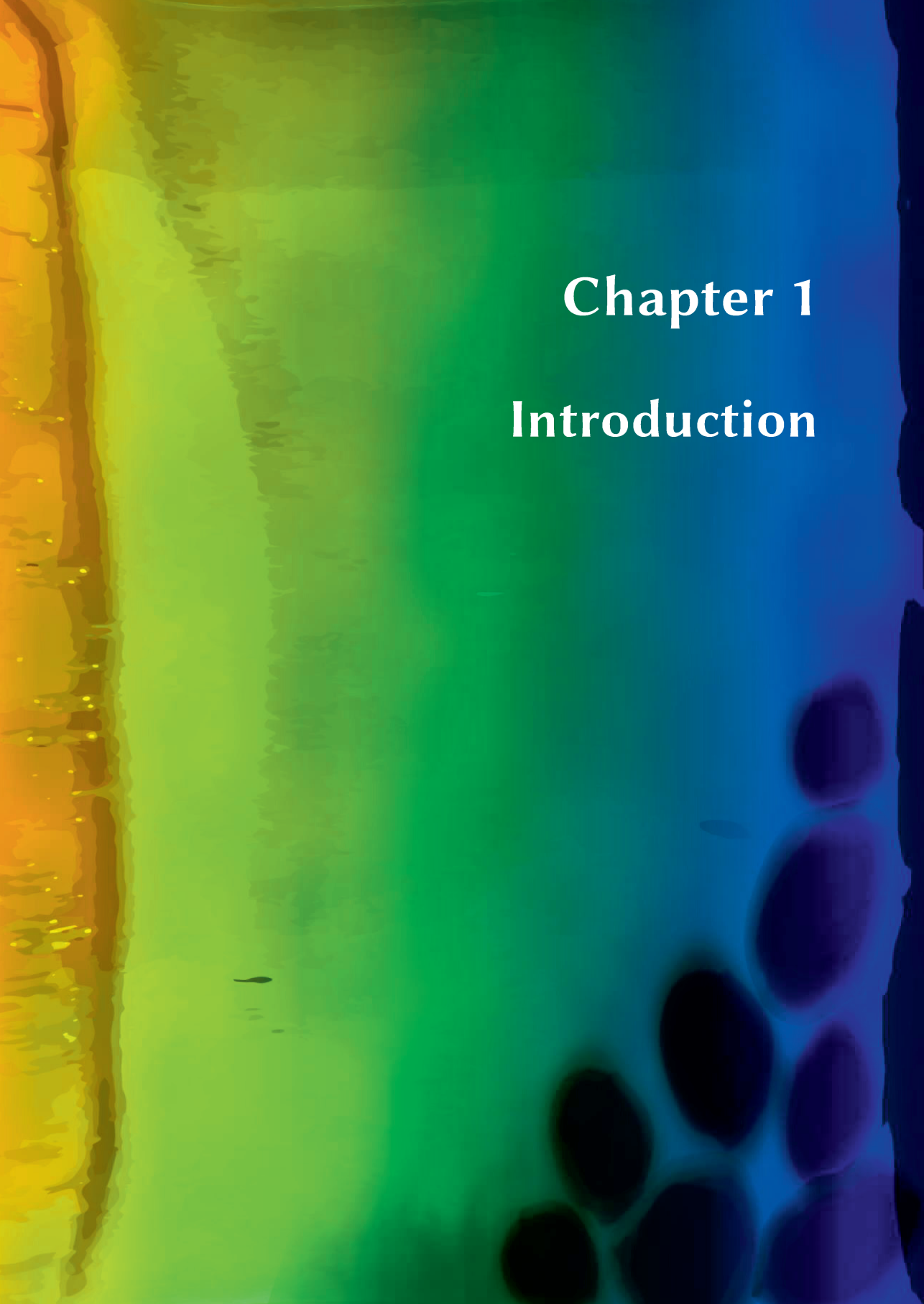
Table of Content

| | |
|---|------------|
| Chapter 1 | 1 |
| Introduction | |
| Chapter 2 | 11 |
| Continuous long-term bioelectrochemical chain elongation to n-butyrate | |
| Chapter 3 | 37 |
| Bioelectrochemical chain elongation of acetate and the role of fermentative and electrode supplied electron donors | |
| Chapter 4 | 59 |
| Bioelectrochemical chain elongation creates steering opportunity for selective production of odd-chain fatty acids | |
| Chapter 5 | 79 |
| Water-based synthesis of hydrophobic ionic liquids [N ₈₈₈][oleate] and [P _{666,14}][oleate] and their bioprocess compatibility | |
| Chapter 6 | 103 |
| Using transport-solvent between two bioprocesses: extraction of fermentation carboxylates with ionic liquid [N ₈₈₈][oleate and microbial solvent regeneration | |
| Chapter 7 | 129 |
| General discussion | |
| Reference list | 146 |
| Summary | 161 |
| List of publications | 165 |
| SENSE certificate | 168 |

Abbreviations

| | |
|------|---|
| BCE | Bioelectrochemical chain elongation |
| BES | Bioelectrochemical system |
| CE | Chain elongation |
| ET | Electron transfer/transport |
| EET | Extracellular electron transfer/transport |
| MET | microbial electrochemical technology |
| MES | Microbial electrosynthesis |
| SCFA | Short chain fatty acid |
| VFA | Volatile fatty acid |

| | |
|-------------------|----------------------------------|
| ATP | adenosine triphosphate |
| NAD ⁺ | nicotinamideadenine dinucleotide |
| NADP ⁺ | NAD-phosphate |
| Fd | ferredoxin |



Chapter 1

Introduction

The origin of bioelectrochemistry

It all started over a century ago, when botany professor M.C. Potter described in 1911 the curious phenomenon of electrical effects during the decomposition of organic compounds by microorganisms.¹ As botany professor he was amongst others active in the field of electro-physiology – the study of electrical properties of cells and tissues. Research in that field in those times had already shown that any physiological process involving chemical changes resulted in an associated electrical change. Potter was inspired by research of professor A.D. Waller, a British physiology professor, who was the first to recognise that cardiac potentials could pass through the chest.² Waller used the in 1872 by Lippmann developed ‘capillary electrometer’ to record electrical pulses of a human’s heart. Such device is a thin tube filled with dilute sulfuric acid and on top some liquid mercury. Two metal wires were emerged into the sulfuric acid at the bottom and in the mercury at the top. If the potential difference between the two wires would change, a small rise of the mercury meniscus would be visible. The bigger the electrical change, the bigger the change in mercury level in the capillary. Waller attached the metal wires to electrodes on a human body, i.e. he placed hands and or feet into jars with saline solution, or put metal objects like a teaspoon into one’s mouth.² The response of the capillary electrometer to a beating human heart was recorded photographically. A light source was placed in front of the electrometer to cast a shadow of the moving mercury meniscus. Behind the electrometer a toy train moved a photosensitive plate to capture the shadows of the liquid in the tube.² This is the first recording of an electrocardiogram, which was developed further over the last 150 years and is still a technique used in modern medicine to record the electrical activity of the heart. In addition to cardiograms, using his electrochemical devices Waller was able to measure electrical responses in plants as well. Living plant leaves were shown to absorb electrical energy when sunlight initiated photosynthesis.³ In that work Waller suggested that during dissociation (i.e. the breakdown of chemical compounds in a living cell) current is liberated. It was this line of enquiry that M.C. Potter followed up upon.

Potter wanted to study the ‘electrical effects’ which occur during degradation of an organic substrate. To do so, he placed a porous cylinder in a glass jar; like a small beaker in a bigger beaker. In both the jar and the inner cylinder he placed a platinum electrode. He filled both the jar and the cylinder with a glucose solution and introduced the yeast *Saccharomyces cerevisiae* (common baker’s yeast) into the outer glass jar. The yeast would consume oxygen as terminal electron acceptor. The compounds of degradation excreted by the yeast, changed the composition of the outer jar compared to the glucose solution put in the inner cylinder. This difference in composition Potter recorded as a potential difference between the two electrodes.¹

Potter's description of this liberation of electrical energy as a result of microbial metabolism is now referred to as the start of bioelectrochemistry.

Although Potter described such considerable interesting interplay between biochemical conversions and electrical signals, it took twenty years to regain some research interest. At that time of history little was known about the chemical processes of microbial metabolism. Cohen, an associate professor of physiological chemistry at John Hopkins School of Medicine,⁴ studied in his early work microbial metabolism using only redox indicators and acid-base indicators.⁴ Following up on this work, Cohen reported in 1931 on potentiometric measurements of microorganisms growing in liquid media. He observed differences in electrical charge, i.e. potential differences, between media he did and did not inoculate with microorganisms. The potential difference which could be observed ranged from 0.5 to 1.0 V compared to the control medium.⁵ This increase in redox potential during microbial conversion was recognised by Cohen as a 'bacterial half-cell'. Similar to a purely electrochemical half-cell, he derived that it should be able to extract electrical energy from it.

It is nowadays known the electrical energy liberated during microbial metabolism is a result of oxidation of organic substrates. The oxidation process transforms these soluble fuels into cellular energy, by transferring electrons from the electron donating substrates towards electron accepting molecules (for example oxygen). The potential difference between substrate and electron acceptor determines the quantity of energy that can be conserved. The energy can be conserved in electron transport (ET) chains, in which membrane bound enzymes transfer electrons from electron donor to the acceptor. The resulting electron flow, normally directed towards oxygen, can instead be directed towards an electrode. When this electrode is connected to a second electrode with a higher redox potential, electrons will flow from the first electrode towards the second. In this way, electrical energy can be harvested from microbial metabolism to perform work.

In the 1930s thereafter, researchers were investigating oxidation-reduction potentials of microbial cultures in the pursuit of discoveries to develop medicine or industrial processes. Or possibly they were striving for a more comprehensive understanding of the fundamentals of biological processes.⁶ For example Gillespie and coworkers,⁶⁻⁸ and Hewitt and coworkers (which he summarised himself in 1950⁹) dedicated series of research articles to the reduction potential changes by microbial activity. The purpose for Hewitt's studies was to get a closer understanding of the metabolism to control bacterial infections.⁹

At that time the interest for it as a source of electricity was limited, because the amount of electricity which could be produced with the microbial cultures was little. In the sixties fuel cell technology research was flourishing, which sparked again the interest microbial electricity generation.¹⁰ In 1962, Davis and Yarbrough were the first to combine the concept of biological energy liberation with a fuel cell, resulting in the earliest report on a microbial fuel cell (MFC).¹¹ The MFC is a technological device to harvest the microbial energy as current. In the years after, several other studies arose exploring this novel technology for electricity generation^{10,12–14} although it took until the end of the nineties for MFC research to intensify.

By then, in the concurrent field of environmental microbiology, several bacterial strains were discovered which are able to use insoluble redox-active minerals such as those containing Fe(III) and Mn(IV) as electron acceptor for their metabolism.^{15,16} Instead of transferring electrons towards oxygen as terminal electron acceptor, such bacteria are able to use solid rocks as terminal electron acceptor. They are able to connect electrically to such minerals and discharge their metabolic electrons by reducing the metal ions in the mineral. In the basis a microbial cell membrane is a sturdy barrier against the extracellular environment, containing both electron transferring and structural components. These latter make the cell wall physically impermeable for minerals.¹⁷ However, over the course of history, specialised mechanisms have evolved for electron exchange between the metabolism inside of a microbial cell and the extracellular environment. The transfer of electrons between the inside (cytoplasmic membrane) and the outside of the cell is named extracellular electron transport (EET).¹⁷

The revival of bioelectrochemistry

The expanding knowledge of these intriguing microbial capabilities connecting microbial metabolism to an insoluble mineral, sprouted the field of bioelectrochemistry. In the early nineties, the first reports emerged in which bacteria were employed again in a MFC to harvest electricity.¹⁸ During degradation of an organic substrate, bacteria release their metabolic electrons to an electrode. Although promising, the electron transfer from bacteria to anode in these early papers was aided by electron carriers. Those are redox-active components which transfer electrons from the cell to the electrode. The early MFC papers depended on electron carriers such as neutral red¹⁹ or anthraquinone2,6disulfonate (AQDS).²⁰ But, in 1999 the breakthrough in bacteria-electrode research came. Kim et al. were the first to connect a Fe(III) reducing bacteria to an electrode without the addition of electron carriers.²¹ Anaerobic cell suspensions of *Shewanella putrefaciens* were shown to exchange electrons with a poised electrode surface. The authors of that paper

proposed to construct a 'biofuel cell' to generate electricity from substrates such as wastewater.²¹ In theory, in this way both a wastewater treatment process as well as electricity generation method could be developed. In 2004 it was Liu et al. who demonstrated the proof of principle of generating electricity while simultaneously treat real waste water.²² After the combination of solving an environmental problem with sustainable electricity production was made, research into bioelectrochemical systems (BESs) heavily intensified, and a myriad of applications were developed in the years after.

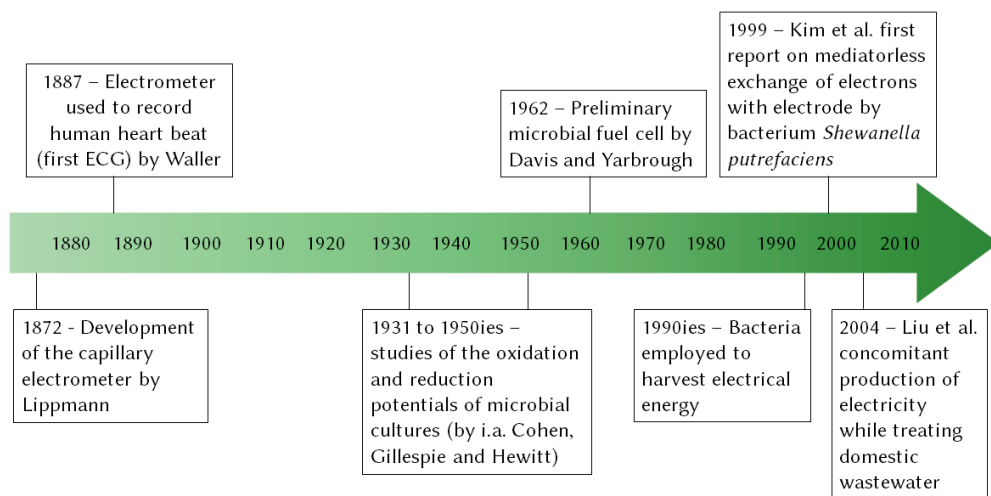


Figure 1.1: Timeline | Major achievements leading to the development of bioelectrochemical systems.

The emerging field of BES applications

BES is a general term for a biotechnological system which consists of two electrodes, where microorganisms catalyse one or both electrode reactions. Over the last decades, the applications of BESs have been expanded greatly incorporating a wide diversity of oxidation and reduction reactions. As written above, BES development started with the application of microorganisms in bioanodes for the concurrent production of electricity during degradation of organic matter. Later microbial electrolysis cells (MECs) emerged, which have a similar setup as the MFCs, except an external energy input is applied to drive the electrode reactions. In the bioanode of MECs organic matter is oxidized, while in most MEC studies the cathodic reaction is protons reduction to H_2 gas, either biocatalysed or not.^{23,24} Additionally, BESs with bioanodes have been applied for desalination purposes,²⁵ and treatment of recalcitrant pollutants and toxic wastewaters.²⁶

Paradigm shift in waste perception: the call for a biobased economy

Our current society heavily depends on fossil resources (oil, coal and natural gas) for amongst others transportation, heating, agriculture and production of commodities like fuels, chemicals, plastic and textiles.²⁷ Nowadays there is clear evidence that anthropogenic activities such as fossil fuel combustion and change of land-use increased the atmospheric concentrations of CO₂, CH₄ and NO_x to unprecedented levels.²⁸ This human influence causes the more and more observed weather extremes and is predicted to lead to a substantial sea level rise by the end of this century.²⁸

The foreseen world population increase²⁹ and the concomitant welfare increase,³⁰ is expected to enlarge human impact on the climate.²⁸ To mitigate these severe and world changing effects – aside from behavioural changes such as limiting world population growth by having fewer children, change to a plant-based diet, and avoid airplane traveling³¹ – it is direly needed to change this dependency on fossil resources to more sustainable resources. The alternative resource which is increasingly acknowledged to replace a large fraction of fossil resources as feedstock for industrial purposes – both energy and non-energy (chemicals and materials) sectors – are plant-based raw materials, i.e. biomass.^{32–35}

Along with the imminent population growth comes an imminent increase of the amounts of organic waste streams humanity will produce.³⁶ Properly managing those waste streams will be crucial to limit further environmental deterioration and to realise the essential transition towards a sustainable society.³⁷ In this nexus of increased amounts of organic waste and the need for alternative resources to substitute fossil resources, lays the challenge and needed paradigm shift: organic residual streams as a resource for valuable fuels and chemicals.

The technological challenge: turning organic waste into a resource

In the so-called carboxylate platform organic feedstocks (agricultural and industrial wastes) are converted into valuable products. Initially, low-grade biomass is anaerobically fermented into a mixture of short chain fatty acids (2 - 5 carbon atoms), carbon dioxide and hydrogen (Figure 1.2, left). The short chain organic acids on themselves are already platform chemicals for the synthesis of value-added chemicals.³⁸ However, due to the relatively low concentrations of SCFAs reached within such fermentations, this is a major bottleneck in the competition with the production of bulk chemicals from petrochemicals. For that reason, often SCFAs serve as substrate for a secondary fermentation, of which microbial chain elongation is an example. During chain elongation the SCFAs are elongated towards medium chain fatty acids (MCFAs, 6-12 carbon atoms) using an exogenously supplied

electron donor (Figure 1.2, right). MCFAs can be used for the synthesis of fuels, lubricants, food additives, plastics and dyes, products which usually are produced using fossil resources.

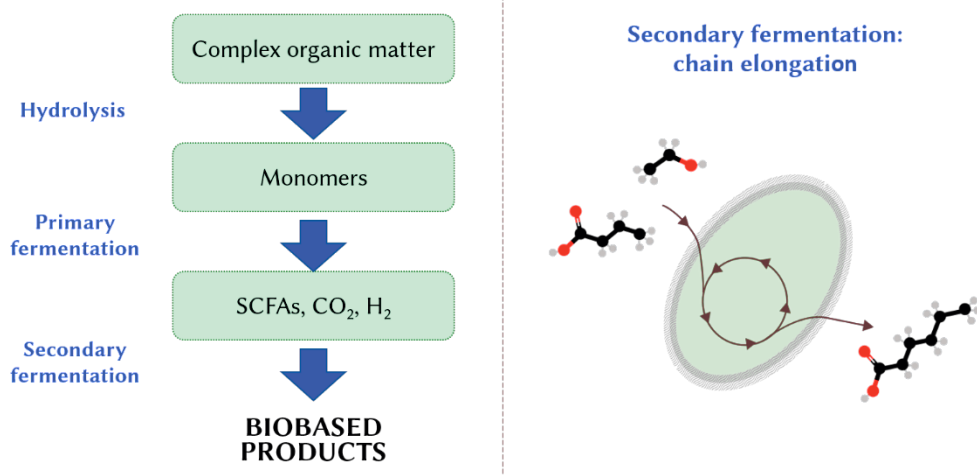


Figure 1.2: Carboxylate platform for the conversion of organic waste streams into biobased products, and right an example of the secondary fermentation chain elongation of n-butyrate to caproate using ethanol as electron donor.

Microbial electrosynthesis – an electrode as waste valorisation technology

Another technology for the conversion of SCFAs is microbial electrosynthesis (MES), an emerging BES technology for the microbially catalysed production of high-value chemicals and fuels compounds.³⁹ An additional feature of this technology is thus that it can convert (renewable) electrical energy into storable chemical energy.

When in 2010 it was demonstrated that microorganisms were able to directly use electrons coming from an electrode,⁴⁰ the production of valuable chemicals in MES systems has gained much interest. To date, mainly CO₂ reduction is studied using mixed microbial cultures.^{41,42,51,43–50} Initially the main product was acetate, however other products have also been produced, such as succinate and glycerol by fumarate reduction,⁵² 1,3-propanediol,⁵³ alcohols from fatty acid reduction,⁵⁴ CO₂ to methane,^{55,56} CO₂ to several organics,⁵⁷ CO₂ to n-butyrate,⁵⁸ and acetate to longer chain fatty acids.⁵⁹ By the start of this thesis research in 2013 sustained bioelectrochemical chain elongation of acetate (or other SCFAs) was not developed yet.

The bioelectrochemical system in which MES takes place, consists of two solid-state electrodes, generally separated by an ion exchange membrane (Figure 1.3). At the

anode electrons are liberated via an oxidation reaction, in this case water oxidation is depicted. The liberated electrons will flow through the external electrical circuit to the cathode compartment where microorganisms grow on the electrode. The transferred electrons will be used in a microbially catalysed reduction reaction (here CO_2 and acetate are depicted as substrates for reduction). The potential difference between the redox reactions occurring at the anode and cathode determines whether net electrical energy is produced or external energy input is required to drive the reactions. In the case of MES, the potential difference is too small or even negative for the cathode reduction reaction to occur spontaneously, i.e. to occur without external energy input. To overcome this thermodynamic barrier, an external electrical power is supplied.⁶⁰

In the above described microbial chain elongation, soluble electron donors are supplied to drive the elongation of SCFAs. In this thesis, the elongation of SCFAs using electrode-derived electrons was studied. This specific sub-type of MES was named bioelectrochemical chain elongation (BCE).

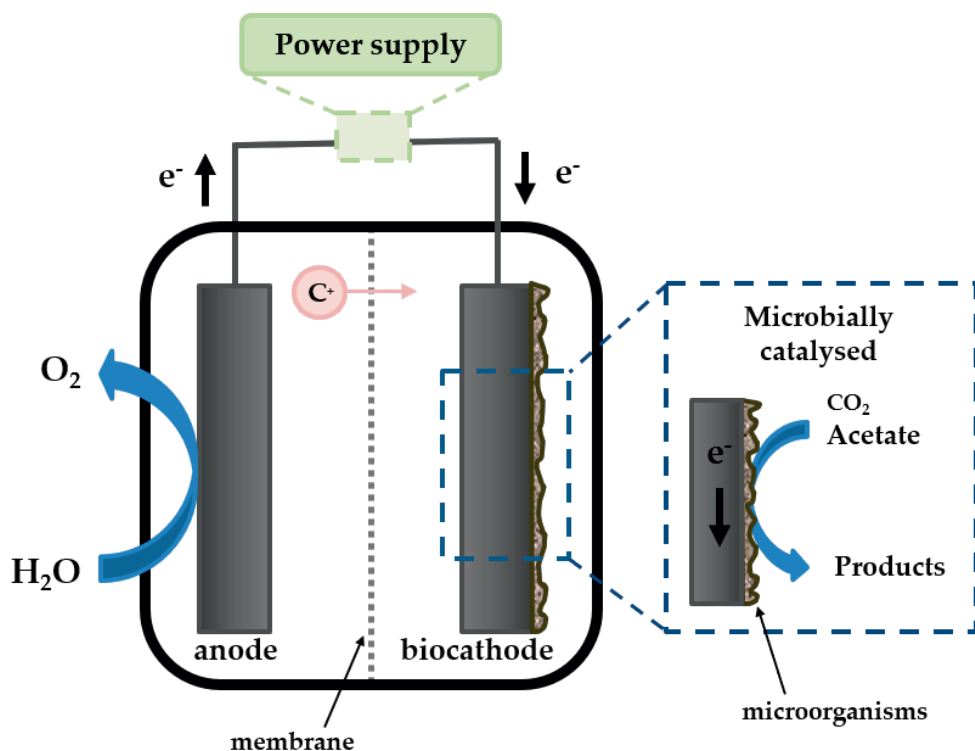


Figure 1.3: Schematic of a microbial electrosynthesis (MES) system using a biocathode to convert acetate and/or CO_2 into valuable products.

Revolutionary new solvents for selective extraction of SCFAs

The work in this thesis was part of the 'MES meets DES - Volatile fatty acid (VFA) production and conversion by microbial electrosynthesis (MES) & recovery by deep eutectic solvent (DES) formation' project (STW-Paques grant 12999). At the collaborating university in Eindhoven designer solvents were developed to recover compounds produced by MES. The solvents which were studied there were ionic liquids (ILs)⁶¹ and deep eutectic solvents (DESs).^{62,63}

In two of the chapters of this thesis ionic liquids were employed for extraction of SCFAs from dilute aqueous solutions. The challenge for fermentative technologies to convert waste into chemicals, is the relatively low concentrations reached and the variable product composition due to heterogeneous feedstocks. Therefore, effective separation of SCFAs from fermentation broths has been studied widely. Liquid-liquid extraction is the one of the oldest and well-established separation technologies.⁶⁴ The conventionally used organic solvents are often flammable, toxic or polluting. In pursuit of more sustainable extraction solvents, ionic liquids were developed, and have been reported in the last decade for the extraction of SCFAs.^{65–70} ILs are molten salts with relatively low melting temperatures, often below 100 °C. They are composed of solely ions, and generally consist of large organic cations combined with organic or inorganic anions.^{65,71} ILs have negligible vapor pressure and are liquid over a wide temperature range. Because of the wide range of possible cation-anion combinations, an IL's physicochemical and toxicological properties can be tailored for specific applications.⁷²

Thesis objective and outline

The objective of this thesis is to explore bioelectrochemical chain elongation and its fatty acid extraction, and to provide a state-of-art discussion on the prospective roles of the electrode as sole electron donor for bioelectrochemical chain elongation.

This thesis consists of two major parts in the valorisation of organic residual waste streams. The first part (**chapter 2, 3, and 4**) focusses on the formation of valuable products from SCFAs using BCE. The second part focusses on the extraction of such bioproducts from dilute aqueous streams using ILs (**chapter 5 and 6**).

At the start of this research the main conversion studied for MES systems was CO₂ to acetate, while no acetate was used as substrate for sustained BCE yet. In **Chapter 2** the proof of concept for bioelectrochemical elongation of acetate and CO₂ to n-butyrate is demonstrated in continuous systems for over 160 days. Compared to production rates obtained in fermentative chain elongation, the rates in that chapter were approximately 20 times lower. To improve the productivity of the BCE systems, a possible approach is to elucidate the mechanisms of n-butyrate formation.

Because the exact mechanism of n-butyrate formation using electrode-derived electrons as electron donor was unknown, several hypotheses on the possible formation of n-butyrate from acetate and electrons are given in that chapter as well. In **Chapter 3** the hypothesis on intermediate electron donor formation is investigated and a major role of current as electron donor is identified.

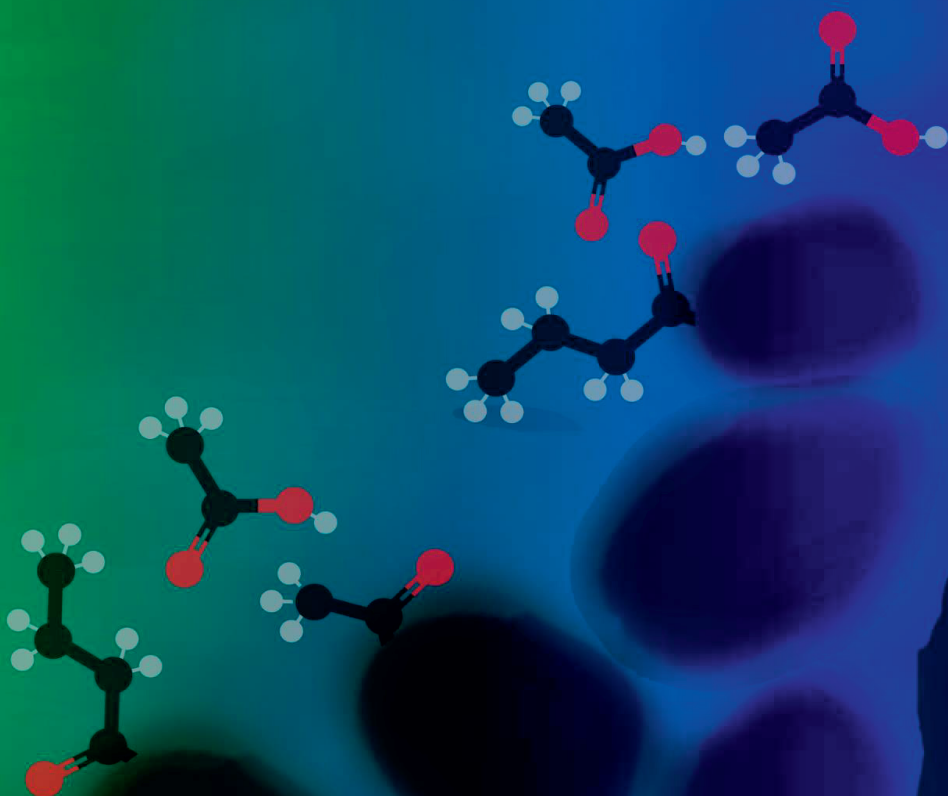
Next to the role of the electron donors, as well the effect of substrate supply, i.e. electron acceptor, is studied (**Chapter 4**). In order for BCE to become an industrially interesting technology for acidified waste valorisation, the substrate spectrum should meet the SCFA spectrum of fermented residual streams, i.e. contain acetate, propionate and n-butyrate. The fate of a mixture of these SCFAs in BCE systems is investigated in **Chapter 4**. The valorisation of solely acetate is compared to combinations of different mixtures of these three SCFAs.

In part 2, the exploitation of ILs for the extraction of SCFAs from fermentation broths are studied. For that reason, the term bioprocess compatibility is introduced to describe the practical applicability of substances with bioprocesses. Firstly, the effect of application of two hydrophobic ILs, [N₈₈₈][oleate] and [P_{666,14}][oleate], on granular methanogenic sludge is studied (**Chapter 5**). Subsequently, in **Chapter 6** the bioprocess compatible [N₈₈₈][oleate] is demonstrated to be reusable as extraction solvent for SCFAs. Additionally, the proof of concept of using microorganisms for solvent regeneration is shown as well in that chapter.

To assess BCE, in **Chapter 7** the general thesis discussion focusses on the role of an electrode as sole electron donor for bioelectrochemical chain elongation based on literature and work in this thesis. It couples the electrode-derived electrons to the bioproduction via the metabolic pathways presumably involved in the product formation as observed in chapter 2 to 4. Finally, an outlook for technology development using electrodes as waste upgrading technology is given.

Chapter 2

Continuous long-term bioelectrochemical chain elongation



Published as: Raes, S.M.T., Jourdin, L., Buisman, C.J.N., Strik, D.P.B.T.B., 2017.
Continuous long-term bioelectrochemical chain elongation to butyrate.
ChemElectroChem 4, 386–395

Abstract

We demonstrate here the long-term continuous bioelectrochemical chain elongation from CO₂ and acetate using a mixed microbial culture. The role of applied current (3.1 A m⁻² versus 9.4 A m⁻²) on the performance was investigated. The main product was n-butyrate which was continuously produced over time. Trace amounts of propionate and n-caproate were also produced, while no alcohols were detected during the whole course of the experiment (163 days). MES systems controlled with more current (9.4 A m⁻²), showed 4.5 times higher n-butyrate concentration (max 0.59 g L⁻¹) and volumetric production rates (0.54 g L⁻¹ day⁻¹) compared to the low current reactors (0.12 g L⁻¹ day⁻¹), at 58.9% and 71.6% electron recovery, respectively. Biocatalytic activity of the microbial consortia was demonstrated. This study revealed that the solid-state electrode does control the chain elongation reaction as an essential electron donor and determines the performance of MES systems. This study highlights MES as a promising alternative for acetate upgrading.

Keywords: Biocatalysis, carboxylic acids, biocathode, microbial electrosynthesis, bioelectrochemical chain elongation

Introduction

In order to decrease our society's dependence on polluting fossil fuels, alternative sources for chemical and fuel production need to be developed. Organic residual streams are a renewable feedstock that can be used to replace these fossil-based fuels and chemicals. Biomass-derived fuels and chemicals and their production processes are expected to reduce net carbon emissions,⁷³ limit dependency on oil exporters, and improve future energy availability.⁷⁴ The production processes should comply with the criteria of decreasing air pollution⁷⁵ and not competing with food production.⁷⁶

The carboxylate platform is suggested as a possible platform for conversion of organic residues into intermediate platform chemicals using undefined mixed cultures.^{36,38} Initially, low-grade biomass is anaerobically fermented into a mixture of short chain carboxylic acids (2-4 carbon atoms), carbon dioxide and hydrogen. The short chain organic acids are mainly acetate, propionate and *n*-butyrate.^{36,77} The most well-known secondary fermentation process to convert these carboxylic acids is methanogenesis. Although, separation of the product methane from the fermentation broth is easy, it is a low-value fuel which needs subsidy to compete with fossil natural gas.^{77,78} Therefore, lately, attention has shifted towards technologies which can produce with high selectivity higher-value compounds from short chain carboxylic acids.⁷⁹

Microbial electrosynthesis (MES) is a technology which might solve this conversion challenge. MES was broadly described as a process where microorganisms catalyse electrochemical reactions converting a substance into a desired product.⁸⁰ Using electrical current and addition of electron mediators to redirect microbial metabolism towards desired products already gained interest in 1979.⁸¹ The addition of electron mediators such as neutral red, methyl viologen and anthraquinone-2,6-disulfonate led to higher yields and increased product concentrations.^{81–86} These processes where small amounts of electron are employed to overcome redox imbalances are defined as electro-fermentation.³⁶ Whereas in MES the main electron donor for microbial metabolism is the electrons coming from the electrode.

Recently it was suggested that microorganisms were able to directly use electrons coming from an electrode, without the addition of electron mediators,⁴⁰ MES research gained further interest. To date, mainly reduction of CO₂ to acetate by electrotrophic mixed microbial consortia was studied.^{41,42,51,43–50} Other biocathode production processes, without the addition of external electron mediator, have been investigated, such as the reduction of fumarate to succinate and glycerol,⁵² glycerol

to 1,3-propanediol,⁵³ fatty acids to alcohols,⁵⁴ CO₂ to methane,^{55,56} CO₂ to several organics,⁵⁷ CO₂ to n-butyrate,⁵⁸ and acetate to longer chain fatty acids.⁵⁹

As complex organic residues can be relatively easily converted (via hydrolysis, acidogenesis, and acetogenesis) into acetate, carbon dioxide and hydrogen, the bioelectrochemical conversion of acetate to higher value chemicals by MES is particularly relevant, and was investigated here. Van Eerten-Jansen et al. (2013) already showed the production of medium chain fatty acids (MCFAs) from acetate and potassium carbonate.⁵⁹ However, their experiment lasted only 18 days and organics production was shown to occur over the first 4 days only. Experimental evidence of sustained production of either n-butyrate, caproate or caprylate over time was not shown. To the best of our knowledge, the bioelectrochemical conversion of acetate to longer chain products was not reported since then. One of the challenges in MES research for organics reduction remains to maintain microbial activity for sustained long term production.⁶⁰ To date, all MES studies from organics lasted less than 70 days. Additionally, to date, most MES research chose the strategy to control the cathode potential. Only few chose an applied current strategy.^{49,87,88} Also the effect of different current densities on the performance of MES systems was not yet reported.

The objective of this study was to evaluate the long term bioelectrochemical conversion of acetate. The cathodic current was controlled to ensure a constant flux of electrons for the conversion of acetate, instead of the cathode potential. Thereby the effect of different applied current densities on the performance of the system was investigated. This work shows that applied current can function as electron donor for bioelectrochemical chain elongation of acetate to n-butyrate over 163 days.

Results and Discussion

The bioelectrochemical conversion of acetate was studied using four continuous microbial electrosynthesis reactors. Two of them were current controlled at 5 mA (low current conditions) and the other two at 15 mA (high current conditions). The performance of the MES systems was evaluated over a period of 163 days.

Bioelectrochemical production of n-butyrate from acetate and CO₂

Figure 2.1 shows the average volumetric production rates of the main identified soluble products over time, at both high (B) and low current conditions (A). Results of duplicate reactors for the high current conditions were in relative good agreement, as can be seen in the standard deviation bars in Figure 1B. Acetate consumption and conversion into longer chain organics started a week after inoculation in both high and low current reactors. The main identified product in all reactors was n-butyrate (n-C₄), and was continuously produced during the whole

experiment. The highest *n*-butyrate production rate was $0.54 \pm 0.06 \text{ g L}^{-1} \text{ day}^{-1}$ under high current conditions (max. conc. $0.59 \pm 0.05 \text{ g L}^{-1}$, data shown in Figure S2.2). This highest production rate at 15 mA was 4.5 times higher than recorded in low current reactors, with maximal production rate of $0.12 \pm 0.04 \text{ g L}^{-1} \text{ day}^{-1}$ (max. conc. $0.15 \pm 0.05 \text{ g L}^{-1}$). Additionally, a maximal production rate of *n*-caproate of about $0.07 \pm 0.04 \text{ g L}^{-1} \text{ day}^{-1}$ (max conc. $0.06 \pm 0.03 \text{ g L}^{-1} \text{ day}^{-1}$) was measured in the 15 mA reactors.

Acetate production rates shown in Figure 2.1 B for high current reactors were continuously negative. Negative production rates indicate that the compound was consumed. The acetate consumption rate in these reactors increased to a maximum of $0.7 \text{ g acetate L}^{-1} \text{ day}^{-1}$. Under low current conditions the acetate production rate was alternating positive or negative, indicating acetate was either net produced or net consumed in these reactors (Figure 2.1 A). Detected hydrogen gas production rates were standardized to projected surface area (psa) of the electrode (here 16 cm^2), and between brackets to catholyte volume. In low current systems detected H_2 gas production was minimal, between 0.001 and $0.38 \text{ L H}_2 \text{ m}^{-2} \text{ psa day}^{-1}$ ($2.10^{-4} - 0.047 \text{ L H}_2 \text{ L}^{-1} \text{ day}^{-1}$), while in high current systems detected hydrogen gas production was significantly higher, between 8.8 and $33.9 \text{ L H}_2 \text{ m}^{-2} \text{ psa day}^{-1}$ ($0.28 - 1.09 \text{ L H}_2 \text{ L}^{-1} \text{ day}^{-1}$). Other identified product in both high and low current reactors was propionate ($< 0.02 \text{ g L}^{-1}$), and in the 15 mA systems *i*-butyrate, and *n*-valerate were also detected in trace amounts ($< 0.02 \text{ g L}^{-1}$). During these experiments no alcohols were detected (detection limit $\sim 0.020 \text{ g L}^{-1}$).

Two clear drops in *n*-butyrate production can be observed in Figure 2.1 B on day 85 and 105 (indicated by the arrows). On these days current control was temporarily impeded, due to technical failure of the potentiostat. In bioelectrochemical systems, negatively charged electrons are transported from anode to cathode, while a charge-balancing ion transport restores the electroneutrality.⁸⁹ In order to keep a constant system composition, ideally the ions transported should exclusively be the ions liberated and consumed by the (bio)electrochemical reactions.⁸⁹ The cathodic pH in this study remained stable without the need for pH control, which indicates that proton transfer from anode balanced proton consumption in the cathode under these conditions. At the moment the applied current was temporarily stopped all the cathodes acidified to pH 3.5 – 4 as a result of diffusion of protons from the acidic anode (pH 2.5 ± 0.5) to the cathode. When current control was restarted, the pH was adapted manually to 5.5 ± 0.2 . The *n*-butyrate production recovered in all four MES reactors within a week after restart. This recovery of *n*-butyrate production shows that the microbial consortium was robust to temporary pH drops.

To the best of our knowledge, only one study reported before on the bioelectrochemical conversion of acetate to more reduced compounds.⁵⁹ The

maximal n-butyrate concentration reached in this study (0.59 g L^{-1}) is 2.2 times higher than the previously reported n-butyrate concentration (0.263 g L^{-1}).⁵⁹ Volumetric production rates were not reported before. In this current study the production of n-butyrate was sustained over 163 days vs. 18 days in previous study.⁵⁹

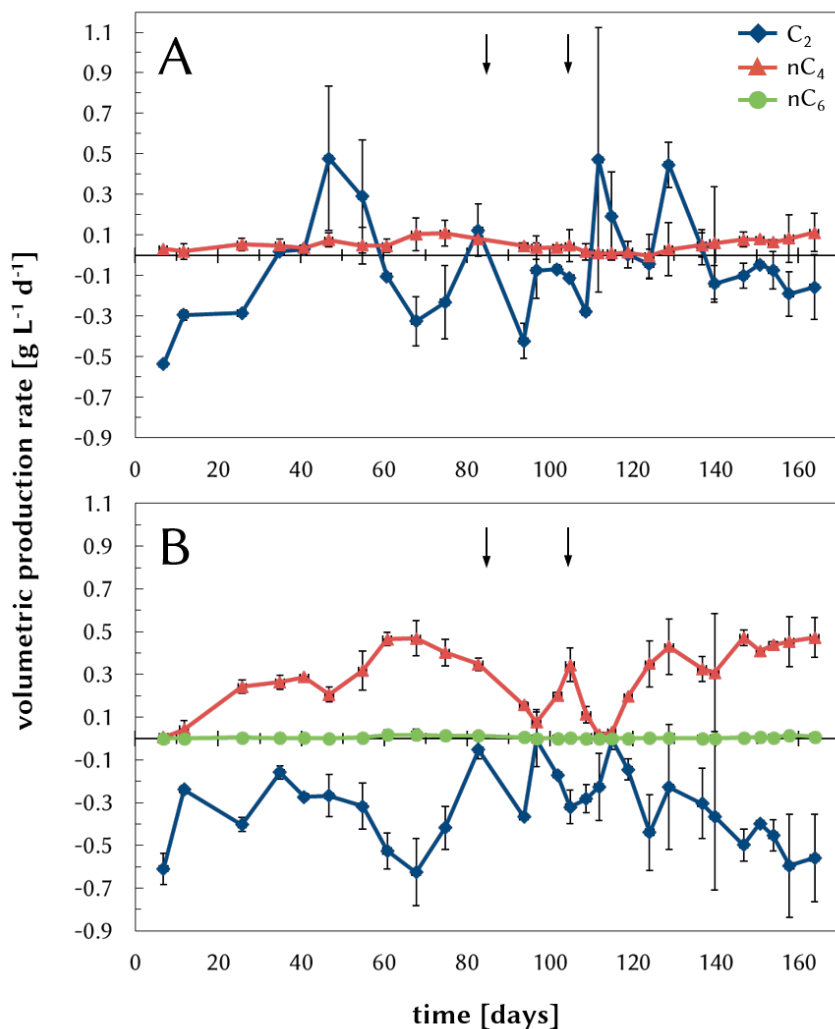


Figure 2.1: Volumetric production rates of the main liquid products produced in the MES reactors applied with 5 mA (A) and 15 mA (B), averages of duplicate reactors are shown including standard deviation bars. Production rates are normalized to catholyte volume. C₂: acetate, nC₄: n-butyrate and nC₆: n-caproate. Arrows indicate moments of temporarily hampered current supply on day 85 and 105.

Carbon and electron recovery

Carbon and electron balances were made to investigate the performance of the MES reactors and can be seen in Figure 2.2. Total electron recovery (i.e. in all identified products; blue line) and electron recovery in soluble organic compounds only (green line) are shown. The carbon balance showed recovery values over 100%. These high recovery values indicate that another carbon source was incorporated into the identified products, since the carbon recovery was calculated based on the supplied acetate as sole carbon source (see materials and methods section). Most likely CO₂ from the influent was used as carbon source by the microbiome besides acetate. Inorganic carbon quantification is necessary to elucidate in more detail the carbon utilisation in the MES microbiomes.

Electrons entered the system via two sources: electrons supplied by the electrode and as acetate in the influent (8 electrons per mole of acetate). The percentage of the electrons supplied by each source relative to the total supplied electrons, varied per applied current level. For 5 mA the ratio $e^-_{\text{acetate}} : e^-_{\text{electrode}}$ was 70% : 30%, while for 15 mA $e^-_{\text{acetate}} : e^-_{\text{electrode}}$ was 45% : 55%. The total supplied electrons were compared with the electrons recovered in the identified products (Equation 2). The average electron recovery for the 5 mA reactors was 73.7 ± 12.6 %, and for the 15 mA reactors 58.9 ± 9.8 % (Figure 2.2). Detected hydrogen led to an average electron recovery loss of 8.8% under high current conditions, while under low conditions no significant electron recovery loss was due to hydrogen production.

Approximately 25% (low current) and 40% (high current) of the electrons were not recovered in the products. Most probable electron sinks were hydrogen diffusion out of the system^{46,90} and diffusion of reduced products towards the anode.⁸⁷ Other possible explanations leading to a loss of electrons are biofilm formation,⁹¹ and unidentified products.⁵⁹ Although the cathode compartment of the MES cells were connected to a gas bag to capture produced gasses, hydrogen still might have diffused through connectors and tubing,⁴⁶ or to the anode compartment where it was flushed out with the CO₂ supply. In order to check whether all the soluble compounds produced were identified, the chemical oxygen demand (COD) of each liquid sample was measured. The COD was converted into mol e^- equivalents and compared to the total amount of electrons in the identified reduced products. Because these amounts matched (results not shown), no significant loss of electrons was accounted for by unidentified products. The anolyte compositions were analysed for accumulation of reduced products only at the end of the experiments. Each of the anodes contained both acetate and *n*-butyrate, in similar concentrations as the cathode compartment of that reactor. As the anolytes were operated in fed-batch, and accumulation of reduced compounds in the anodes was only identified

as a possible electron sink at the end of the experiment, sufficient data was not available to fulfil the electron balance. To put this possible electron sink into perspective, in 0.3 L of anolyte, a concentration of 1.5 g L⁻¹ of acetate would result in 60 mmol e⁻ equivalents, and 0.2 g L⁻¹ of n-butyrate represents 14 mmol e⁻ equivalents. Total electron supply per day was 16 mmol.day⁻¹ (low) or 24 mmol.day⁻¹ (high). As the anolyte was operated in fed-batch mode, the accumulation of reduced products could only reach similar concentrations as in the catholyte. Then the driving force for diffusion (concentration gradient) would be gone. Compared to total electron supply for the total length of the experiment (approx. 2500 (5 mA) or 3900 mmol e⁻ equivalents (15mA)), the accumulation of reduced compounds in the anolyte could not have represented a significant electron loss in this experiment.

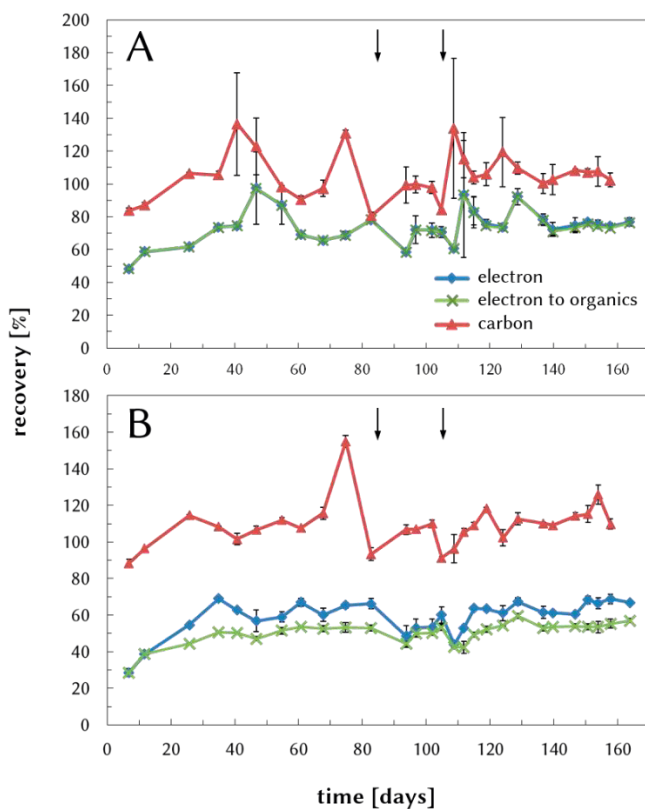


Figure 2.2: Electron and carbon recovery of MES cells applied with 5 mA (A) and 15 mA (B), averages of duplicate reactors are shown including standard deviation bars. Electron recovery: percentage of total supplied electrons recovered in the identified products. Electron to organics recovery: percentage of total supplied electrons detected in the dissolved organic products. Thus the difference between the 'electron' and 'electron to organics' recovery is the amount of electrons identified in H₂. Carbon recovery: carbon supply of acetate in the influent compared to carbon atoms in identified products, both liquid and gaseous.

Current enhances *n*-butyrate production

A main question to valorise MES as an alternative technology for acetate upgrading, is whether current is indeed needed for product formation. To analyse the electron input compared to the output, the cumulative electron distribution at the end of the experiment was calculated (Figure 2.3). For the 15 mA cells the amount of electrons supplied by acetate (1757 mmole e^- equivalents – blue part of the bar Figure 2.3 B) was less than the total sum of electrons recovered in the products identified (2331 mmole e^- equivalents). This shows that (a part of) the electrons supplied by the electrode had contributed to the production of compounds. Under low current conditions the contribution of current to production was not so apparent. The difference between supplied electrons as acetate and the electrons in identified products was 30 mmole electron equivalents, which represents 1.2% of the total amount of supplied electron equivalents (Figure 2.3 A). In the 15 mA reactors most electrons were recovered as *n*-butyrate (25%), hydrogen (16%) and acetate (55%), while in the 5 mA reactors most electrons were recovered as acetate (92%). *n*-Butyrate accounted in these low current reactors only for 6% and hydrogen for 0.04% of total identified electrons.

It was not previously validated experimentally whether current was needed for the conversion of acetate to *n*-butyrate in these MES systems. To confirm this, two control MES reactors were set up identical to the other four reactors. In the MES reactors which were inoculated and applied with 15 mA (9.4 A m^{-2}), the *n*-butyrate concentration was approximately 0.4 g L^{-1} after 40 days (Figure S2.3).

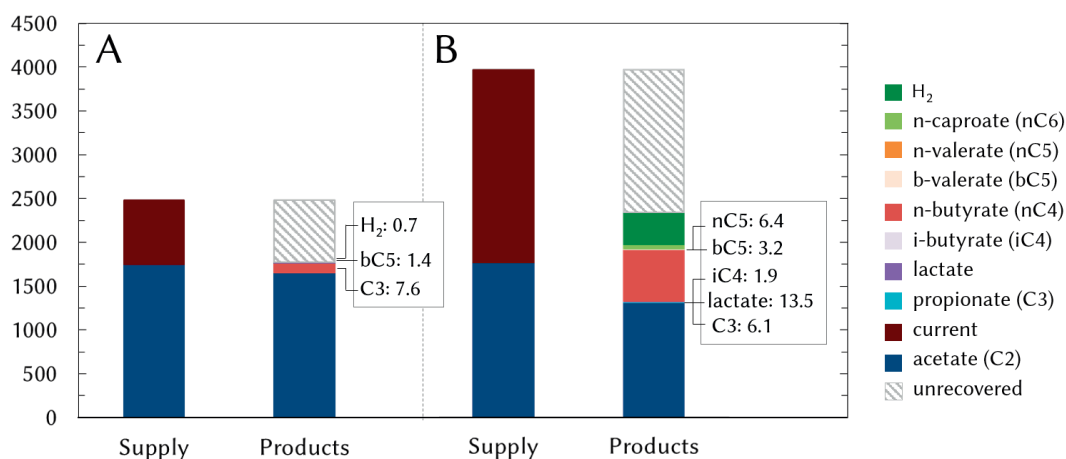


Figure 2.3: Cumulative electron distribution after 163 days of operation for one duplicate of 5 mA (A) and 15 mA (B) reactors. Total electron recovery was for 5 mA reactors 71.6 % and for 15 mA reactors 58.9 %.

Control 1 was set up to assess whether pure electrochemical reduction of acetate could lead to similar concentrations of n-butyrate in a similar timespan. Therefore, the current of control 1 was controlled at 15 mA (9.4 A m^{-2}) and operated for 37 days with a non-inoculated cathode. Maximal n-butyrate concentration was 0.053 g L^{-1} at the end of the run (results shown in Figure S2.3). These limited amounts of n-butyrate were most probably detected due to the difficulty to keep the reactors sterile and were a result of minor microbial activity.

Control 2 was used to assess whether biological anaerobic conversion of acetate in these specific MES reactors without applied current as electron donor could lead to n-butyrate production. After 71 days of operation, the maximal n-butyrate concentration reached 0.025 g L^{-1} (Figure S2.4).

These controls show that pure electrochemically or fermentative production of n-butyrate in these MES systems resulted in significantly lower n-butyrate production in the same amount of time. Therefore, it is evident that in the inoculated reactors under current controlled conditions the n-butyrate was primary bioelectrochemically produced. Furthermore, the cumulative electron distribution (Figure 2.3) and the control experiments demonstrated that when current was applied to the MES reactors, more n-butyrate was produced than when no current was applied. This shows that the application of current enhances the n-butyrate production from acetate and CO_2 in these MES reactors.

Moreover, the amount of current applied (i.e. high or low current) influenced the bioelectrochemical conversion of acetate. As showed in Figure 2.1, 15 mA applied current resulted in 4.5 times higher production rates and n-butyrate concentration than in low current cells controlled with 3 times lower current. Although a lower production was recorded in the 5 mA reactors, the electron efficiency was in these reactors higher than under high current conditions. These results demonstrate clearly that the applied current level affected the performance of MES reactors in such a way that more current resulted in higher production rates, higher concentration and more reduced compounds in the products spectrum. A plausible explanation for the higher production when more current was applied is that a higher current density led to a higher H_2 production, which could be either electrochemically or bioelectrochemically produced.^{59,92} H_2 has been shown to be the main electron flux carrier from cathode to electron acceptor.⁹³ Their study showed as well that H_2 production was biologically induced by surface modifications with catalytic active redox species. In our experiment, more H_2 was produced when more current was applied, and therefore more H_2 was available for microbial metabolism to reduce acetate. In chain elongation fermentation ethanol is needed as an electron donor and the H_2 partial pressure in the reactor should be kept high ($> 0.1 \text{ atm}$) to

prevent its oxidation to acetate.^{94,95} In our reactors an elevated H_2 partial pressure would prevent oxidation of produced carboxylates.⁷⁹ Under low current conditions, only very small amounts of H_2 left the aqueous phase. This might indicate *n*-butyrate was partly oxidized after it was produced when not sufficient H_2 was present near the biofilm (i.e. electrode surface). Limited H_2 partial pressure could have been caused by its full consumption by acetogenic bacteria for the conversion of CO_2 to acetate, as showed in Figure 2.1 A (occasional net production). In that case, lower amount of H_2 would be available to further elongate acetate to *n*-butyrate than in high current reactors. Consequently, it was hypothesised that an excess of H_2 in the high current reactors caused the 4.5 times higher *n*-butyrate production while only 3 times more current was applied. Furthermore, the production of reduced compounds in the low current reactors was also hypothesised to be limited by the lower H_2 production.

Although more current applied led to higher production rates/concentration, more electrons were lost to H_2 (ca. 25 mL H_2 day⁻¹, ca. 2 mmole e^- equivalents or ca. 8.8% electron recovery loss). For further implementation of MES as an acetate conversion technology, extensive electron losses need to be prevented. Hence what was limiting the H_2 consumption in these reactors needs to be elucidated. A first possible explanation could be that CO_2 supply was insufficient in the reactors. Jourdin et al. (2016)⁹³ showed that when they supplied sufficient CO_2 to a highly active homoacetogenic microbiome in their biocathode, all H_2 was consumed. The observations that 5 mA reactors had roughly the same concentration of acetate in effluent as in influent (Figure S2.2), that part of the inoculum consisted of acetogens from a running biocathode, and that limited H_2 was detected, led to the hypothesis that in the low current reactors acetate was formed from CO_2 and H_2 at the same rate than acetate was converted into other products (e.g. *n*-butyrate). Although acetate was continuously consumed more than it was produced in the high current reactors (Figure 2.1 B), it was not excluded that CO_2 reduction to acetate did happen in these reactors. The CO_2 supply was assessed to verify whether sufficient CO_2 was supplied to the reactors. All four MES reactors were supplied from the same influent tank, and thus were supplied with the same concentration of dissolved CO_2 . By modelling of our medium at a temperature of 303 K, and a pH of 5.5 using OLI Studio 9.2, it was determined that 32.5 mmol CO_2 L⁻¹ can be dissolved. At the applied inflow rate and HRT this equals 1.3 mmol CO_2 per 20 hours available. If all the electrons supplied (5 mA) were converted into H_2 , this would give 2.59×10^{-8} mol H_2 s⁻¹, while 15 mA would produce 7.77×10^{-8} mol H_2 s⁻¹. Per HRT (20 hours) this would give a production of 1.87 mmol H_2 or 5.60 mmol H_2 . According to stoichiometry of CO_2 reduction to acetate using H_2 as an electron donor, the molar ratio CO_2 : H_2 is 1 : 2.

The CO₂ consumption needed to convert this H₂ without losses into acetate, would be 0.93 mmol or 2.8 mmol CO₂ respectively. Moreover, the anode was sparged continuously with pure CO₂, assuming the anolyte to be CO₂ saturated. If the concentration of dissolved CO₂ in the cathode would be lower than in the anode, diffusion of dissolved CO₂ over the CEM towards the cathode would occur because of the concentration gradient. In the low current reactors the modelling showed the CO₂ concentration in the medium would be sufficient to fully consume the produced H₂, and CO₂ supply would not limit H₂ consumption. In the high current reactors the CO₂ supply would not be sufficient to consume the produced H₂ fully, which could explain the higher H₂ production rate in these reactors. Although calculations show that CO₂ could be limiting the H₂ consumption, it might not have limited the n-butyrate production in these reactors, because diffusion of CO₂ from the anode could have occurred. Total inorganic carbon measurements are needed to verify this possible CO₂ limitation under high current conditions.

Possible alternative explanations for the limited H₂ consumption under high current conditions could be non-homogeneous biofilm development on the electrode,⁹⁶ causing spaces on the electrode where H₂ was not consumed and consequently could leave the reactor. Furthermore, non-ideal electrode design could have resulted in mass transfer limitations,⁴⁶ either for substrate or nutrient supply to the microorganisms, as well as local pH stresses due to proton reduction at the cathode surface leading to a local extreme pH. For future implementation of MES technology, reactor and electrode design optimisation is needed to tackle these H₂ consumption limitations.⁹⁷

Potential biological pathways for electrochemical chain elongation

Understanding the electron transfer mechanisms involved in MES could help improve the technology for enhanced production of organics.⁹⁸ Unravelling the possible pathways in MES reactors can give insight on how to steer the process towards more specific products.

The first step in elucidating the possible metabolic pathways in MES reactors, is verifying whether the reactors were biologically catalysed. For this purpose, linear sweep voltammetry at constant pH 5.7 ± 0.3 was performed in abiotic condition (before inoculation) and at the end of the experiment on day 163 (Figure S2.5). A clear shift in the onset of current towards higher potentials can be observed after the experiment (ca. -0.8 V) compared to abiotic conditions (ca. -1 V). This was an indication of biological catalytic activity.^{42,46,92,99,100}

The inoculum consisted of acetogenic microorganisms from active CO₂ reducing biocathodes, chain elongating microorganisms and fermentative microorganisms.

These sources combined give several possible pathways to produce n-butyrate, H₂ and traces of n-caproate of which an overview is depicted in Figure 2.4.

A first possible part of the pathway to produce n-butyrate could have been the reduction of CO₂ to acetate via the reductive acetyl-CoA pathway using H₂ as an electron donor (Figure 2.4 - A3 and B1). This acetate producing pathway has been studied widely and was reviewed recently.¹⁰¹ In MES research this CO₂ reduction to acetate was the first to be shown to be driven by electrode derived electrons.⁴⁰ Since then, high rate and specific acetate production from CO₂ has been achieved in MES reactors.¹⁰⁰ Some acetogens can form n-butyrate as an end product¹⁰² by a pathway involving the aldol condensation of two acetyl-CoA molecules.¹⁰³

Another possible pathway to produce n-butyrate is elongation of acetate via the reverse β -oxidation pathway using ethanol or lactate as an electron donor (Figure 2.4 - A6 and B2).^{104,105} Several acetogenic species have been reported to produce ethanol directly from CO₂ derived acetyl-CoA or via acetate reduction to acetaldehyde.¹⁰² In mixed cultures ethanol has been shown to be produced from acetate and H₂ as electron donor,¹⁰⁶ or using the redox mediator methyl viologen in a bioelectrochemical cell.⁸⁶ In other bioelectrochemical studies ethanol was a by-product of CO₂ reduction,^{58,87} or VFA reduction,^{54,59} showing ethanol production in bioelectrochemical systems can occur (Figure 2.4 - A4). Although acetate reduction to ethanol with hydrogen as electron donor by mixed cultures is feasible both in fermentation and in MES, the kinetics are reported to be sluggish.^{79,106,107} Hydrogen partial pressures play an important role in the thermodynamic feasibility of the reduction of acetate to ethanol using H₂ as electron donor.¹⁰⁶ The higher the hydrogen partial pressure, the more energy could be gained by the microorganisms upon reduction of acetate.¹⁰⁶

When a fixed current was applied in our MES reactors, an excess of H₂ at the surface of the electrode (i.e. H₂ was present in headspace) was created. In this atmosphere of excess of H₂ and acetate in the catholyte, it could have been thermodynamic favourable for the microbial community to reduce acetate to ethanol. The observation of 4.5 times higher n-butyrate production rates in our high current reactors compared to the low current reactors where only 3 times less current was applied, suggests H₂ (and/or current) was of importance for the production of n-butyrate.

In literature H₂ was postulated as an electron donor for direct n-butyrate or n-caproate production by mixed culture fermentation,¹⁰⁸ a kinetic and thermodynamic modelling study showed kinetic limitations for this reaction. It was predicted that direct acetate conversion to n-butyrate by H₂ is most likely not feasible

even under high H_2 partial pressures.¹⁰⁹ Therefore, several reviewers assumed not H_2 , but instead ethanol as the real electron donor in that previous study.^{79,107}

In our experiments we did not detect any ethanol, still it could still have been the electron donor for the detected chain elongation of acetate to n-butyrate. The kinetically slow conversion of acetate to ethanol (in excess of H_2) could be predicted to be the limiting step in our MES reactors if the production went through the reverse β -oxidation using ethanol as electron donor.

Alternatively, ethanol could not have been produced at all. Therefore, we hypothesize on a new bioelectrochemical pathway (excluding the need of ethanol, lactate or even hydrogen) in which acetate is elongated using CO_2 , protons and electron equivalents directly taken-up from the solid electrode (Figure 2.4 - A7). This potential new route is supported by the fact that we did not detect any ethanol in our study. In the first part of the experiments reported by Ganigué et al. they as well demonstrated n-butyrate production without ethanol formation.⁵⁸ This speculative new pathway can be an explanation for their n-butyrate production, in which first acetate was produced by CO_2 and H_2 and this acetate was further converted into n-butyrate by CO_2 , protons and electron equivalents.

Usually in chain elongation fermentations mostly n-caproate (nC6) and only fractions of n-butyrate is produced when acetate and ethanol are supplied.^{110,111} In this study the main product was n-butyrate and only traces of n-caproate were detected in the high current reactors. It has been shown that the ratio electron donor (which in chain elongation fermentation was ethanol) to acetate supplied influences the product ratio n-butyrate/n-caproate.^{112,113} A higher availability of electron donor compared to acetate results in longer carbon chains.^{79,113–115} In our MES reactors only acetate was available, and if n-butyrate was produced via ethanol, it had to be produced before it could be used for chain elongation. This could explain the observation that mainly n-butyrate was produced and only traces of n-caproate were detected.

An alternative explanation for mainly producing n-butyrate could be that n-butyrate was mainly produced via acetyl-CoA reduction instead of via the reversed beta-oxidation. Acetyl-CoA can be formed via acetogenic pathways (Figure 2.4 – B1) in which the reducing power is delivered via H_2 or via the newly proposed bioelectrochemical pathway.

In summary, n-butyrate production in this study could have been either a result of a new bioelectrochemical pathway, or a result of a combination of pathways: i) CO_2 reduction to acetate via the reductive acetyl-CoA pathway, ii) acetate bio(electro)conversion to ethanol, iii) and chain elongation of acetate using ethanol

as electron donor. Thorough investigation of the present microbiome and an in-depth microbial metabolic analysis will be required to confirm these mechanisms.

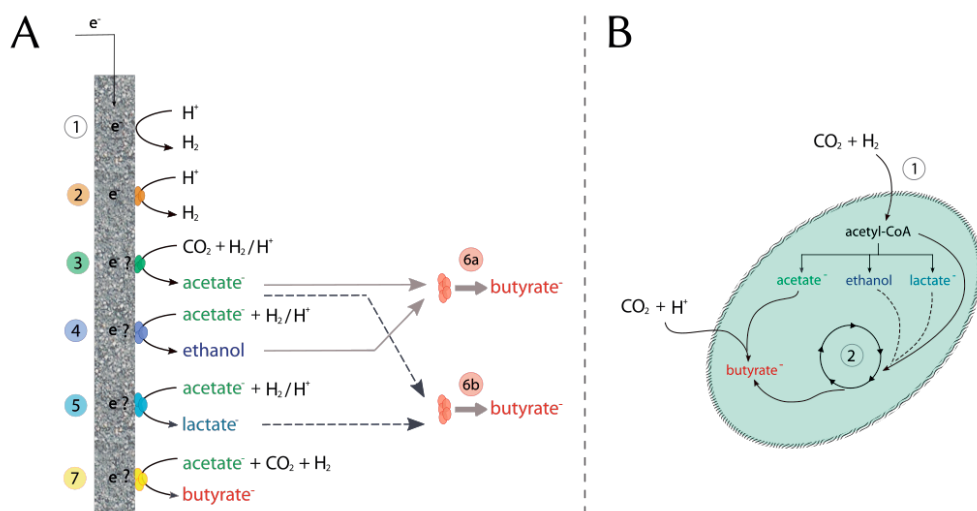


Figure 2.4: Schematics of microbial pathways contributing to n-butyrate production in microbial electrosynthesis cells. A: All possible pathways occurring in our MES cells, 1) electrochemical reduction of protons to H_2 B) bioelectrochemical reduction of protons to H_2 , 3) CO_2 reduction to acetate by acetogens, 4) acetate reduction to ethanol, 5) acetate conversion to lactate, 6) chain elongation of acetate to n-butyrate using ethanol (6a) or lactate (6b) as electron donor, 7) bioelectrochemical direct conversion of acetate to n-butyrate. Question marks indicate reactions where the exact electron transfer is not yet elucidated. Electron could be used by the microorganisms directly from the electrode, or hydrogen is first produced and subsequently the microorganisms use hydrogen as electron donor for their metabolism. B shows how the described metabolic pathways occur in microbial cells. The pathways are depicted in one microbial cell, in practice these reactions would occur in several types of microorganisms. Pathway B1 is the reductive acetyl-CoA pathway, B2) reverse β -oxidation, B3) new proposed bioelectrochemical pathway.

Perspective

Here, bioelectrochemical conversion of acetate was shown to reach n-butyrate concentrations and production rates up to 0.59 g L^{-1} and $0.54 \text{ g L}^{-1} \text{ day}^{-1}$, respectively, without the detection of ethanol. The highest n-butyrate concentrations in MES studies without external added mediators so far were 0.263 g L^{-1} ⁵⁹ and 0.445 g L^{-1} ⁵⁸ (see Table S2.1). Their production rate for n-butyrate was $0.334 \text{ g L}^{-1} \text{ day}^{-1}$ ⁵⁸ and Eerten-Jansen et al. did not report on production rates.⁵⁹ Therefore, to the best of our knowledge the concentration and production rate achieved in our study are the highest reported for MES converting acetate to more reduced carboxylates, to date.

However, compared to chain elongation (CE) of acetate using ethanol as electron donor, our n-butyrate production rate was approximately 20 times lower than the highest CE production rate reported to date¹¹⁰ (Table S2.1). Further research and development are required to reach similar rates. In-situ electron supply has several advantages over supplying ethanol as electron donor for fermentation: 1) no infrastructure for supply of hydrogen is needed, 2) the electron donor is renewable when renewable electricity is used, 3) in-situ supply results in locally high hydrogen partial pressures, which are favourable for reduction reactions.⁵⁹ Therefore, MES shows great promise as alternative for acetate elongation.

As stated before, previously reported reduction of acetate to ethanol¹⁰⁶ has been described as sluggish.^{79,107} Steinbusch and coworkers produced 0.309 mmol ethanol L⁻¹ day⁻¹. In our study we found a maximal n-butyrate production of 0.54 g L⁻¹ day⁻¹ (= 6.1 mmol L⁻¹ day⁻¹). When one presumes only chain elongation of acetate and ethanol to n-butyrate, according to stoichiometry, the molar ratio acetate : ethanol : n-butyrate is 1 : 1.5 : 1.25.¹⁰⁷ For the observed production of n-butyrate, an ethanol consumption rate of 1.2 times the n-butyrate production would have been needed, which is a consumption of 7.3 mmol ethanol L⁻¹ day⁻¹. As no traces of ethanol were detected in our study, the ethanol production should have been at the same rate as the ethanol consumption needed for n-butyrate production. This indicates our ethanol production rate was ca. 4.9 times as high as the previously reported rate.

In our experiments we used different electron donor to acceptor ratios. The electron acceptor (acetate) contains per mole 8 electrons, and the electron donor (ethanol, presumed to be produced from electrons) twelve electrons per mole. This gives according to abovementioned stoichiometry the electron acceptor to electron donor ratio of 8 to 14.4 (12 times 1.2). This indicates that for a stoichiometrically optimal reaction the ratio of electrons in electron acceptor and electron donor should be 36% : 64%. In our reactors approximately 1 g L⁻¹ of acetate was still in the effluent. The ratio of electrons supplied by acetate and by current in our systems, were 70% : 30% (5 mA) and 50% : 50% (15mA). Thus, in our reactors we supplied more electron acceptor than stoichiometrically needed. This indicates that for the process to be optimised, the ratio acetate supply compared to current can be used to improve n-butyrate production further.

Conclusions

In this study we showed continuous long term bioelectrochemical chain elongation of acetate to n-butyrate. In contrast to most MES studies, here the MES reactors were current controlled to ensure a constant flux of electrons. Variation in applied current had an effect on both product spectrum and production rate. It was shown that current was indeed needed for the production of reduced compounds compared to no current applied. Higher current applied (15mA) led to 4.5 times higher production rate of n-butyrate compared to 5 mA applied. Most electrons were recovered as n-butyrate (25 %) under high current conditions. Bioelectrocatalytic activity was confirmed. The microbial production route might have been a new proposed bioelectrochemical pathway, or it was a combination of the reductive acetyl-CoA pathway, (bio)electrochemically reduction of acetate to ethanol, and chain elongation of acetate and ethanol to n-butyrate.

Experimental Section

Electrochemical setup

Six identical electrochemical cells were set up. Each cell consisted of two Plexiglass flow through compartments (volume 33 cm³), one flat cathodic current collector plate (graphite 160 x 70 x 10 mm), one anodic current collector plate (Pt/IrO₂ coated Ti, Magneto Special Anodes, Schiedam, The Netherlands), and two Plexiglass support plates.¹¹⁶ Cathode and anode compartment were separated by a cation exchange membrane (Fumasep FTCM-E, Fumatech, projected surface area (psa) 22 cm²). The cathode compartments were filled with 6 layers of graphite felt (3 mm thick, CTG Carbon GmbH, Germany; total psa was 16 cm², total electrode volume was 24 cm³). The felt layers were cut off to leave 1.5 cm empty space at both bottom and top to promote homogenous liquid mixing before flowing through the felt. The anode compartment was fully filled with glass beads (ca. 0.5 cm diameter) to press the membrane against the graphite felt in the cathode chamber and to disperse the gas flow through the anode compartment. The cathode headspace was connected to a gas bag, in order to identify and quantify gas production. A pH sensor (QMP108X, Q-is, Oosterhout, the Netherlands) was placed in the catholyte recirculation circuit to log the pH every 10 minutes (D230 datalogger, Consort, Belgium). CO₂ gas was sparged at 10 mL min⁻¹ through the anode compartment, to scavenge produced O₂ and to limit CO₂ loss from the cathode by diffusion. Schematic of the setup is shown in Figure S2.1.

Electrolytes and inoculum

The total catholyte volume was 50 mL (electrochemical cell and tubing), and was recirculated at 5.2 L h⁻¹. The catholyte medium consisted of 0.25 g L⁻¹ (NH₄)₂CO₃, 10 mg L⁻¹ MgSO₄·7H₂O, and 2,9 mg L⁻¹ Ca(OH)₂, 2 mL·L⁻¹ micronutrient solution, 1 mL·L⁻¹ vitamin solution, 20 mM potassium phosphate buffer (pH 5), 20 mM potassium acetate, 10 mM acetic acid and 3 g L⁻¹ sodium 2-bromoethanesulfonate. The micronutrient solution contained 2 g L⁻¹ FeCl₂·4H₂O, 1 g L⁻¹ COCl₂·6H₂O, 0.5 g L⁻¹ MnCl₂·4H₂O, 0.05 g L⁻¹ ZnCl₂, 0.05 g L⁻¹ H₃BO₃, 0.04 g L⁻¹ CuCl₂·2H₂O, 0.07 g L⁻¹ (NH₄)₆Mo₇O₂₄·5H₂O, 1 g L⁻¹ NiCl₂·6H₂O, 2 mL of 37% HCl. The vitamin solution was optimised for fatty acid synthesis and contained 0.5 g L⁻¹ biotin, 0.02 g L⁻¹ folic acid, 0.5 g L⁻¹ nicotinic acid, 0.1 g L⁻¹ pyridoxine-HCl, 0.1 g L⁻¹ riboflavin, 0.01 g L⁻¹ thiamin-HCl, 0.01 g L⁻¹ vitamin B12, 0.25 g L⁻¹ lipoic acid, and 0.05 g L⁻¹ D-Ca-Pantothenate. The catholyte was supplied to the reactors continuously which resulted in an hydraulic retention time (HRT) of 20 hours. The pH of the influent was adjusted to 5.4 with 1 M KOH. The catholyte influent vessel was sparged continuously with pure CO₂ gas at 1 L h⁻¹.

The anolyte consisted of potassium phosphate buffer (20 mM, pH 5), 0.25 g L⁻¹ (NH₄)₂CO₃, 10 mg L⁻¹ MgSO₄·7H₂O, and 2,9 mg L⁻¹ Ca(OH)₂. The pH was adjusted to pH 2.5 ± 0.1 using 0.5 M H₃PO₄. The total anolyte volume was ca. 300 mL, and the anolyte was recirculated at 5.2 L h⁻¹. The anolyte was operated in fed-batch. Once every 1-2 weeks the anolyte was replenished with fresh anolyte solution in order to correct for liquid loss due to CO₂ sparging and electrolysis of water.

For inoculation of the MES cells, several sources were mixed: 1) effluent from two different running chain elongation reactors,^{117,118} 2) effluent from two running CO₂ reducing biocathodes,^{51,88} 3) primary sludge (WWTP Bennekom, the Netherlands), and 4) VFA producing granular sludge (provided by Paques BV, the Netherlands). The mixture was washed 3 times by centrifugation for 10 min at 10000 rpm followed by resuspension of the pellet in fresh buffer solution, and was used as inoculum for the four MESs. 10 mL of inoculum (COD of inoculum was 1475 mg O₂·L⁻¹) was added to each reactor.

MES reactor operation

A multichannel potentiostat (n-stat, Ivium, the Netherlands) was connected to the three-electrode electrochemical cells to control the current and record the cathode potentials. The cathode was equipped with a 3M Ag/AgCl reference electrode (QM710X, Q-is, Oosterhout, the Netherlands). All potentials are reported versus this reference electrode unless stated otherwise (E°=+0.207 V vs SHE at 303 K). Two of the cells were controlled at 5 mA (3.1 A/m² psa) and two others were controlled at 15 mA (9.4 A/m² psa).

Two of the six reactors were used as controls. These controls were used to study whether sole electrochemical reduction of acetate could lead to *n*-butyrate production (control 1), and whether acetate would be reduced to *n*-butyrate by microorganisms without current as electron donor (control 2). Therefore, control 1 was not inoculated, and control 2 was inoculated with 5 mL effluent of each of the four running MES cells. Control 1 was controlled at 15 mA, and control 2 was left on open cell voltage (OCV).

The cathode pH was manually controlled at 5.5 ± 0.5 , using 0.5 M H_3PO_4 or 1 M KOH dosing. The reactors were operated in a temperature-controlled cabin at 30 °C.

Before inoculation, the reactors were operated abiotically for 7 days to stabilize the pH due to ion balancing between anode and cathode and to characterise the systems.

Analyses

Once or twice a week, 5 mL liquid samples were taken from the cathodes to analyse catholyte composition. Concentration of volatile fatty acids (C2 to *n*-C6) was analysed by gas chromatography (HP 5890 series II, Germany) on a packed column (2 m x 6 mm x 2 mm) with 10 % Fluorad 431 on Supelco-port 100-120 mesh. The detector (FID) temperature was 280°C, inlet temperature 200°C and column temperature 130°C. N_2 saturated with formic acid was used as carrier gas at a flow of 40 mL/min. 1 µL of sample was injected on the column, and isothermally analysed. Concentration of alcohols (ethanol to hexanol) was analysed by a similar GC setup. The temperature program was: 75°C (6 min), temperature ramp of 5°C.min⁻¹ until 130°C, temperature ramp of 49°C.min⁻¹ until 160°C (8.5 min).

Concentration of formate, succinate and lactate was measured using high pressure liquid chromatography (HPLC, Ultimate 3000, Dionex). 0.2 µL was loaded on a OA-1000 organic acids column (300 mm x 6.5 mm; Alltech). Column temperature was 60°C, flow rate 0.6 mL min⁻¹, mobile phase 1.25 mM H_2SO_4 . For detection a RI detector was used.

In order to check whether all reduced components were identified, chemical oxygen demands (COD) was measured using the Hach Lange LCK014 cuvette test, according to fabricant's instructions.

Headspace samples were taken at the same time liquid samples were taken. Gas samples were taken from the gas sampling port located between the gasbag and the cathode liquid level. Hydrogen was analysed by gas chromatography, injecting 100 µL sample directly on column (HP 5890 series II, TCD detector). A Molesieve 5 Å column (30 m x 0.53 mm x 25 µm) was used. Inlet temperature 110°C, oven temperature 40°C, and detector temperature 150°C. The carrier gas was argon 5.0 on 220 kPa. Nitrogen, carbon dioxide, methane and oxygen were analysed loading ca.

1.5 mL gas sample on a gas chromatograph (2010, Shimadzu, TCD detector). 50 μ L gas was injected via loopinjection on a parallel combination of Parabond Q column (50 m x 0.53 mm x 10 μ m) and a Molesieve 5Å column (25 m x 0.53 mm x 50 μ m). Inlet temperature 120°C, oven temperature 80°C, and detector temperature 150°C. The carrier gas was helium 5.0 on 0.95 bar.

Headspace volume was measured by manually emptying the gasbag using a 100 mL syringe.

At the start (day 0) and at the end of the experiment (day 163) cyclic voltammetry was performed by scanning 3 cycles, from -0.2 V to -1.1 V at a scan rate of 1 mV.s⁻¹ and the pH was controlled at 5.7 \pm 0.4. The 3 cycles were reproducible and only the last reductive wave is showed here as a representative.

Calculations

To analyse the influence of current on the production of compounds, an electron balance was calculated. Based on Eerten-Jansen (2013), the production (mol e⁻ equivalents) of each product at each sampling moment t ($p_{i,t}$) was calculated:

Production_{i,t} = accumulation_{i,t} + out_{i,t} - in_{i,t}

$$p_{i,t} = \left[V_{cat}(C_{i,t} - C_{i,t-1}) + Q \frac{(C_{i,t} + C_{i,t-1})}{2} \Delta t - Q C_{in,i} \Delta t \right] n_{e,i} \quad (1)$$

where subscript i refers to the product (that is, all organics which were quantified and mentioned in the section Analyses), V_{cath} the total catholyte volume (0.050 L), C_i the concentration of product (mol L⁻¹), Q the influent and effluent flow rate (L h⁻¹), Δt the time between sampling time t and t - 1 (h), $C_{in,i}$ the concentration of product i in the influent (mol L⁻¹), and $n_{e,i}$ the number of electrons per mole of product.

The coulombic efficiency, or electron recovery η_e (%), represents the fraction of electrons recovered in products compared to the electrons supplied by either current or acetate. The electron recovery was calculated according to:

$$\eta_{e,t} = \frac{(accumulation_{total,t} + out_{total,t})}{(in_{current,t} + in_{acetate,t})} \quad (2)$$

where accumulation_{total} represents the sum of the accumulation of all products (each one in mol e⁻ equivalents.), out_{total} the sum of out, in_{current} the amount of electrons supplied by the electrode, and in_{acetate} the amount of electrons supplied by acetate.

The volumetric production rate (g L⁻¹ day⁻¹) was calculated by:

$$Volumetric\ production\ rate_{i,t} = \frac{p_{i,t} M_i}{\Delta t V_{cath} n_{e,i}} \quad (3)$$

where M_i refers to the molar weight of product i (g.mol⁻¹).

The carbon recovery η_c (%) represents the fraction of carbon supplied by acetate that was recovered in the identified reduced products (acetate also regarded as product), and was calculated based on equation 1:

$$\eta_{c,t} = \frac{(\text{accumulation}_{c,t} + \text{out}_{c,t})}{\text{in}_{c,t}} \quad (4)$$

in which subscript c,t refers to total carbon, and concentration is expressed in mM.

Averages and standard deviations for production rate, electron and carbon recovery were calculated based on the duplicate reactors per current condition.

Acknowledgements

Financial support from the Dutch Technology Foundation STW and the company Paques (project nr. STW-Paques 12999) is grate-fully acknowledged. SR acknowledges S.D. Molenaar for his valuable contribution to the experimental design and the fruitful discussions.

Chapter 2 - Supplementary information

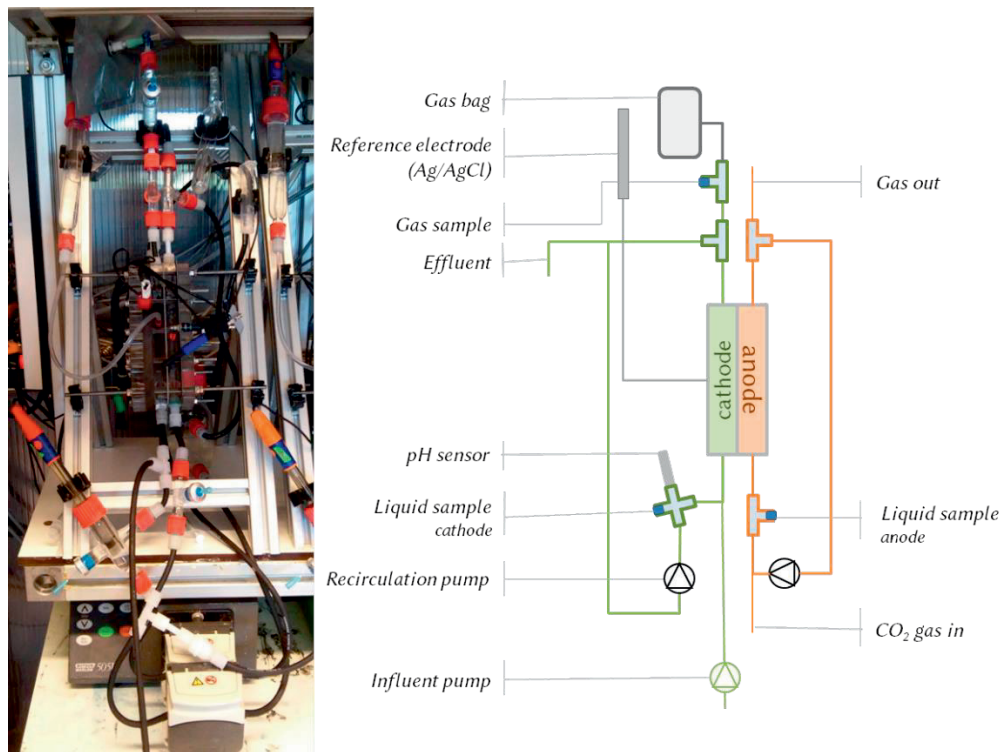


Figure S2.1: Photo and schematic of microbial electrosynthesis setup used in this study. Cathode consisted of several layers of graphite felt with a graphite plate as current collector. The anode was a Pt/Ir coated Ti plate.

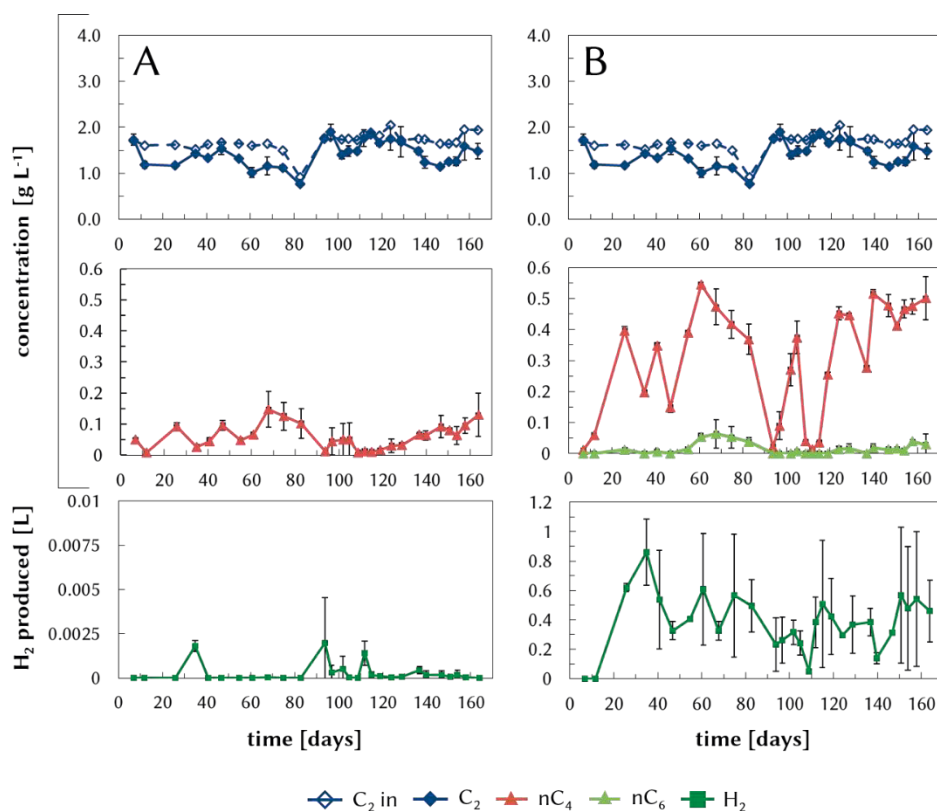


Figure S2.2: Concentration of the main products for MES reactors applied A) with 5 mA (3.1 A/m²) and B) 15 mA (9.4 A/m²). Average of duplicate reactors are shown, standard deviation is indicated by the bars. C₂-in: acetate in influent, C₂: acetate in effluent, nC₄: n-butyrate, nC₆: n-caproate. Detected H₂ depicts the amount of H₂ that was produced in between two sample points.

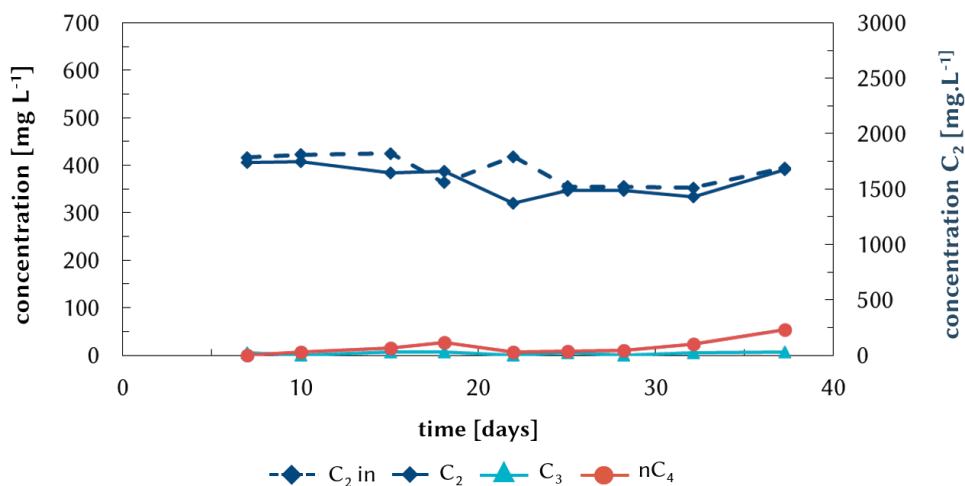


Figure S2.3: Concentration of acetate and main liquid products in Control 1. To verify whether electrochemical reduction of acetate could lead to a n-butyrate concentration of 0.4 g L^{-1} within 20-40 days, this reactor was applied with 15 mA (9.4 A m^{-2}), but was not inoculated and operated for 37 days. C2: acetate, C3: propionate, nC4: n-butyrate.

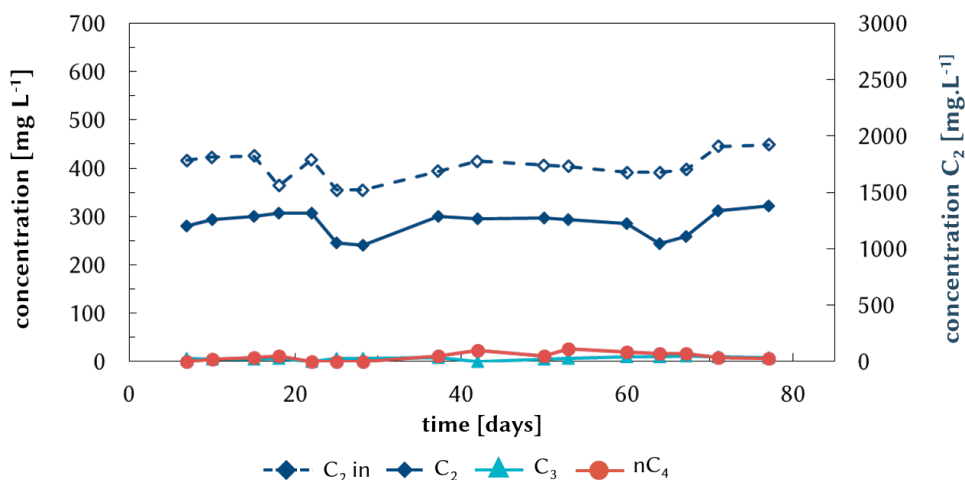


Figure S2.4: Concentration of acetate and liquid products in Control 2. To verify whether anaerobic biological conversion could lead to n-butyrate concentration of approximately 0.5 g L^{-1} , this reactor was inoculated with 5 mL from the four running MES reactors and no current was applied to it.

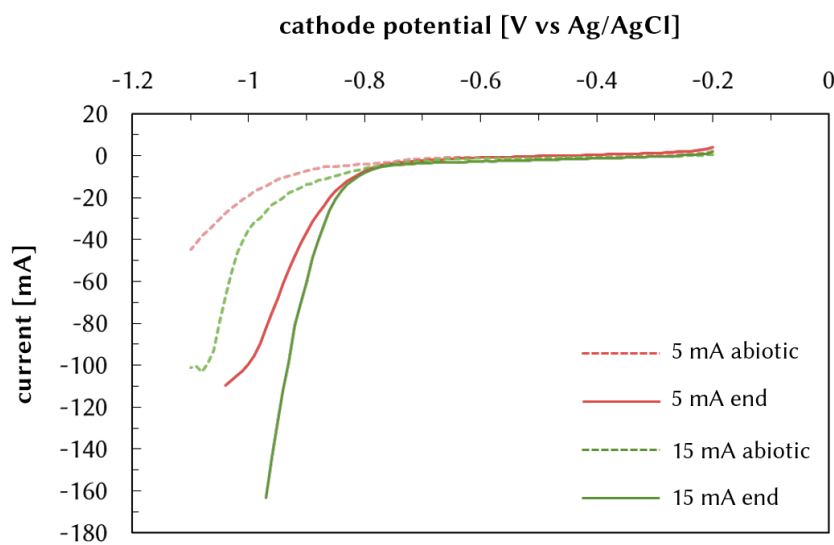


Figure S2.5: Reductive waves of cyclic voltammetry on cathodes at day 0 (abiotic - dashed lines) and after the experiment on day 163 (end - solid lines), scan rate 1 mV s^{-1} . A clear shift in onset potential is observed for both low (5 mA , 3.1 A m^{-2}) and high (15 mA , 9.4 A m^{-2}) current, indicating that the reactions occurring in the reactors were biologically catalysed.

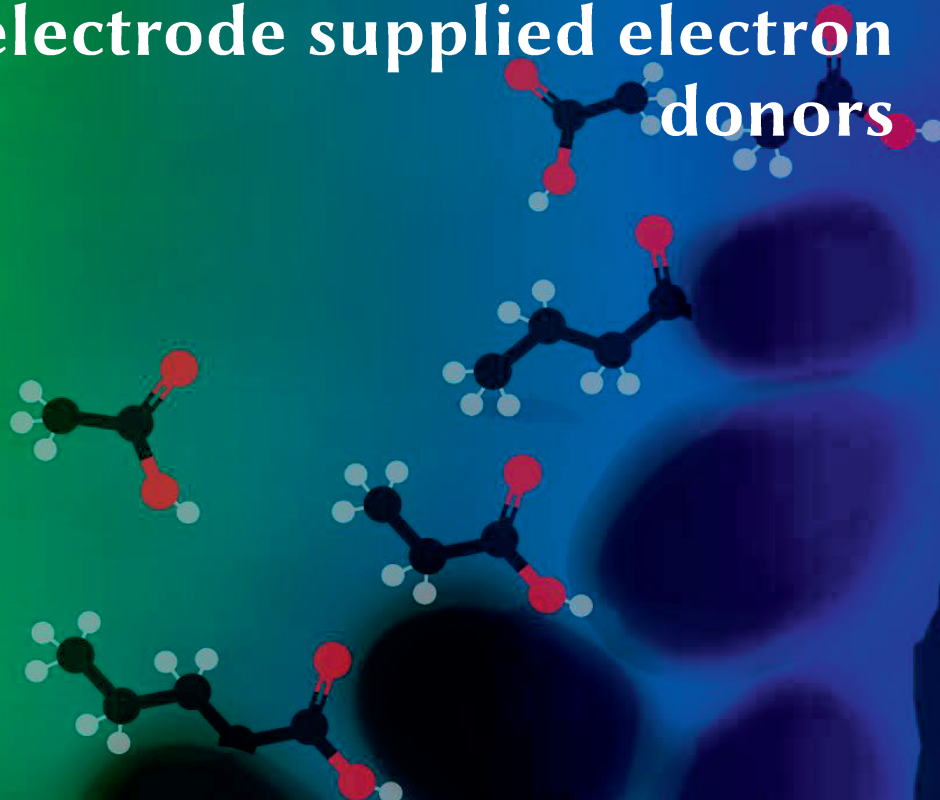
Table S2.1: Key parameters and highest production rate of acetate reduction to n-butyrate in MES studies and chain elongation fermentation studies.

| Ecath (V vs SHE) | Current density (Am ⁻²) ^I | Electron recovery (%) | Substrate/ C-source | Main products | Max. conc. Products (g L ⁻¹) | Production rate (g L ⁻¹ day ⁻¹ or gas: L L ⁻¹ day ⁻¹) ^{II} | Operation mode | Experiment length (days) | Reference |
|------------------------|--|-----------------------------|---|--|--|--|-------------------|--------------------------------|--|
| -0.9 | 1.8 ± 0.6 | 45 | acetic acid (100mM) + K ₂ CO ₃ (4 g L ⁻¹) | n-butyrate, caproate, caprylate | 0.263, 0.739, 0.036 | n.d. | Continuous | 17 | Van Eerten Jansen, 2013 ⁵⁹ |
| -0.8 | 3 - 20 | 32 | CO ₂ (gas, sat conc. 26.9 mM) | Acetate n-butyrate, ethanol | 1.664 0.445 0.709 | n.d. 0.334 n.d. | Fed-batch | 34 | Ganigué, 2015 ^{58 III} |
| -0.85 | 37 | n.d. | NaHCO ₃ (0.5 - 2 g L ⁻¹) | Acetate | 1.65 | n.d. | Fed-batch | 140 | Jourdin, 2014 ⁴⁶ |
| -0.85 | 102 - 150 | 100 ± 4 | NaHCO ₃ (1 - 4 g L ⁻¹) | Acetate | 11 | 0.373 | Fed-batch | 63 | Jourdin, 2015 ¹⁰⁰ |
| -0.55 | 0.27 - 1.33 | 49 - 12 | Acetic acid (50mM) | Ethanol, H ₂ , n-butyrate | 0.083 - 0.062 | 5.8 · 10 ⁻⁵ 0.012 - | Batch | 10 | Steinbusch, 2010 ⁸⁶ |
| - | - | - | Acetate (4.8 -36.0 g L ⁻¹), ethanol (7.4 - 82.8 g L ⁻¹) and K ₂ CO ₃ | n-butyrate, caproate, caprylate | 1.7 12 0.9 | 9.6 55.8 1.8 | Continuous | 69 | Grootscholten, 2013 ¹¹⁰ |
| -0.63 ± 0.1 | 3.125 | 71.6 | Acetate (30 mM) + CO ₂ | n-butyrate | 0.11 | 0.08 | Continuous | 163 | This study |
| -0.72 ± 0.2 | 9.375 | 58.9 | Acetate (30 mM) + CO ₂ | n- butyrate | 0.59 | 0.54 | Continuous | 163 | This study |

| | | | |
|----|---|------|--|
| I | normalized for projected electrode surface area | III | second experiment of paper is used for this table (best results) |
| II | normalized for total catholyte volume | n.d. | not defined |

Chapter 3

Bioelectrochemical chain elongation of acetate and the role of fermentative and electrode supplied electron donors

The image displays several ball-and-stick molecular models of carboxylate anions. In the upper right, there is an acetate ion (CC(=O)[O-]). Below it and to the left are several butyrate ions (CCCC(=O)[O-]). The atoms are color-coded: carbon is black, oxygen is red, and hydrogen is white. The molecules are arranged in a diagonal pattern across the right side of the page.

Abstract

Bioelectrochemical chain elongation (BCE) is an emerging biotechnology to convert residual biomass or CO₂ into precursors for liquid fuels and chemicals. However, a number of kinetic aspects are unknown which are required for an efficient and optimal BCE process. To elucidate whether BCE is driven by intermediate produced known electron donors for fermentative chain elongation, i.e. ethanol and lactate, these compounds were separately introduced in triplicate BCE reactors. Both compounds did not significantly affect the rate of n-butyrate production. Next to these compounds, the effect of formate was tested. The effect of increased formate levels led to the induction of acetate production. The induced acetate production competed for electrons associated with acetate elongation to n-butyrate. To investigate the role of the electrode as electron donor, the current was doubled, which resulted in doubled production rates of n-butyrate. Hence, in this study we showed that acetate conversion towards higher value-products in our BCE reactors was not limited by intermediate production of well-known electron donors, but was driven by electrons supplied by the electrode. This finding supports the postulation that BCE occurred via (bio)electrochemically induced H₂ production and/or direct electron uptake mechanisms.

Introduction

The synthesis of commodity chemicals and liquid fuels from renewable resources is essential to achieve the envisioned circular economy and independence from fossil fuels. Renewable biomass, such as organic residual streams, holds great potential to become that alternative sustainable feedstock. Commonly, organic residues are anaerobically digested into methane containing biogas which can be used for heat and/or electricity production.⁷⁷ However, the formation of biogas is associated with methane emissions and in addition, biogas has a relatively low economic impact.⁷⁷ Therefore, the research efforts on the valorisation of organic residues has been intensified in the last decades. Amongst other valorisation methods, microbial chain elongation is a promising emerging technology reaching commercial demonstration.¹¹⁹

Chain elongation is a bioconversion process that uses open anaerobic microbial communities to produce value-added chemicals and fuel precursors from organic waste.^{79,107} For chain elongation (CE), low-grade biomass is biochemically pretreated via hydrolysis and acidification, to produce short chain fatty acids (SCFA; 2-5 carbon atoms; mainly acetate, propionate and n-butyrate). These short building blocks are subsequently elongated towards medium chain fatty acids (MCFAs) by supplying an external electron donor. Reported electron donors in microbial chain elongation of SCFAs are ethanol,^{111,120} lactate,^{121,122} H₂,^{123,124} methanol,¹¹⁸ propanol,^{125,126} and electrode-derived electrons.¹²⁷ Recently, the sustainability of n-caproate (nC6 MCFA) production via chain elongation of mixed organic waste with ethanol as electron donor was assessed.¹²⁸ Ethanol was identified to have the biggest negative environmental impact. To reduce this environmental impact, electrode-derived electrons can be supplied, designating this as bioelectrochemical chain elongation (BCE). Replacing ethanol or lactate with electrons as electron donor, has the potential to increase the LCA of chain elongation processes.

The supply of electrons for the reduction of SCFAs by an electrode was described as a promising valorisation technology for the conversion of acetate into longer chain fatty acids,^{59,127} and as well for the elongation of CO₂ to n-caproate (nC₆).^{129,130} In previous work the long-term continuous elongation of acetate (C₂) to n-butyrate (nC₄) was demonstrated.¹²⁷ To gain insight in the dominating reaction mechanisms of the formation of nC₄ in the BCE process, the nC₄ production pathways described for fermentative chain elongation were reviewed.¹²⁷ The microbial production route either might be a novel postulated bioelectrochemical pathway, or a via conventional pathway locally produced electron donor and subsequent chain elongation of acetate with that electron donor to nC₄. During the experiments the concentration of all possible soluble (intermediate) electron donors were always

below detection limit in the BCE reactors. However, this pathway could not be excluded yet.

Several studies have reported the production of nC₄ in bioelectrochemical reactors,^{58,129–135} however ethanol was detected as well in these studies except for Jourdin et al (2018).¹²⁹ Ethanol can be produced by acetate reduction by carboxytrophic bacteria such as *Clostridium autoetanogenum*, *C. ljungdahli*, *C. ragsdalei*.¹³⁶ For such bacteria, a pH shift is required from near neutral to pH 4.5 - 5.0 to change its metabolism from acidogenesis to solventogenesis.¹³⁶ The reduction of SCFA to alcohols have been reported with H₂ as electron donor¹⁰⁶ and therefore the availability of H₂ influences the alcohol production.¹³⁷

In bioelectrochemical systems (BESs), H₂ has been described as an important electron mediator reducing CO₂ to acetate.^{93,138,139} For instance, Batlle-Vilanova (2017) reported that a requirement for nC₄ production was a built up H₂ partial pressure in the headspace of their batch microbial electrosynthesis (MES) systems.¹³¹ Due to this H₂ partial pressure, acetate in the liquid phase could be reduced to ethanol and subsequently nC₄ production occurred.¹³¹

Besides being described as an important reductant in BESs, H₂ plays an important role in syntrophic microbial communities as electron carrier, as well as formate.^{140,141} H₂ and formate can either be electrochemically formed or be formed by microbially excreted redox-active enzymes sorbed to a cathode surface.¹⁴² In case of the methanogenic archaea *M. maripaludis* H₂ and formate formation was catalysed by extracellular hydrogenases and formate dehydrogenases.¹⁴² Formate was detected in trace amounts in several studies accompanying nC₄ production,^{132,134,135} indicating a possible role of formate in the production of nC₄.

Despite a number of studies produced possible intermediate electron donors in BCE processes, still the actual electron donor(s) used and the consequent carbon fluxes are poorly understood. Studies often use (undefined) mixed cultures and report on various intermediates (e.g. ethanol as electron donor) while diverse mixtures of products were formed. Hence, the key electron donor in BCE remains speculative, especially when no known electron donor is detected for CE.¹²⁷

In such BCE systems where no soluble electron donors are detected, it is also possible that electrode-derived electrons are the source of metabolic electrons for chain elongators similar as shown for various acetogens.¹⁴³ In previous work, it was demonstrated that current was required for nC₄ production (control experiments) as well as that nC₄ production rate was increased when more current was applied.¹²⁷ Vassilev et al. showed that an applied cathode potential of -0.8V vs SHE was needed

to reduce CO_2 .¹³⁰ These results indicate that energy supply via poised electrode or applied current might play a pivot role as electron donor in bioelectrochemical CE.

The objective of this study was to elucidate the key electron donor in the bioelectrochemical elongation of acetate to nC_4 . It was hypothesised that the production of nC_4 in our BCE reactors was limited by intermediate electron donor production. When the limitation would be removed, i.e. the presumed electron donor was externally supplied into the reactors, the nC_4 production would instantly increase. Therefore, to elucidate the involved electron donor in nC_4 production, the known electron donors for fermentative CE (ethanol and lactate), and formate were independently spiked in nC_4 -producing MES reactors and the effects on nC_4 production were studied for several days after the spike. Additionally, to validate the postulated requirement for a high H_2 partial pressure in the headspace, the headspace was flushed continuously with N_2 . Lastly, to verify the role of current in the production of nC_4 , the applied current was doubled.

Experimental Section

MES reactor setup and operation

Three identical electrochemical reactors were operated for these experiments. The reactor setup was described in detail previously.¹²⁷ Two of the three reactors were previously applied with 5mA (3.1 A m^{-2} projected electrode surface area; psa was 16 cm^2), and prior to the experiments the current was increased to 15mA (9.3 A m^{-2} psa). The third reactor was already applied with 15 mA prior to the experiments.

The catholyte (50 ml) medium consisted of 0.25 g L^{-1} $(\text{NH}_4)_2\text{CO}_3$, 10 mg L^{-1} $\text{MgSO}_4 \cdot 7\text{H}_2\text{O}$, and 2.9 mg L^{-1} $\text{Ca}(\text{OH})_2$, 2 mL L^{-1} micronutrient solution, 1 mL L^{-1} vitamin solution, 20 mM potassium phosphate buffer (pH 5), 3 g L^{-1} sodium 2-bromoethanesulfonate, and 30 mM acetic acid. The micronutrient solution and vitamin solution were identical to previous work.¹²⁷ pH of the influent was adjusted to 5.2 with KOH. The HRT was 25 hours. The catholyte influent vessel was sparged continuously with pure CO_2 gas at 1 L h^{-1} to keep it anaerobically and to supply dissolved CO_2 . Manually the catholyte pH in the reactors was controlled by addition of 1 M KOH or 0.5 M H_3PO_4 in case the catholyte was deviating more than 0.5 from pH 5.5. The anolyte (300 ml) consisted of demiwatier acidified with H_3PO_4 to pH ~ 2.1 , and was operated in fed-batch. Weekly approximately 10% of the total anolyte volume was added to compensate for evaporation and reduced volume as a result of water oxidation. The reactors were operated in a temperature-controlled cabin at 30°C .

Electron donor experiments

To study the role of known electron donors, the electron donor was spiked in the reactors and the effect on nC₄ production was studied for several days after the spike (Table 3.1). The used electron donors ethanol, lactate and formate were added to the reactors via a syringe. To prevent a pH shock in the reactors, first the catholyte recirculation pump was stopped, 5-10 mL of catholyte was extracted from the system in a beaker glass. The electron donor was added to the beaker glass and the pH was adapted to ~5.5. The subsequent mixture of catholyte and electron donor was reintroduced in the reactor using the syringe, and the recirculation pump was started again.

The amount of electron donor added to the system was selected in such a way that the stoichiometric conversion with the 30 mM acetic acid in the system would not be limited. For ethanol, the stoichiometric acetate : ethanol ratio is 1 : 1.5,¹⁰⁷ and hence 0.18 ml ethanol (96 % pure, Merx) was added to the reactor. This would result in a concentration of 2.76 g L⁻¹. Two spiking series in the three reactors gave 6 replicates for ethanol. The ratio acetate : lactate for n-butyrate production is 1 : 1,¹⁰⁷ so to the reactor 92 µL lactic acid (90% pure, VWR) was added, resulting in ~ 2 g L⁻¹. For LA only three replicates are included, as another spiking series yielded unusable results due to potentiostat failing during the second spiking series. As no literature is available on direct formate conversion to n-butyrate, and therefore no stoichiometric ratio was known beforehand, during preliminary formic acid spiking tests (data not shown), the equal amount of electrons as supplied by ethanol (36 mmol e⁻) were added as formic acid (18 mmol, leading to 0.36 M or 16.5 g L⁻¹ reactor concentration). Because of this high FA concentration, the nC₄ production was temporarily impeded. Upon recovery of the reactors after this spike, a lower concentration of 1-2 g L⁻¹ was aimed for in the spiking of FA as well. For that reasons 50 µL of FA (98-100%, Sigma Aldrich) was introduced in the reactors, which would result in 1.21 g L⁻¹. Of formic acid four replicates are included in this study.

To verify the hypothesis a pH₂ in the headspace was needed as electron donor for nC₄ production,¹³¹ the gasbags were removed from the systems and continuous N₂ headspace flushing was applied (Table 3.1). After 4 weeks of operation in this way, N₂ flushing was stopped and the gasbags were attached again.

The ideal electron ratio between donor and acceptor is 18 : 8 mol e⁻ based on the stoichiometric ratio of ethanol to acetate of 1.5 : 1 in chain elongation.¹⁰⁷ To study whether the current had an effect on the n-butyrate production keeping the influent concentration of acetate the same, the applied current in two different already running reactors was increased from 15 mA to 29 mA (18.1 A m⁻² psa) (Table 3.1).

Table 3.1: Electron donor experimental conditions

| Electron donor | Treatment |
|--------------------------|---|
| Ethanol | Spike reactors – 0.18 ml 96% pure ethanol |
| Lactate | Spike reactors – 92 µl 90% lactic acid |
| Formate | Spike reactors - 50 µl 98-100% formic acid |
| H ₂ headspace | Remove gasbag and continuously sparge headspace with N ₂ |
| Current | Increase current from 15 mA to 29 mA |

Analyses

To investigate whether n-butyrate production would increase upon the spike of the electron donor, liquid samples were regularly taken from the cathodes to analyse the dissolved organic products. When the reactors were spiked with electron donor, samples were taken at least once a day for 4-5 subsequent days after each spike, and 2-3 times per week during the headspace flushing period as well as during the period of applied current doubling. The concentrations of volatile and medium-chain fatty acids (C2 to C8) and alcohols (methanol to hexanol) in the liquid phase were determined as previously reported.¹²⁹

The concentration of formate and lactate was measured using high pressure liquid chromatography (HPLC, Ultimate 3000, Dionex). 0.2µl was loaded on a OA-1000 organic acids column (300 mm x 6.5 mm; Alltech). Column temperature was 60°C, flow rate 0.6 mL min⁻¹, mobile phase 1.25 mM H₂SO₄. For detection a RI detector was used.

Chemical oxygen demand (COD) Hach Lange LCK014 cuvette test was regularly used according to fabricant’s instructions to verify if all reduced components were identified.

The volumetric production rates of organics were calculated as previously described.¹²⁷

Mathematical model and parameter estimation

A mathematical model for the fate of the electron donors ethanol, lactate and formate in the bioelectrochemical cell was developed. As mentioned in the previous sections, the setup consists of an electrochemical reactor with continuous supply of fresh medium containing acetate. After administering a peak injection of electron donor, the system can be represented with the following mass balances:

$$\frac{dVC_B}{dt} = (\gamma_e \cdot k_e \cdot V - \emptyset) \cdot C_B \quad \text{eq. 1}$$

$$\frac{dVC_e}{dt} = -(\emptyset + k_e \cdot V) \cdot C_e + R_e^F \quad \text{eq. 2}$$

Where V is the reactor volume (L), C is the concentration in the bulk of the solution of respectively n-butyrate (subscript B) and electron donor (subscript e , L h⁻¹), t is time (h), k_e the first order reaction rate of electron donor converted into n-butyrate (h⁻¹), \emptyset the flow rate of fresh medium (L h⁻¹) containing a concentration of n-butyrate, γ_e the stoichiometric ratio for conversion of electron donor to n-butyrate and R_e^F the reaction rate of electron donor formation from CO₂ (mmol L⁻¹ h⁻¹). Notice that the reaction kinetics assumed first order.

The stoichiometric ratios γ_e used in this study are taken from Spirito et al. (2014):¹⁰⁷ γ_e (ethanol : nC4) is 5/6, and γ_e (lactate : nC4) is 1.

After solving the differential equation 2, the following equation for electron donor concentration is obtained:

$$C_e(t) = C_{0,e} \cdot e^{-\left(\frac{\emptyset}{V} + k_e\right)t} + R_e^F \frac{\left(1 - C_{0,e} \cdot e^{-\left(\frac{\emptyset}{V} + k_e\right)t}\right)}{Q + k_e \cdot V} \quad \text{eq. 3}$$

Where $C_{0,e}$ is the concentration of electron donor in the bioelectrochemical cell after spiking (in mmol L⁻¹). To be able to compare all tests, which are performed in at least triplicate, the concentration of electron donor was normalized ($\overline{C_e}$), according to:

$$\overline{C_e}(t) = \frac{C_e(t)}{C_{0,e}} = e^{-\left(\frac{\emptyset}{V} + k_e\right)t} + R_e^F \frac{\left(\frac{1}{C_{0,e}} - e^{-\left(\frac{\emptyset}{V} + k_e\right)t}\right)}{Q + k_e \cdot V} \quad \text{eq. 4}$$

The hypothesised increase of n-butyrate concentration following electron donor conversion could not be directly calculated. Therefore, instead, a normalized Δ concentration was determined, according to:

$$\overline{\Delta C_B} = \frac{C_B - C_B^{feed}}{C_B^{feed}} \quad \text{eq. 5}$$

Given the proposed model structure for the electron donor and experimental data, a non-linear least square parameter estimation routine was used to calibrate the model structure of which details are provided in the supplementary information.

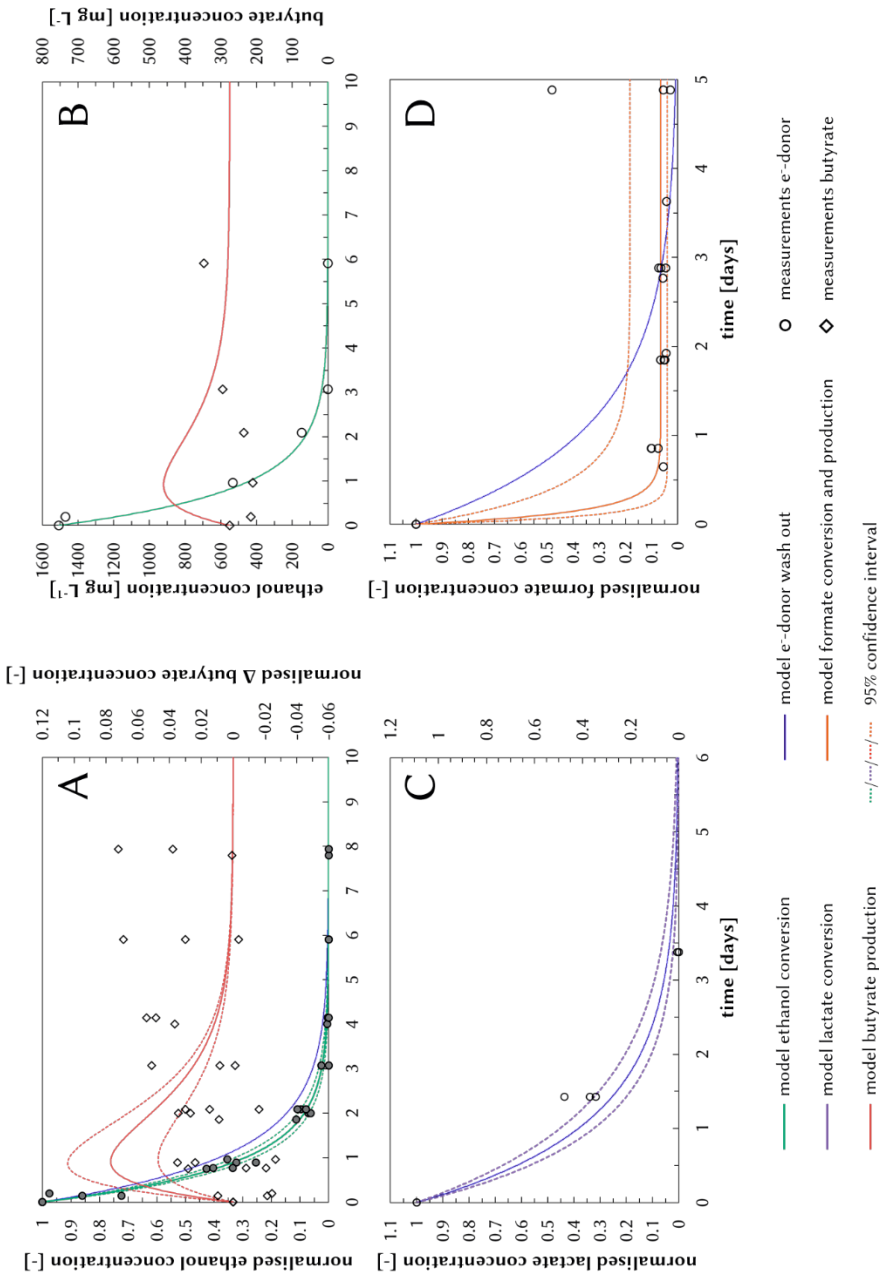


Figure 3.1: Spiking experiments – models (lines) and measurements (circles and diamonds) for the spiking of ethanol (A and B), lactate (C) and formate (D). A, C, and D show the normalised electron donor concentration over time. For the ethanol spikes the model indicated conversion of ethanol and could have been converted into n-butyrate. The resulting production of n-butyrate as a consequence of ethanol conversion was modelled and is plotted in A as Δ n-butyrate concentration and for one replicate as the resulting concentration (B). The lactate model resulted in such a small conversion rate, that the conversion model was not significantly different from the wash-out model shown in C. The conversion model for formate (D) includes formation.

Results & Discussion

Ethanol, lactate and formate were one by one spiked in bioelectrochemical chain elongation (BCE) reactors to verify the possible role in the production of nC₄. Subsequently, the concentrations of substrate and products were followed for several days (more than 3 HRTs). The spiked electron donor could have two fates upon introduction in the reactors: i) no conversion, and the electron donor was only washed out, or ii) the electron donor was converted and (partly) washed out. The experimental data were used to estimate kinetic conversions rates to verify whether the electron donors were converted.

Ethanol and lactate: no intermediates in nC₄ production in bioelectrochemical chain elongation

Given the proposed model structure, the parameter estimation routine was used to calibrate the models. As for ethanol and lactate the concentrations decreased below detection limit after several days after injection, it was assumed that the formation rates of both electron donors were not significant, i.e. both $R^F_{ethanol}$ and $R^F_{lactate}$ were 0. The resulting model fit with optimized parameters is shown in Figure 3.1. It was found that $k_{ethanol} = 0.27 \pm 0.06 \text{ h}^{-1}$ and $k_{lactate} = 0.00 \pm 0.08 \text{ h}^{-1}$.

Figure 3.1 shows the washout and conversion models for ethanol (A and B), and lactate (C). To compare all the spiking replicates of one electron donor, i.e. all ethanol spikes for example, the measured concentration ($C_{ethanol}$) was normalised ($\overline{C_e}$) to the initial concentration at t_0 ($C_{0,ethanol}$). In A and C these normalised concentrations are plotted for ethanol and lactate, both for the modelled concentrations as well as for the measurements.

For ethanol, the measurements lay within the 95% confidence range of the conversion model (Figure 3.1 A). This indicates that the spiked ethanol was converted in the reactors. Following the hypothesis that ethanol was converted into nC₄, the ethanol conversion rate was used to predict an nC₄ concentration change. For the stoichiometric ratio of ethanol conversion in n-butyrate, 5 : 6 was assumed based on the stoichiometry of acetate and ethanol in fermentative chain elongation.¹⁰⁷ To show the predicted nC₄ concentration in the reactor ($\overline{\Delta C_B}$) based on the conversion of ethanol per spike, the resulting concentration of nC₄ was calculated as well and compared to the actual measured concentration (Figure 3.1B and Figure S3.1). Clearly, the measurements of n-butyrate are not within the 95% confidence interval and do not show an increase after the spike. This indicates that the hypothesised conversion of ethanol into n-butyrate did not occur.

The estimated rate of lactate conversion was close to zero and therefore much smaller than the wash out rate ($\frac{1}{HRT}$; 0.96 h^{-1}). Hence, the model assuming

conversion for lactate is not significantly different than assuming wash out only (Figure 3.1 C). In combination with the 95% confidence interval, it is safe to conclude that lactate was not converted. The decrease in concentration can only be explained by wash out of the reactors.

Hence, these results demonstrate that both ethanol and lactate were no evident intermediates in the nC4 production.

Formate: competition for electrons

After more than 3HRTs after injection with formate, it was still detected in the reactor solution. The measured concentrations could not be explained by the washing out of the initially spiked amount, formate seemed to be formed as well. Hence, parameters were estimated using $R_e^F > 0$, resulting in $k_{\text{formate}} = 6.08 \pm 2.25 \text{ h}^{-1}$ and $R_e^F = 20.03 \pm 5.72 \text{ mmol L}^{-1} \text{ h}^{-1}$.

The wash out and the conversion model of formate are plotted in Figure 3.1D in which the normalised actual measured concentrations of formate ($\overline{C_e}$) are shown as well. The estimated conversion rate of formate is significantly higher than the wash out rate, indicating that formate was converted fast. This was backed up by two omitted spikes due to failing setups. The first sample (t_0) after introduction of the electron donor was taken 1-2 hours after injection to ensure homogeneity of the catholyte solution. In two measurement series after formate injections, the $t_{0,\text{formate}}$ concentrations were 1075 mg L^{-1} and 892 mg L^{-1} , compared to 523, 379, 419, and 394 mg L^{-1} for the other four series which were not impeded. Approximately 1200 mg L^{-1} should have been the resulting concentration in the reactor after spiking. These results support that formate is indeed converted fast.

Because there is no stoichiometric conversion of formate to n-butyrate directly known, the concentration of n-butyrate resulting from the formate could not be estimated and therefore is not visible in Figure 3.1D. Hence, the electron balance was used to evaluate where the spiked electron equivalents possibly went. In all replicates, after spiking formate, the acetate production rate increased, while the n-butyrate production rate dropped (Figure S3.2). Formate (HCOO^-) can reversibly be converted by formate hydrogenases (FDHs) into CO_2 , H^+ , and 2e^- , and therefore formate can also be regarded as soluble CO_2 and H_2 . In other BESs studies formate dehydrogenases were described to be excreted by microorganisms to facilitate electron uptake.^{142,144} The excretion of enzymes as FDHs in the biofilm matrix offers the explanation that formate was formed faster than it washed out, so that formate could be detected even after the spiked amount should have been washed out.

In the galvanostatic controlled cathodes not all supplied electrons were recovered in the organic products, i.e. the electron recovery was about 50% during non-spiking

periods (data not shown). This typically results in a continuous H₂ production, supported by the headspace gas composition analysis (data not shown). Therefore, H₂ was assumed not to be limiting the n-butyrate formation in the BCE reactors. Hence, the spiking of formate increased the soluble CO₂ concentration. The observed acetate production rate increase could therefore be explained by the conversion of the increased soluble CO₂ to acetate. This homoacetogenesis could under normal reactor operation conditions could occur as well, though it shows to be limited CO₂ supply which limited acetate formation and mostly acetate was elongated to n-butyrate. Alternatively, formate could directly have been used for the formation of acetate, since formate is the precursor of the methylgroup of acetate in *Clostridium sp.*¹⁴⁵ Presumably *Clostridium sp.* were present in the microbiome, in which case direct conversion to acetate could have taken place without enzymatic conversion into CO₂.

The observation that n-butyrate production was limited by the formate spike (Figure S3.2), indicates that the production of acetate competed with the production of n-butyrate for electrons. In case formate derived CO₂ was converted into acetate, H₂ or electrode derived electrons were the electron donor. The conversion of acetate to n-butyrate is most likely current driven¹²⁷ and in this could explain the acetate formation competition with n-butyrate production.

Conclusively, formate is simultaneously produced and converted fast in the BCE reactors. Most likely formate was converted into acetate. Nevertheless, formate did not increase the n-butyrate production from acetate.

High hydrogen partial pressure not necessary for bioelectrochemical chain elongation

To verify the postulated requirement for an elevated partial hydrogen headspace in the formation of nC₄,¹³¹ the headspace of three reactors was changed to continuously flushing with N₂. Before removing the gasbags, the headspace composition was 84.1 ± 5.1 % H₂ and 16.6 ± 3.4 % N₂. The concentration of n-butyrate after headspace change was compared with the concentration before (for details see Text S3.2). The difference between the average concentration with gasbag headspace and headspace flushing (Δ average) is smaller than the standard deviation for these averages (Δ standard deviation). Hence, it can be concluded that for these BCE reactors, the requirement for an elevated H₂ partial pressure in the headspace did not apply to our systems.

In the CO₂ to nC₆ BCE systems of Jourdin et al. (2018),¹⁴⁶ the catholyte was continuously flushed with a CO₂: N₂ gas mixture, signifying that H₂ could not build up in the headspace and was not required for BCE. Therefore, it can be postulated

in case the BCE is a biofilm-based process, there is no requirement for H_2 partial pressure in the headspace for product formation to occur.

Doubling the applied current doubled nC₄ production rate

Lastly, the influence of increasing the current on nC₄ production was investigated in two reactors. The ideal chain elongation ratio known of acetate to ethanol is 1 : 1.5.^{107,111} To supply the stoichiometrical ideal amount of electrons, this ideal ratio corresponds to an electron ratio of 8 to 18 ($= 1.5 \times 12 \text{ e}^-/\text{mol ethanol}$). When optimising the current to the acetate inflow rate ($30 \text{ mM} \times 2 \text{ ml h}^{-1}$), the ideal applied current would be 29 mA ($13.2 \text{ A m}^{-2} \text{ psa}$). After an initial period of 29 days, the current was increased from 15 mA to 29 mA (dashed lines in Figure 3.2, duplicate reactor in Figure S3.3). The current increase caused the nC₄ production rate to increase gradually and the acetate consumption rate to increase even more (Figure 3.2 A). After approximately 10 days the nC₄ production rate reached a plateau, indicating another steady state was reached. The steady state concentration of acetate was decreased two to three times, while the nC₄ concentration was doubled. Interestingly, the production rates increased gradually, indicating that the current did affect the conversion of acetate to nC₄ though the current was not kinetically limiting. The relatively slow increase (more than 3 HRT to stabilise) indicates that the biology needed to adapt to the changed circumstances. If the microorganisms would have been able to process the increased flux of electrons straight away, the nC₄ and acetate concentrations would reach steady state faster.

Next to nC₄ and acetate, also trace amounts (below 50 mg L^{-1}) of propionate (C₃) and n-caproate (nC₆) were detected before and after current increase. Though the concentrations of these compounds were so low, that the effect of increase in current on their production could not be evaluated.

The cathode potentials of the reactors were not significantly changed when the current was increased (Figure 3.2B). When averaging all the measured cathode potentials at 15 mA and compare them with the average at 29 mA, then the difference was 35 mV for reactor 1 and for the second 2 mV (Table S3.1). The observation that the cathode potentials did not change indicates that the (bio)electrocatalytic capacity of the biofilm was possibly well developed to divert electrons from the electrode surface.

After increasing the current, the electron recovery into organics decreased approximately 15 to 20 % for both reactors (Figure 3.2 C and Figure S3.3). The unrecovered electrons most likely ended up in biomass formation or more H_2 production. The gradual change in acetate and nC₄ concentrations supports the loss of electrons to biomass. Additionally, the gas production (data not shown) increased

in the days after the current increase, which confirms the increased H₂ production. Although more electrons were unrecovered after current increase, the percentage of nC₄ in the recovered electrons was higher. This is in correspondence with our previous study in which a higher applied current, more electrons were recovered in nC₄.¹²⁷

The experiments in this study show that it is highly unlikely that the bioelectrochemical production of nC₄ was limited by intermediate production of ethanol and lactate. The spiking of formate presumably increased the soluble CO₂ concentration and incited acetogenesis and not chain elongation. In that process it competed for electrons with acetate elongation to n-butyrate. Based on these soluble electron donor experiments it cannot fully be excluded that other soluble electron donors for chain elongation (like methanol^{118,126} or sugars¹⁴⁷ affect n-butyrate production.

The only electron donor tested to increase the nC₄ production, both in production rate as in percentage of electrons recovered in nC₄, was increase of current. Even though at this point it is still unclear whether electrons, or (bio)electrochemically induced H₂, formate or redox active molecules serve as the electron donor for microbial metabolism, these experiments demonstrate that the production of n-butyrate was current-driven. Also, thermodynamic calculations support the formation of n-butyrate from acetate either using electrode-derived electrons or hydrogen is both feasible (see Table S3.3). This finding holds promise for BCE as a waste valorisation technology using current driven electron donor which eliminates the need for exogenous soluble electron donors supply.

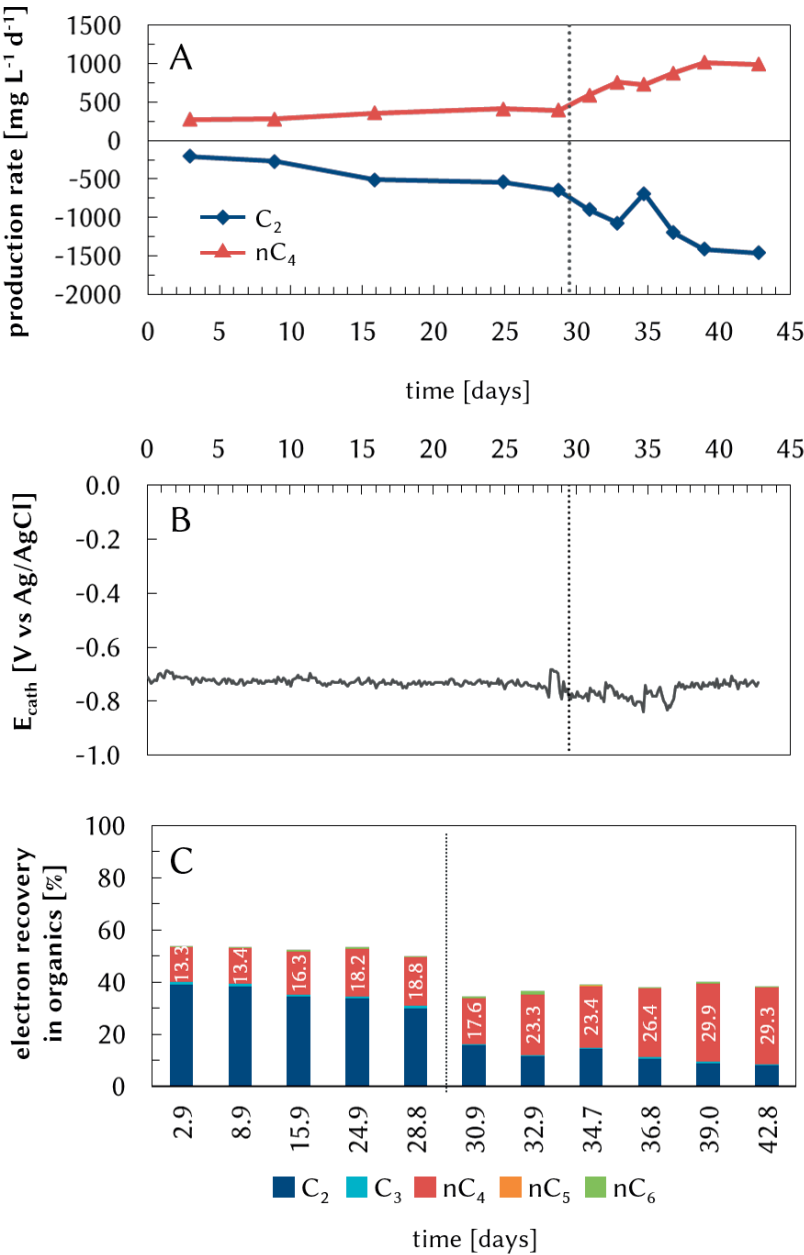


Figure 3.2: Data of increase of current experiments. A shows the production rate profiles of acetate (C₂) and n-butyrate (nC₄) over time. Dashed line indicates increase of the applied current. B shows the corresponding cathode potential and C shows the electron recovery in organic products.

Chapter 3 - Supplementary information

Text S1 – Non-linear least square parameter estimation for model structure calibration

The model parameter k_e^F , the conversion rate of electron donor towards n-butyrate (first order kinetics), was estimated via non-linear least square parameter estimation. The concentrations of electron donor over time after the spikes were used to estimate this parameter. When in the experiments it was found, that no electron donor was formed, i.e. \bar{C}_e at the end of the experimental run was below detection limit, R_e^F was assumed 0 when estimating the parameter. The unknown rate was estimated for the different electron donors with its corresponding standard deviation using the model described in the main text.

Unknown rate parameters in the kinetic model, represented by the parameter vector θ , are estimated using the experimental data. Via a least square routine, the estimated single-output gives:

$$\hat{\theta}_N = \arg \min_{\theta \in D} \sum_{k=1}^N \varepsilon(t_k | \theta)^2 \quad \text{eq. SI-3.1}$$

Where $\varepsilon(\cdot | \theta) = y(k) - \hat{y}(\cdot | \theta)$ is the output error at index k of time vector t , $y(k)$ the experimental normalized electron donor concentration at k , $\hat{y}(\cdot | \theta)$ the predicted electron donor concentration at k given estimate of θ ($\hat{\theta}$), D is the prior parameter domain. The error variance σ_ε^2 , a measure for the model fit, is given by:

$$\sigma_\varepsilon^2 = \frac{1}{N-p} \sum_{k=1}^N \varepsilon(t_k | \theta)^2 \quad \text{eq. SI-3.2}$$

with p the number of parameters.

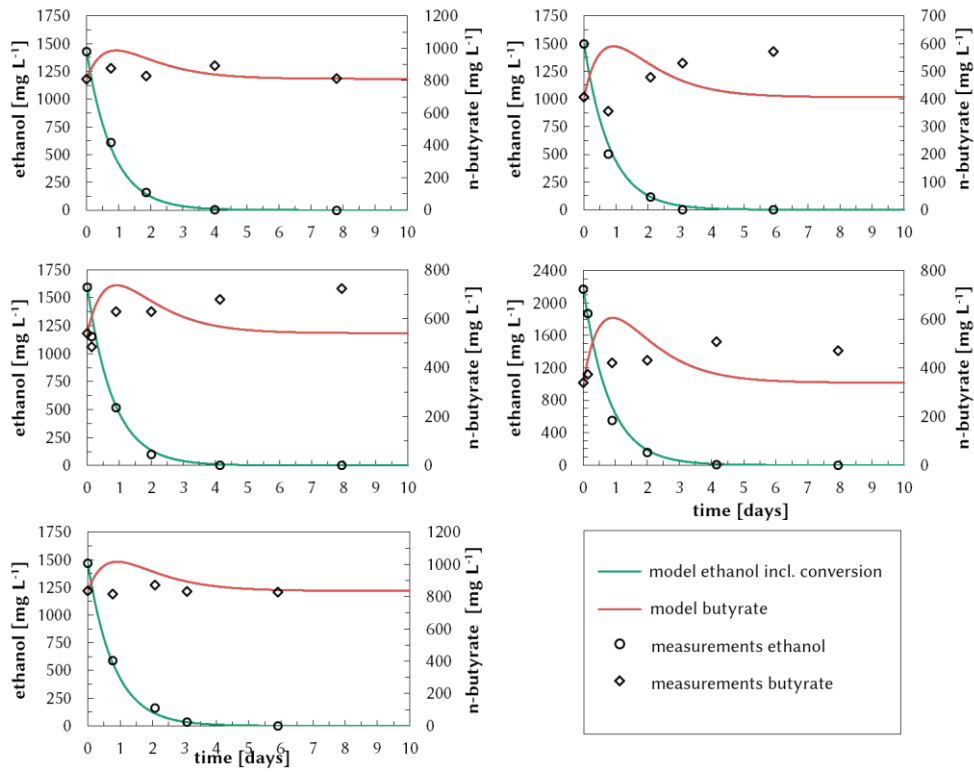


Figure S3.1: Concentrations ethanol and n-butyrate (conversion model) and measurements for each individual reactor.

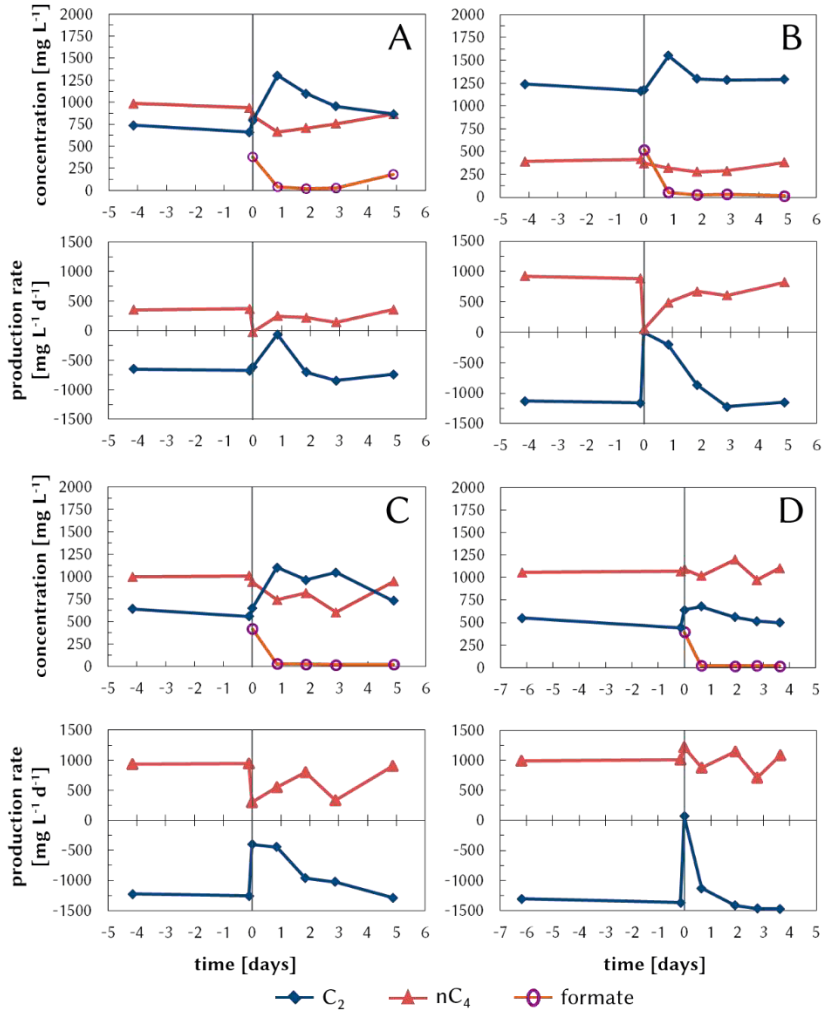


Figure S3.2: Individual spikes formate (A to D). Measured concentrations and calculated production rates of acetate (C_2) and n-butylate (nC_4). Formate was spiked at $t = 0$ d. Negative production rates indicate acetate consumption.

Text S2 – analysis on the effect of changing the headspace from gasbag to continuous N₂ sparging

n-Butyrate concentration measurements before and after change headspace in mg L⁻¹.

| | t [day] | Reactor 1 | Reactor 2 | Reactor 3 |
|-------------------------|---------|--------------------------|-----------|-----------|
| gas bag | -5.1 | 494.97 | 557.25 | 1197.33 |
| | -2.0 | 439.89 | 557.16 | 1121.46 |
| | -0.2 | 534.3 | 579.63 | 1097.52 |
| | 0.0 | <i>changed headspace</i> | | |
| N ₂ sparging | 0.9 | 563.7 | 582.69 | 1067.76 |
| | 1.8 | 489.99 | 600.36 | 1245.96 |
| | 4.8 | 432.93 | 479.55 | n.d. |
| | 5.8 | 544.32 | 606.75 | 1332.3 |
| | 6.8 | 446.49 | 506.97 | 1340.01 |

To analyse the effect, the average and standard deviations of the nC₄ concentrations were calculated of the measurements before and after change of headspace.

| | | Reactor 1 | Reactor 2 | Reactor 3 |
|-------------------------|----------------------|-----------|-----------|-----------|
| gasbag | average | 489.72 | 564.68 | 1138.77 |
| | standard deviation | 47.42 | 12.95 | 52.11 |
| N ₂ sparging | average | 495.49 | 555.26 | 1246.51 |
| | standard deviation | 57.84 | 58.10 | 126.56 |
| comparison | Δ average | -5.77 | 9.42 | -107.74 |
| | Δ standard deviation | 74.80 | 59.52 | 136.87 |

The comparison is calculated as the average gasbag minus average N₂, and the difference for the standard deviation is calculated as

$$\sqrt{(stdev_{gasbag})^2 + (stdev_{N_2})^2}$$

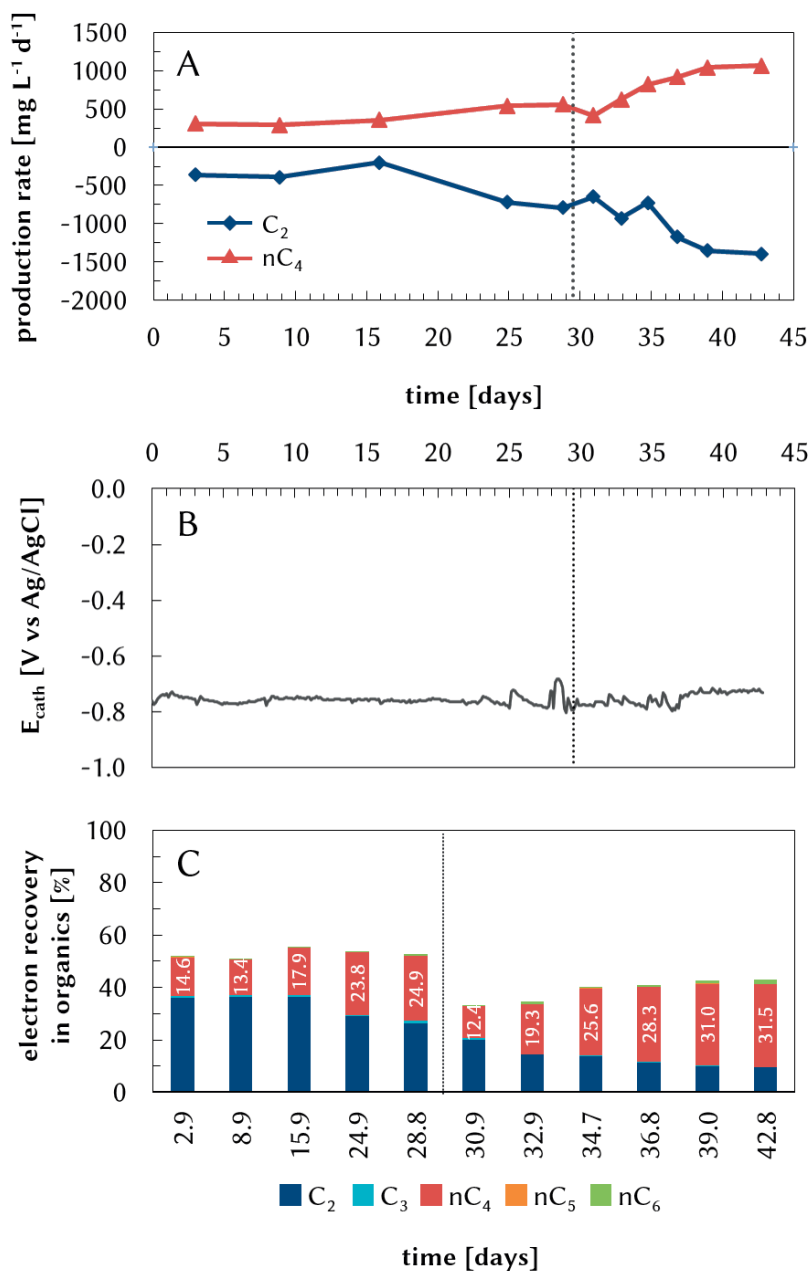


Figure S3.3: Data of increase of current experiments of the duplicate reactor. A shows the production rate profiles of acetate (C_2) and n-butyrate (nC_4) over time. Dashed line indicates the moment when the applied current was increased. B shows the corresponding cathode potential and C shows the electron recovery in organic products.

Table S3.1: averages and standard deviation of the cathode potential before and after current increase.

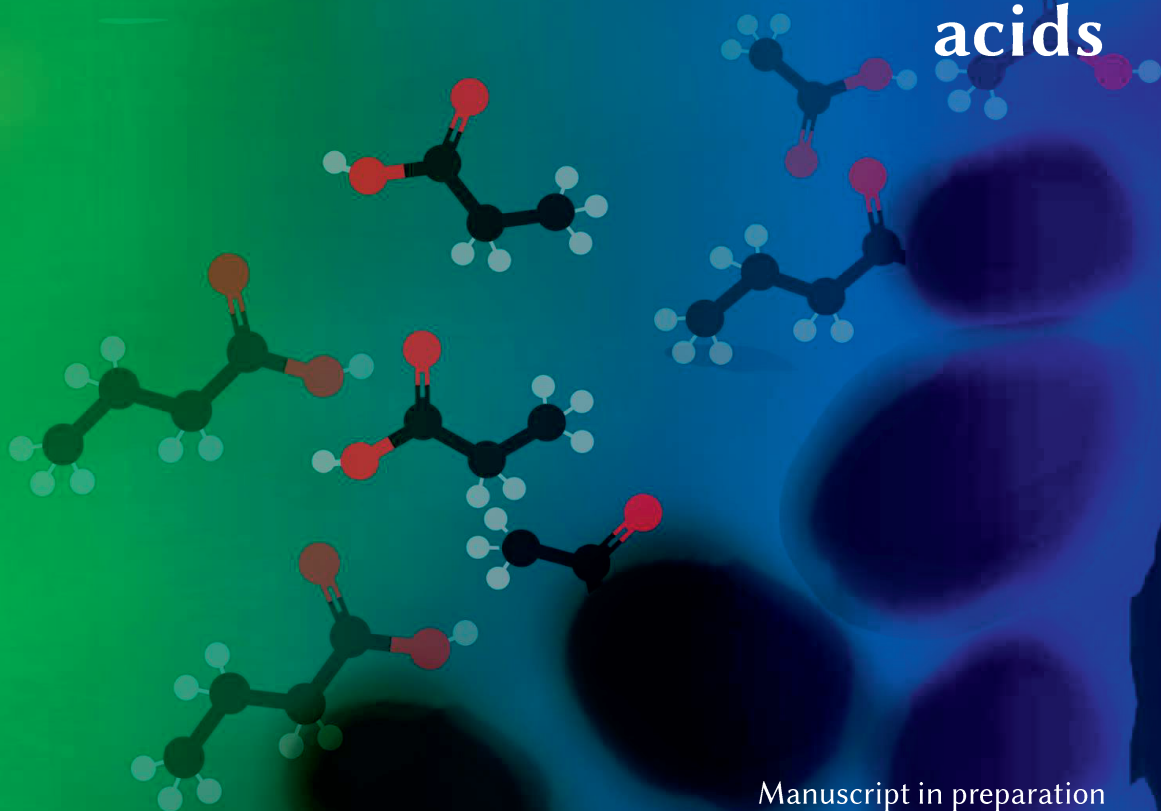
| | Reactor 1 | | Reactor 2 | |
|-----------------|---|----------|---|----------|
| Applied current | Average E_{cath} [V vs Ag/AgCl] | σ | Average E_{cath} [V vs Ag/AgCl] | σ |
| 15 mA | -0.728 | 0.030 | -0.751 | 0.024 |
| 29 mA | -0.763 | 0.028 | -0.753 | 0.024 |

Table S3.2: Standardised and reactor conditions used for thermodynamic calculations (Table S3.3 below). H_2 was assumed to be present at 1 bar as a result of continuous electron supply on the electrode.

| | Unit | Standar- -dised conditions | Reactor 1 | | Reactor 2 | | Reactor 3 | |
|----------------------|----------------|----------------------------------|-----------|--------|-----------|--------|-----------|--------|
| | | | 15mA | 29 mA | 15mA | 29 mA | 15mA | 29 mA |
| C_2 (aq) | mM | 1,000 | 11.2 | 7.8 | 17.0 | 9.5 | 18.9 | 8.2 |
| nC_4 (aq) | mM | 1,000 | 8.4 | 11.6 | 6.4 | 12.9 | 5.0 | 11.2 |
| Protons (pH) | 10-pH | 7.0 | 5.65 | 5.65 | 5.65 | 5.65 | 5.65 | 5.65 |
| H_2 (g) | Bar | 1 | 1 | 1 | 1 | 1 | 1 | 1 |
| E_{cathode} | (V vs. SHE) | -0.507 | -0.529 | -0.550 | -0.541 | -0.543 | -0.518 | -0.553 |
| Temperature | (K) | 298.15 | 303.15 | 303.15 | 303.15 | 303.15 | 303.15 | 303.15 |

Chapter 4

Bioelectrochemical chain elongation creates steering opportunity for selective production of odd-chain fatty acids



Manuscript in preparation
Raes, S.M.T., Jourdin, L., Buisman, C.J.N., Strik, D.P.B.T.B.

Abstract

Bioelectrochemical chain elongation (BCE) of short chain fatty acids (SCFA) was steered to high selective product formation efficiencies. n-Butyrate, n-valerate, n-caproate were in different experimental conditions formed from supplied SCFA and electrons by the cathode at respectively 94.1, 95.4 and 83.4 % carbon-based selectivity. These results were obtained by adjusting the supplied electron acceptor composition and studying the effects on product formation in triplicate continuous BCE reactors. Four different substrate feeding strategies were tested: I) acetate, II) acetate and propionate, III) acetate and n-butyrate, and IV) a mixture of acetate, propionate and n-butyrate. The reactor microbiomes adapted to the new feeding conditions within a few days. Remarkably, propionate elongation appeared to be preferred over acetate elongation. Propionate elongation resulted in highly selective formation of the odd-chain fatty acid n-valerate; this seems contradictory to ethanol chain elongation studies in which acetate is concurrently formed leading to straight fatty acids as by-products.

Introduction

The necessary reduction of the environmental footprint of fossil-based chemicals and liquid fuel precursors can be achieved by replacing them with biomass-derived ones. Organic residual streams are an alternative renewable feedstock that can contribute to the transition towards biobased chemicals. To convert organic feedstocks into intermediate chemicals, the carboxylate platform was suggested in which mixed microbial cultures hydrolyse and acidify (primary fermentation) residual organics to a mixture of short-chain fatty acids (SCFAs).³⁶ These SCFAs are valuable intermediate platform chemicals when separated, or used in a secondary (bio)conversion. Chain elongation is such a secondary fermentation, which produces medium chain fatty acids (MCFAs) from SCFAs and an electron donor.

So far, chain elongation bioreactor studies have focussed mainly on elongation of acetate towards n-caproate (C6 MCFA) with ethanol as electron donor.⁷⁹ Because of heterogeneity of primary fermentation broths, it is important to extent the knowledge on the metabolic capabilities of microbial communities to deal with varying feedstocks. Currently, there is only limited understanding on how open microbiomes respond to different substrates (electron acceptors) and/or mixtures of substrates.

In open culture studies, Grootcholten and co-workers supplied propionate (C3) as electron acceptor and ethanol as electron donor, producing a mixture of mainly n-valerate (nC5) and n-heptanoate (nC7).¹⁴⁸ The same compounds were used by Roghair et al, and were converted into mainly n-caproate and n-valerate.¹⁴⁹ An extensive study was performed by Coma et al. on the product diversity resulting from several combinations of electron donors and electron acceptors.¹²⁶ They showed ethanol and propanol as suitable electron donors for elongation of acetate, propionate, and n-butyrate as electron acceptors. However, the supply of mixtures of electron acceptors and the corresponding metabolic response are not systematically investigated yet.

In a recent assessment of the sustainability of n-caproate production by chain elongation of acetate with ethanol as electron donor, ethanol was identified to have the biggest environmental impact.¹²⁸ To reduce the impact of the process, recently electrons supplied by an electrode were demonstrated to be an attractive alternative electron donor for chain elongation,^{54,127,129} designating this as bioelectrochemical chain elongation (BCE).

To investigate the potential for BCE as organic waste valorisation technology, here the substrate spectrum was extended beyond acetate. In this study continuous BCE reactors were sequentially supplied with I) acetate, II) acetate and propionate,

III) acetate and n-butyrate, and IV) a mixture of acetate, propionate and n-butyrate. The resulting effects on SCFA utilisation and product formation were studied. Hereby we present the first insights on using mixed organic acids as substrate for BCE.

Materials and Methods

Reactor set-up and experiment

Three identical bioelectrochemical reactors were operated for these experiments of which the reactor setup was described previously in detail.¹²⁷ The reactors were running for over 300 days, of which the last 44 days of two reactors were presented in a previous study (Chapter 3). In short, three already running continuous reactors were operated at 30°C, pH 5.5 ± 0.3 (by addition of 1 M NaOH or 0.5 M H₃PO₄), HRT of 25 h and applied with 29 mA (18.1 A m² projected surface area, psa was 16 cm²). The reactors (50 ml catholyte volume) were fed with synthetic medium as described in Chapter 3. During the study the electron acceptor in the medium was varied from only acetate, to propionate and/or n-butyrate (nC₄, Table 4.1). Acetate was not excluded from the medium to sustain biomass growth, as it is required for protein synthesis of the well-known chain elongator *C. kluyveri*.¹⁵⁰ The total extracellular concentration of acids in phase II, III, and IV was kept constant (60 mM). Analytical procedures for fatty acids (C₂-C₈) and alcohols (C₁ to C₆) were the same as described before.¹²⁹

Table 4.1: Overview of the experimental phases and the supplied electron acceptors in each phase.

| Phase | Days after start of experiment | Influent concentration [mM] | | | Influent concentration [mMC] | | |
|-------|--------------------------------|-----------------------------|----------------|-----------------|------------------------------|----------------|-----------------|
| | | C ₂ | C ₃ | nC ₄ | C ₂ | C ₃ | nC ₄ |
| I | Day 1 to day 10 | 30 | - | - | 60 | - | - |
| II | Day 11 to day 42 | 30 | 30 | - | 60 | 90 | - |
| II | Day 43 to day 85 | 30 | - | 30 | 60 | - | 120 |
| IV | Day 86 to day 95 | 20 | 20 | 20 | 40 | 60 | 80 |

Calculations

The volumetric production rate of compound i was derived via mass balance because fluctuations in concentrations occurred, and consequently no steady state assumption was made for these calculations:

Production_{i,t} = accumulation_{i,t} + out_{i,t} - in_{i,t}

$$p_{i,t} = \left[\frac{V_{cat}}{\Delta t} (C_{i,t} - C_{i,t-1}) + Q \frac{(C_{i,t} + C_{i,t-1})}{2} - Q C_{in,i} \right] n_{e,i} \quad \text{eq. 1}$$

where subscript *i* refers to the product (that is, all organics which were quantified and mentioned in the section analyses), *p_{i,t}* the production of product (mol e⁻ d⁻¹), *V_{cath}* the total catholyte volume (0.050 L), *C_i* the concentration of product (mol L⁻¹), *Q* the influent and effluent flow rate (L d⁻¹), Δt the time between sampling time *t* and *t*-1 (d), *C_{in,i}* the concentration of product *i* in the influent (mol L⁻¹), and *n_{e,i}* the number of electrons per mole of product. To express the production rate as mol carbon per day, instead of *n_{e,i}* the number of carbons per mole of product is used (*n_{c,i}*).

Carbon and electron recovery represent the fraction of either carbon atoms or electrons which was recovered in the identified products compared to the total carbon atoms or electrons supplied to the system in that time period. The calculations for these recoveries are the same as described previously.¹²⁷ Because acetate, propionate and n-butyrate in the influent also contain electrons and carbons, these were also incorporated as such.

Formation selectivity is here defined based on carbon basis and is calculated via:

Selectivity [%] = product formation rate (mMC d⁻¹) / total substrate consumption rate (mMC d⁻¹).

To compare the formation selectivity to other studies, it was also expressed on an electron basis according to Roghair et al. (2018).¹⁴⁹

Results and discussion

Figure 4.1 shows the concentration and production rate profiles over time of one of the triplicate reactors. The data for the other two reactors can be found in Figure S4.1. Unless stated otherwise, the replicate reactors exhibited similar behaviour.

Supply of acetate and propionate promotes formation of n-valerate over n-butyrate

In phase I when only acetate was supplied as substrate for BCE, n-butyrate (nC4) was the only identified chain elongation product (Figure 4.1 B and C). The nC4 concentration was 40 mMC (0.9 g L⁻¹), and was produced at 39.7 mMC d⁻¹ with a carbon selectivity of 94 % (Table 4.3; selectivity data for other two reactors can be found in Supplementary info). From here selectivity is carbon based unless stated otherwise. Directly after adding propionate (start phase II – day 10), it was consumed and valerate (nC5) production was initiated. The nC5 concentration

reached a maximum concentration of 60.6 mMC (1.2 g L^{-1}) at day 24, at a production rate of 57.5 mMC d^{-1} with a remarkable high 73.8 % formation selectivity (Table 4.3 Table 4.). Whilst, propionate was consumed at 40.5 mMC d^{-1} . Apparently, the biomass was capable to change its metabolism from acetate elongation to propionate elongation without delay. These observations are in line with the experiments of Grootcholten et al. (2013), who also showed nC5 production directly after propionate addition.¹⁴⁸

Besides nC5, also nC4 was produced but at lower rates compared to phase I (14.1 mMC d^{-1} vs. 39.7 mMC d^{-1}). Although the exact mechanism of acetate conversion in BCE systems is not yet unravelled, it can be hypothesised based on the consumed substrates and formed compounds, that acetate was not only consumed for propionate elongation, but was partly elongated to nC4 as well (Table 4.4 reaction 2 and 1 respectively). This co-production of nC4 was observed before in open chain elongation reactors when fed with propionate and ethanol.^{126,148,149} Additionally, propanol formation was also observed in these previous studies, presumably as a result of propionate reduction.^{110,126,149} Here, we did not detect any alcohol formation, which was in agreement with previous BCE studies^{127,129} and Chapter 3. In phase II also traces of n-caproate were measured, of which the maximal concentration was 2.1 mMC (0.040 g L^{-1}) corresponding to a 2.5% selectivity.

Interestingly, in this phase the consumption patterns of acetate and propionate were highly similar (Figure 4.1 C). Similar consumption in mMC translates to 1.5 times more consumption of propionate than acetate based on molar concentrations. The molar stoichiometric reactions (Table 4.4, reaction 2) correspond to a carbon-molar stoichiometry for nC5 production of 0.4 molC acetate to 0.6 molC propionate resulting in 1 molC of nC5. Stoichiometric analysis of the consumption and production rates in this phase is shown in Table 4.2. The conversion of both acetate to nC4 and the production of nC5 from acetate and propionate accounts on day 24 for 90.4 % and 85.3 % for the acetate and propionate consumption respectively. This stoichiometric analysis fits well with the formation of nC5 and nC4 and the observed consumption of acetate and propionate.

The addition of propionate to the medium did not significantly affect the cathode potential (Figure S4.3). Even though in this phase more electrons were supplied via the influent by addition of 60 mMC propionate, the electron recovery increased in phase II from 38 % to 65 % (Figure 4.2). This electron recovery included as well the electrons supplied by the substrates in the influent.

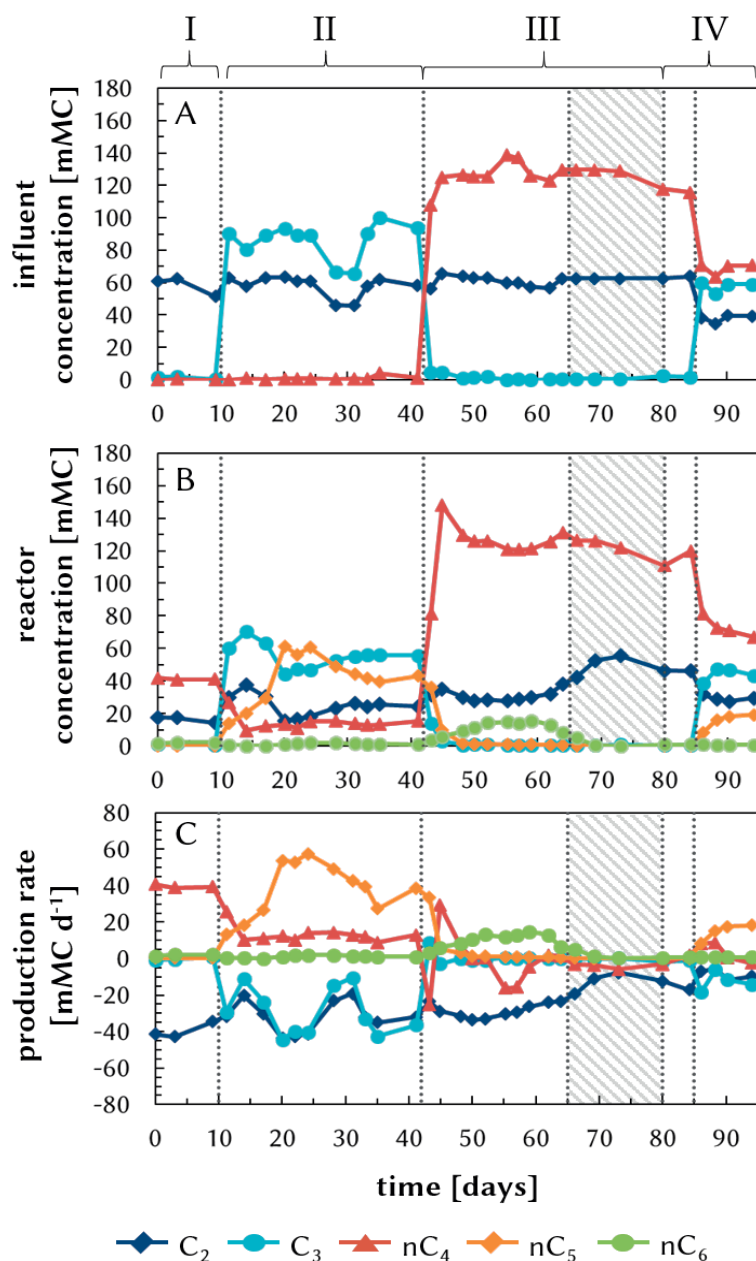


Figure 4.1: Concentration of organic acids in the influent (A) and in the reactor (B) over time and the corresponding production rate (C). Reactor was operated at 18.1 A m^{-2} . Roman numbers indicate different feeding strategies as indicated in the text: I) 30 mM acetate, II) 30 mM acetate + 30 mM propionate, III) 30 mM acetate + 30 mM n-butyrate, IV) 20 mM acetate + 20 mM propionate + 20 mM n-butyrate. Shaded area in phase III indicates the amperostatic control was impaired.

Table 4.2: Production rates at day 24, when nC5 production was the highest [all in mMC d⁻¹]. Last three columns represent the percentage of consumed C2 or C3 which was converted to the products nC4 or nC5. Reactor was applied with 18.1 A m⁻² and at that moment fed with 30 mM acetate and 30 mM propionate in the influent.

| Day | Production rate [mMC d ⁻¹] | | | | | Substrate conversion | | |
|-----|--|----------------|-----------------|-----------------|-----------------|------------------------------------|-----------------------------------|------------------------------------|
| | C ₂ | C ₃ | nC ₄ | nC ₅ | nC ₆ | %C ₂ to nC ₄ | %C ₂ to C ₅ | %C ₃ to nC ₅ |
| 24 | -41.1 | -40.5 | 14.1 | 57.5 | 2.0 | 34.4 | 56.0 | 85.3 |

Supply of n-butyrate and acetate steers to more selective n-caproate formation

In phase III nC4 (~120 mMC) was co-supplied with acetate to the reactors starting on day 43 (Figure 4.1 A). Upon the change of medium, propionate and nC5 were washed out of the reactor. As a result of less acetate consumption, the acetate concentration in the reactor increased in the first 5 days of this third phase. The nC4 concentration was for the first days higher than the influent concentration, signifying that conversion of acetate to nC4 occurred at a higher rate than nC4 was consumed. After ~10 days a stable n-caproate (nC6) production was observed. The maximum nC6 concentration was 15.8 mMC (0.3 g L⁻¹), at a production rate of 13.3 mMC d⁻¹ and formation selectivity of 83.4 %. During nC6 production, the nC4 consumption rate was fluctuating around 0 mMC d⁻¹. Because nC4 was supplied via the influent, this value means that nC4 was consumed and produced at a similar rate, resulting in a net consumption rate of 0 mMC d⁻¹. Compared to phase I when solely acetate was supplied, the co-supply of nC4 steered to more selective formation of nC6 (from 4.6 % to 83.4 %).

Comparing the nC4 production in phase I to the nC6 production in phase III, 39.7 mMC d⁻¹ compared to 13.3 mMC d⁻¹, the elongation rate decreased with increasing chain length. This is in agreement with previous studies where the production rate of longer chain FAs was slower than of shorter ones.^{114,148}

Although the precise chain elongation mechanism remains hypothetical, possibly simultaneously nC4 was produced from acetate elongation as well as nC4 was elongated towards nC6 (Table 4.4 reaction 1 and 4 respectively). Alternatively, it could be hypothesised that acetate was directly elongated to n-caproate (Table 4.4 reaction 3). In both the possible reactions (reactions 3 and 4), the origin of 1 molC of nC6 can be 1 molC of acetate or 0.33 molC acetate and 0.67 molC nC4. The elongation of acetate to nC4 has also a 1 molC acetate to 1 molC of nC4, so based on stoichiometric analysis the exact elongation mechanism could not be determined in this study.

Table 4.3: Formation selectivity of bioelectrochemical chain elongation to products during the four experimental phases. Values presented are averages and standard deviations of the last three values per phase, except for phase IV where the last two datapoints were averaged (indicated with *).

| Phase | Selectivity <i>carbon</i> based [%] | | | Selectivity <i>electron</i> based [%] | | |
|-------|-------------------------------------|------------|------------|---------------------------------------|------------|------------|
| | nC4 | nC5 | nC6 | nC4 | nC5 | nC6 |
| I | 94.1 ± 0.3 | 0.7 ± 0.1 | 4.6 ± 0.9 | 93.8 ± 1.7 | 0.8 ± 0.1 | 4.9 ± 1.0 |
| II | 23.7 ± 0.9 | 73.8 ± 0.8 | 2.5 ± 0.5 | 23.0 ± 0.9 | 74.4 ± 0.8 | 2.6 ± 0.6 |
| III | 14.5 ± 2.7 | 5.8 ± 0.5 | 83.4 ± 7.4 | 13.8 ± 2.6 | 5.7 ± 0.5 | 84.1 ± 7.2 |
| IV* | - | 95.4 ± 1.9 | 4.6 ± 0.1 | - | 95.3 ± 1.9 | 4.7 ± 0.1 |

n-Caproate production was sustained until a period where amperostatic control was twice temporary impaired (shaded area in Figure 4.1 and Figure 4.2). As a consequence of two short periods of no applied current (day 65.5 till 66; day 70 till day 72), protons from the acid anolyte (pH 1.5 to 2.0) could diffuse through the membrane to the catholyte. These technical issues led to a ceasing acetate consumption and as a consequence at day 70 the acetate concentration in the reactor was similar to the influent concentration. Together with the ceased acetate consumption, the associated nC4 and nC6 production were ceased as well. At day 72 the amperostatic control was re-established, and after a week (from day 80) the elongation process had started again. At day 84 the substrate in the influent was changed to a mixture of acetate, propionate and nC4 to investigate the effect of a mixture on the product spectrum.

Electron equivalent supply by electrode steers towards selective odd-chain fatty acid production

In phase IV the three electron acceptors were supplied in a molar ratio of 1 to 1 to 1. Upon re-addition of propionate in the reactors after 41 days feeding on nC4 and acetate, directly propionate was consumed and nC5 production commenced (Figure 4.1, phase IV). The nC5 concentration at the end of the experiment reached 19.3 mMC (0.4 g L⁻¹). The acetate concentration in the reactor was decreased again to concentrations lower than the influent, signifying its consumption. n-Caproate production was not re-established before the end of the experimental period.

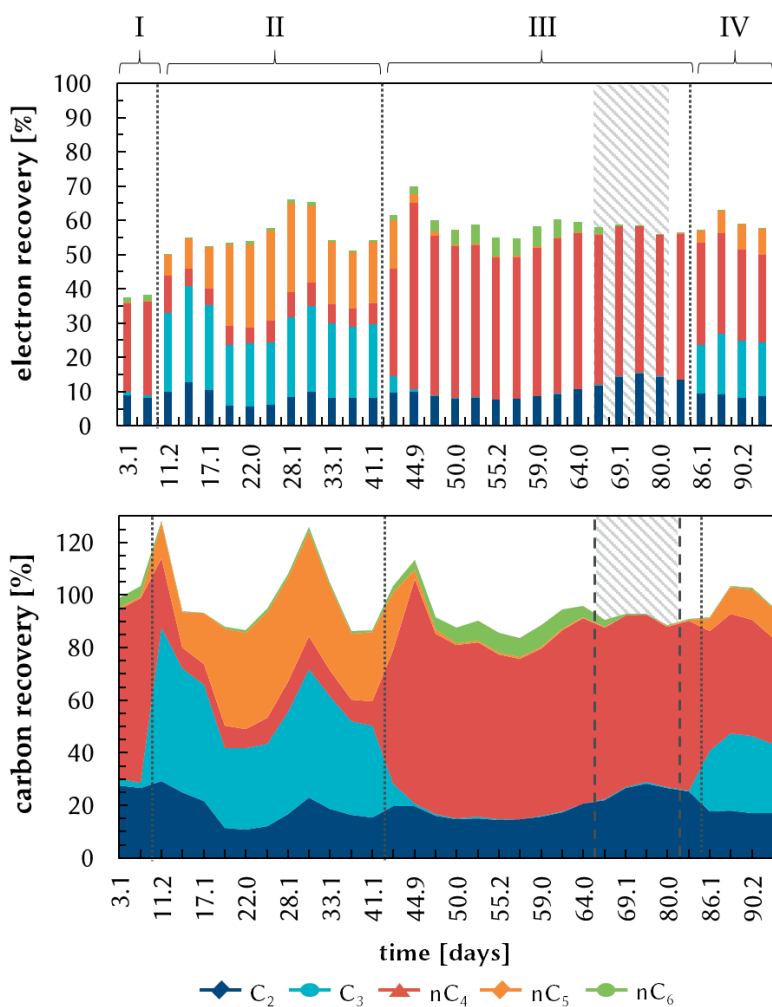


Figure 4.2 Electron recovery and carbon recovery over time.

This last phase in which a mixture of three SCFAs was fed to BCE reactors resulted in a highly selective nC5 production. n-Valerate was produced at a rate of 18.3 mMC d⁻¹ at a selectivity of 95.4%. Propionate was consumed at 14 mMC d⁻¹. Both the propionate consumption and the nC5 production in phase IV were approximately three times lower than in phase II. Stoichiometric analysis showed that 74.7 % and 77.8 % of respectively the acetate and propionate consumption could be explained by nC5 production.

In open chain elongation reactors where propionate and ethanol were fed, the selectivity towards n-valerate and n-heptanoate production together was maximally 56 %.¹⁴⁹ Interestingly, stoichiometric analysis of data of Roghair et al., similar

portions of the propionate consumption accounted for the nC5 production, i.e. 73-79 % of the propionate consumption was used for nC5 production. Although such stoichiometrics were not systematically studied here and by Roghair et al., these calculations might indicate a similar odd-chain substrate utilisation mechanism for chain elongation unrelated to electron donor supply.

When using ethanol, the selectivity towards odd-chain fatty acids (nC5 and nC7) could not be improved further due to ethanol oxidation and subsequent butyrate and caproate production (26.9 % selectivity towards nC4 and nC6).¹⁴⁹ Similar loss of selectivity towards odd-chain fatty acids was observed by Grootcholten et al., where nC5 selectivity was maximally 39% (electron based).¹⁴⁸ In the reverse β -oxidation pathway, 6 moles of ethanol are oxidised to 5 moles of acetyl-CoA and 1 mole of acetate.⁷⁹ Therefore, when applying ethanol as electron donor, even-chain fatty acid production cannot be prevented and decreases the selectivity towards odd-chain products. Ethanol oxidation in the reverse β -oxidation generates reducing power in the form of NADH to elongate a carboxylate with two carbon atoms. The observations here in this study indicate that an electrode can supply the chain elongation process with reducing equivalents without the production of acetate. Therefore, the usage of an electrode for the chain elongation process might be beneficial when high selectivities towards odd-chain products is required.

Additionally Roghair et al. posed the hypothesis that acetate and propionate compete for the same enzyme system in chain elongating microorganisms, and that this enzyme system could have a higher affinity for acetate.¹⁴⁹ Presuming similar dominant microbial metabolic pathways in our microbiome, the results obtained in this study indicate a contradiction of Roghair et al. Here propionate elongation appeared to be preferred over acetate elongation in phase II and in phase IV. The addition of propionate to the medium from phase I to phase II, showed that the microbiome was capable of utilising both substrates, which is in accordance to literature.^{114,126,148} Assuming the same microbes to elongate acetate as well as propionate, the enzyme affinity hypothesis does not explain the propionate preference observed here. A recent open microbiome chain elongation study showed that not the reverse β -oxidation pathway played a role in the production of MCFAs, but another pathway: the fatty acid biosynthesis (FAB) pathway.¹⁵¹ In that study ethanol and acetate were supplied in a fermentative batch CE reaction, producing a mixture of propionate, nC4, nC5 and nC6. Based on metagenomic and metatranscriptomic analysis the authors demonstrated that the FAB was more active in the chain elongation to n-caproate than the reverse β -oxidation pathway. Even though the present study was not designed to elucidate the exact chain elongation

pathways, together with the study of Han et al.¹⁵¹ it emphasises that the CE pathways involved are yet insufficiently characterised.

Thermodynamics favouring electrons as electron donor for chain elongation

Step by step progress is being made to elucidate how exactly electrodes are used as electron donor for microbial metabolism in biocathode processes, e.g. via (bio)electrochemically induced H₂ or other redox active molecules.^{152,153} In the BCE systems studied in this thesis, most likely intermediary formation of known electron donors, i.e. ethanol and lactate, do not play a role (Chapter 3). Therefore, direct electron transfer – direct electrically contact of microbial cell with the electrode – or mediated electron transfer mechanisms via H₂ or formate are most likely driving the BCE production. However, to examine whether H₂ or electrons could indeed serve as electron donor for the chain elongation reactions, thermodynamic calculations were performed (Table 4.4). The Gibbs free energy of the presumed elongation reaction in every experimental phase was calculated with either H₂ or electrons as electron donor.

All the included chain elongation reactions (1a to 4b, Table 4.4) showed to be thermodynamically feasible, which seems to contradict the kinetic study of Gonzalez-Cabaleiro.¹⁰⁹ The study of Gonzalez-Cabaleiro and co-workers modelled the described metabolic pathway for acetate elongation to n-butyrate with H₂ as electron donor. Their metabolic model included a threshold energy yield needed to transport protons across the membrane and subsequently produce ATP. H₂ could not achieve enough energy to support the needed proton gradient. Therefore they concluded that H₂ itself could not serve as electron donor. However, in electrode driven systems, such as BCE, it is not yet understood how energy is conserved by the microorganisms, nor if this happens via the same mechanisms as in fermentative conditions with a soluble electron donor. The thermodynamic calculation here thus demonstrates only the feasibility of certain potential pathways, of which the exact steps need to be elucidated yet.

Interestingly, electron driven reactions (all reactions b) yield a higher energy gain compared to H₂ driven ones (all reactions a). Which is in a sense logical, as in these reactions no ΔG^0 for protons and H₂ were incorporated. Therefore, there is a clear energetic benefit of using an electrode as electron donor for microbial metabolism instead of H₂.

Acetate elongation towards n-butyrate in phase I (reaction 1, Table 4.4) yield similar energy gains compared to propionate elongation in phase II (reaction 2, Table 4.4) regardless of the electron donor employed. The Gibbs free energies for these

reactions (1 and 2) were similar as well in phase IV when the three SCFAs were simultaneously supplied. The observed preference for propionate elongation over acetate elongation during phase IV, can thus not be explained by thermodynamics, but is likely related to enzyme specificity and/or bioenergetics.

n-Caproate formation can occur via solely acetate elongation (reaction 3, Table 4.4) or directly via n-butyrate (reaction 4, Table 4.4). The energy gain for the hypothesised reaction of solely acetate towards caproate yields the most energy. Even though this theoretical higher energy gain, in phase IV mainly n-valerate was produced. This might indicate that direct caproate formation from acetate (reaction 3) did not occur. Alternatively, the energy yield of reaction 4 during phase IV is slightly higher than reaction 1 and reaction 2. In contrast to the observed n-valerate production preference in the last experimental phase, caproate formation via reaction 4 is thermodynamically more favourable.

Here we report on the bioelectrochemical chain elongation of SCFAs, which led to highly selective production of n-valerate when propionate was supplied as substrate together with acetate. The observed preference for propionate elongation over both n-butyrate formation or caproate formation is in contrast to fermentative chain elongation studies. Further research in which mixtures of SCFAs derived from real fermentation broths, could validate whether these curious preferences occur as well, and whether electrodes could be employed to steer chain elongation towards desired chemicals.

Table 4.4: Thermodynamic calculations of potential (bioelectrochemical) chain elongation reactions using either hydrogen or electrons as electron donor. Gibbs free energy of all reactions is given under standardised (indicated with ¹) and reactor conditions. For electron-based reactions, cathode potentials are reported as well under standardised (Ecat¹) and reactor (Ecat) conditions. For these thermodynamic calculation the methods described in ⁹¹ and ²⁸⁷ were followed. Reactor conditions and Gibbs free energies of formations which are used for these calculations are supplied in

| Nr | | | Description | Catabolic rection | Standardised conditions* | | | | Experimental phase | | | | | | | |
|----|---|--|-------------|-------------------|---------------------------|---|------------------------------|------------------------------|------------------------|---|---|---|------|--|--|--|
| | | | | | I | | II | | III | | IV | | | | | |
| | | | | | kJ reaction ⁻¹ | H ₂ ⁻¹ or kJ (2e ⁻) ⁻¹ | ΔG _r ¹ | ΔG _r ¹ | Ecat ¹ Ecat | ΔG _r ¹ Ecat ¹ Ecat | ΔG _r ¹ Ecat ¹ Ecat | ΔG _r ¹ Ecat ¹ Ecat | | | | |
| 1a | n-butyrate formation from acetate and hydrogen | $2CH_3COO^- + H^+ + 2H_2 \rightarrow CH_3(CH_2)_2COO^- + 2H_2O$ | -48 | -24 | -41 | n.a. | -46 | n.a. | -43 | n.a. | -42 | n.a. | n.a. | | | |
| 1b | n-butyrate formation from acetate and electrons | $2CH_3COO^- + 5H^+ + 4e^- \rightarrow CH_3(CH_2)_2COO^- + 2H_2O$ | -80 | -40 | -112 (-0.534) | -0.243 (-0.534) | -123 (-0.549) | -0.231 (-0.549) | -110 (-0.524) | -0.238 (-0.524) | -103 (-0.507) | -0.239 (-0.507) | | | | |
| 2a | n-valerate formation from acetate, propionate and hydrogen | $2CH_3COO^- + C_3H_5O_2^- + 2H_2 + H^+ \rightarrow C_5H_9O_2^- + 2H_2O$ | -48 | -24 | n.a. | n.a. | -45 | n.a. | n.a. | n.a. | -46 | n.a. | n.a. | | | |
| 2b | n-valerate formation from acetate, propionate and electrons | $2CH_3COO^- + C_3H_5O_2^- + 5H^+ + 4e^- \rightarrow C_5H_9O_2^- + 2H_2O$ | -80 | -40 | n.a. | n.a. | -122 (-0.549) | -0.234 (-0.549) | n.a. | n.a. | -107 (-0.507) | -0.299 (-0.507) | | | | |
| 3a | n-caproate formation from acetate and hydrogen | $3CH_3COO^- + 2H^+ + 4H_2 \rightarrow CH_3(CH_2)_4COO^- + 4H_2O$ | -96 | -24 | -92 | n.a. | -97 | n.a. | -93 | n.a. | -97 | n.a. | n.a. | | | |
| 3b | n-caproate formation from acetate and electrons | $3CH_3COO^- + 10H^+ + 8e^- \rightarrow CH_3(CH_2)_4COO^- + 4H_2O$ | -160 | -40 | -235 (-0.534) | -0.230 (-0.534) | -235 (-0.549) | -0.245 (-0.549) | -211 (-0.524) | -0.251 (-0.524) | -202 (-0.507) | -0.245 (-0.507) | | | | |
| 4a | n-caproate production from acetate, n0butyrate and hydrogen | $C_4H_7O_2^- + CH_3COO^- + H^+ + 2H_2 \rightarrow C_6H_7O_2^- + 2H_2O$ | -48 | -24 | -51 | n.a. | -52 | n.a. | -50 | n.a. | -55 | n.a. | n.a. | | | |
| 4b | n-caproate formation from acetate, n-butyrate and electrons | $C_4H_7O_2^- + CH_3COO^- + 5H^+ + 4e^- \rightarrow C_6H_7O_2^- + 2H_2O$ | -80 | -40 | -122 (-0.534) | -0.208 (-0.534) | -129 (-0.549) | -0.215 (-0.549) | -118 (-0.524) | -0.218 (-0.524) | -123 (-0.507) | -0.206 (-0.507) | | | | |

¹ indicates value that is calculated using standardised conditions.

* standardised conditions: pH 7, 1 M of soluble compounds, 1 bar for gasses. However, for reactions using electrons as electron donor, no ΔG_r⁰(25°C) are reported in literature. Therefore, -0.507 V vs NHE was used for these thermodynamic calculations, and was chosen because this represents the cathode potentials in the BCE systems here. For that reason the term ‘standardised’ instead of standard was applied.

Chapter 4 – Supplementary information

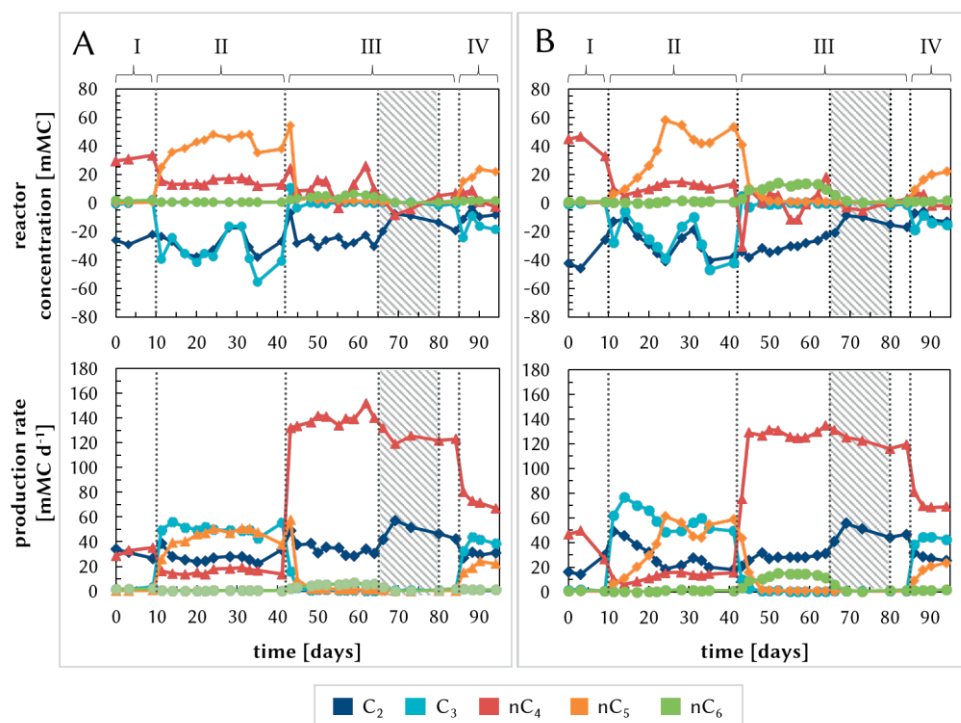


Figure S4.1: concentration and production rate of organic acids in the duplicate and triplicate reactor. Roman numbers indicate different feeding strategies. I: 30 mM acetate, II: 30 mM acetate + 30 mM propionate, III: 30 mM acetate + 30 mM n-butyrate, IV: 20 mM acetate + 20 mM propionate + 20 mM n-butyrate. Shaded area indicates temporary amperostatic impairment.

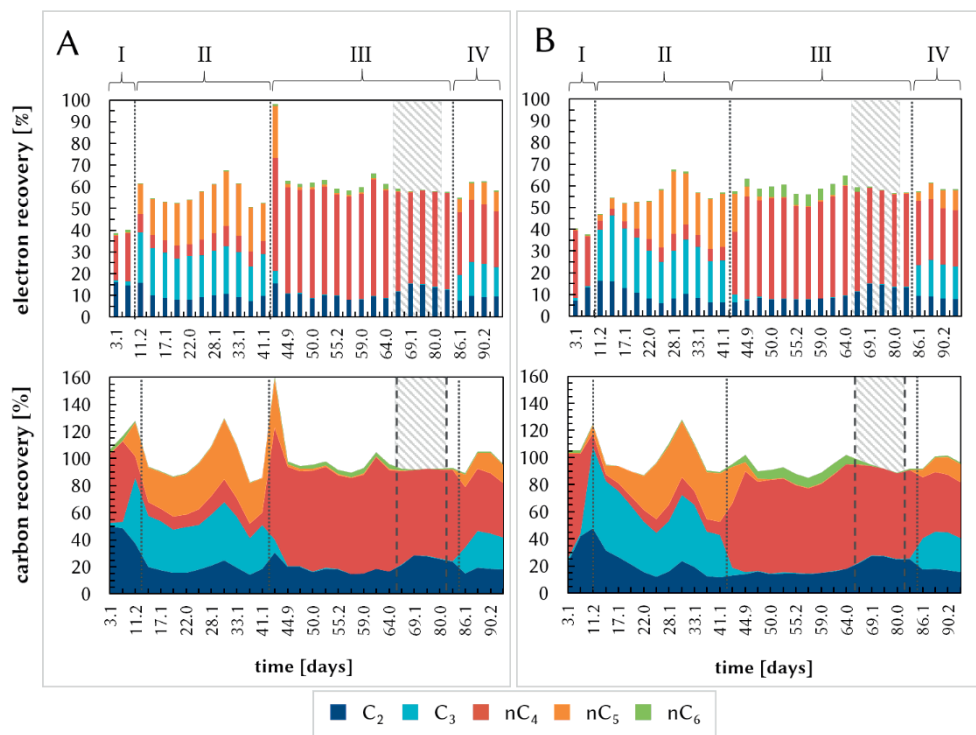


Figure S4.2: Electron recovery and carbon recovery of duplicate and triplicate reactor.

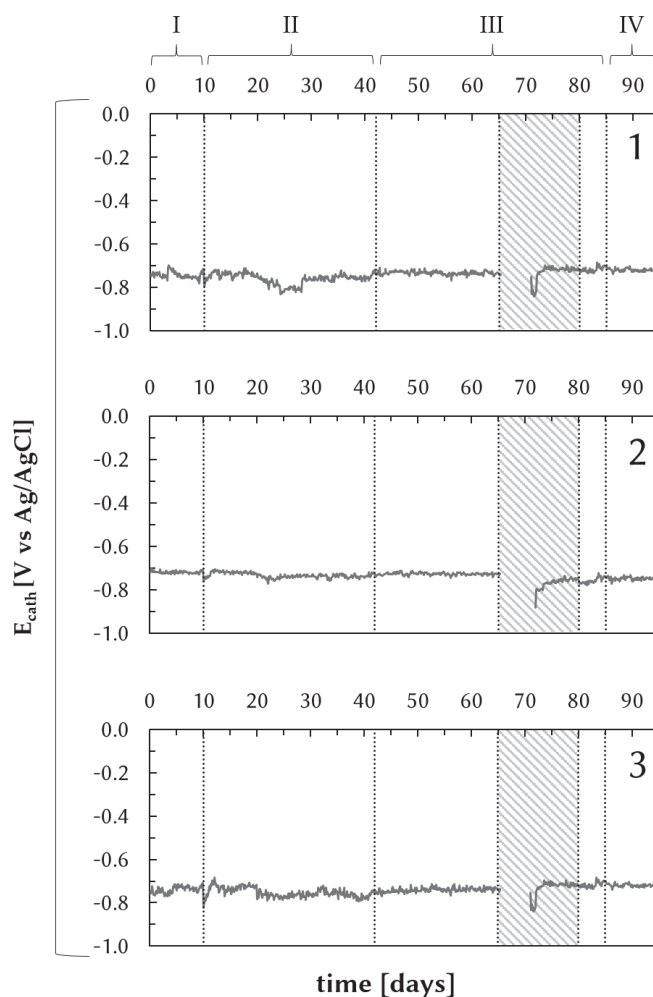


Figure S4.3: Cathode potential of triplicate reactors (designated by right top numbers) during all the experimental phases. Roman numbers indicate different feeding strategies. I: 30 mM acetate, II: 30 mM acetate + 30 mM propionate, III: 30 mM acetate + 30 mM n-butyrate, IV: 20 mM acetate + 20 mM propionate + 20 mM n-butyrate. Shaded area indicates temporary amperostatic impairment. The reference electrode Ag/AgCl has a redox potential of +0.210 V vs NHE.

Table S4.1: Formation selectivity of bioelectrochemical chain elongation to products during the experimental phases for reactor 2 and reactor 3.

| Reactor 2 | Selectivity carbon based [%] | | | Selectivity electron based [%] | | |
|-----------|------------------------------|-----------------|-----------------|--------------------------------|-----------------|-----------------|
| Phase | nC ₄ | nC ₅ | nC ₆ | nC ₄ | nC ₅ | nC ₆ |
| I | 91.7 ± 3.6 | 0.9 ± 0.3 | 5.4 ± 0.6 | 91.4 ± 3.4 | 0.9 ± 0.3 | 5.7 ± 0.7 |
| II | 25.7 ± 0.3 | 73.5 ± 0.4 | 0.9 ± 0.2 | 24.6 ± 0.3 | 74.4 ± 0.4 | 1.0 ± 0.2 |
| III | 68.1 ± 10.4 | 5.9 ± 1.9 | 25.1 ± 7.8 | 66.9 ± 10.6 | 6.0 ± 2.0 | 26.3 ± 8.0 |
| IV* | - | 93.5 ± 1.8 | 5.0 ± 0.4 | - | 93.4 ± 1.7 | 5.1 ± 0.4 |

| Reactor 3 | Selectivity carbon based [%] | | | Selectivity electron based [%] | | |
|-----------|------------------------------|-----------------|-----------------|--------------------------------|-----------------|-----------------|
| Phase | nC ₄ | nC ₅ | nC ₆ | nC ₄ | nC ₅ | nC ₆ |
| I | 96.4 ± 2.0 | 0.8 ± 0.4 | 2.2 ± 0.7 | 96.2 ± 2.0 | 0.8 ± 0.4 | 2.4 ± 0.7 |
| II | 20.5 ± 1.9 | 77.8 ± 1.8 | 1.7 ± 0.3 | 19.8 ± 1.9 | 78.4 ± 1.8 | 1.8 ± 0.3 |
| III* | 46.5 ± 24.2 | 3.3 ± 1.3 | 50.2 ± 0.3 | 45.2 ± 24.1 | 4.3 ± 1.9 | 64.8 ± 28.1 |
| IV* | - | 93.7 ± 0.8 | 6.3 ± 0.8 | - | 93.5 ± 0.8 | 6.5 ± 0.8 |

*: only last two datapoints of phase were included in average

Table S4.2: Reactor conditions used for thermodynamic calculations in Table 4.4. CO₂ and H₂ were presumed to be present at 1 bar as results of continuous electron supply on the electrode and gaseous CO₂ supply in the influent bottle.

| Unit | | Standardized conditions | Experimental phase | | | |
|----------------------|-------------|-------------------------|--------------------|--------|--------|--------|
| | | | I | II | III | IV |
| C ₂ (aq) | mM | 1,000 | 8 | 12 | 20 | 14 |
| C ₃ (aq) | mM | 1,000 | 0.3 | 18 | 0.2 | 15 |
| nC ₄ (aq) | mM | 1,000 | 10.3 | 3.5 | 31 | 17 |
| nC ₅ (aq) | mM | 1,000 | ~0 | 8.5 | 0.1 | 4 |
| nC ₆ (aq) | mM | 1,000 | 0.3 | <0.1 | 2.5 | 0.15 |
| Protons (pH) | 10-pH | 7.0 | 5.8 | 5.8 | 5.8 | 5.8 |
| H ₂ (g) | Bar | 1 | 1 | 1 | 1 | 1 |
| CO ₂ (g) | Bar | 1 | 1 | 1 | 1 | 1 |
| E _{cathode} | (V vs. SHE) | -0.507 | -0.534 | -0.549 | -0.524 | -0.507 |
| Temperature | (K) | 298.15 | 303.15 | 303.15 | 303.15 | 303.15 |

Table S4.3: Gibbs free energies of formation of the elements used for thermodynamic calculations ¹⁵⁴

| Component | $\Delta G_f^0 (25^\circ\text{C})$ [kJ mol ⁻¹] |
|-------------------------------|--|
| C ₂ (aq) | -369.41 |
| C ₃ (aq) | -361.08 |
| nC ₄ (aq) | -352.63 |
| nC ₅ (aq) | -344.34 |
| nC ₆ (aq) | -355.96 |
| H ₂ | 0 |
| HCO ₃ ⁻ | -568.85 |
| proton | 0 |

Chapter 5

Water based synthesis of hydrophobic ionic liquids [N₈₈₈₈][oleate] and [P_{666,14}][oleate] and their bioprocess compatibility

Published as: Raes, S.M.T. Carlucci, L., van den Bruinhorst, A., Strik, D.P.B.T.B., Buisman, C.N.J.. Water-Based Synthesis of Hydrophobic Ionic Liquids [N₈₈₈₈][oleate] and [P_{666,14}][oleate] and their bioprocess compatibility. *ChemistryOpen* 7, 878–884 (2018).

Abstract

The conversion of organic waste streams as renewable feedstocks into carboxylic acids results in relatively dilute aqueous streams. Carboxylic acids can be recovered from such streams using liquid-liquid extraction. Hydrophobic ionic liquids are novel extractants which can be employed for carboxylic acid recovery. To integrate these ionic liquids (ILs) as *in situ* extractants in several biotechnologies, the ionic liquid must be bioprocess compatible. Here the ionic liquids [P_{666,14}][oleate] and [N₈₈₈₈][oleate] were synthesised in water and their bioprocess compatibility was assessed by temporary exposure of an aqueous phase containing methanogenic granular sludge to an IL phase. Upon transfer of the sludge into fresh medium, [P_{666,14}][oleate] exposed granules were completely inhibited. Granules exposed to [N₈₈₈₈][oleate] sustained anaerobic digestion activity, although moderately reduced. Contaminants of the ILs, bromide (5 to 500 ppm) and oleate (10 to 4000 ppm), were shown not to inhibit the methanogenic conversion of acetate. [P_{666,14}] was identified as a bioprocess incompatible component. However, our results showed that [N₈₈₈₈][oleate] was bioprocess compatible and therefore has potential use in bioprocesses.

Keywords: microbial compatibility, ionic liquid, extraction, oleate, [N₈₈₈₈], [P_{666,14}], toxicity

Introduction

Fermented organic residual streams are a renewable feedstock that have the potential to (partially) replace the fossil-based platform chemicals now used for synthesis of value-added chemicals.^{155,156} The conversion of these waste streams into chemical building blocks, i.e. carboxylic acids, can be achieved via fermentative routes either using soluble electron donors^{36,79,157} or electrodes.¹²⁷ The relatively low concentrations reached in these bioprocesses form the major bottleneck in the competition with petrochemical production of bulk chemicals. Hence, separation of carboxylic acids from dilute aqueous solutions is direly needed.¹⁵⁸

Separation of volatile fatty acids (VFAs), the main carboxylic acids produced during fermentative pathways, can be achieved in several ways which have been described before.¹⁵⁹ One of the most applied affinity separation methods is liquid-liquid extraction, in which the VFAs are transferred from an aqueous phase into a suitable solvent.¹⁶⁰ Conventional extractions make use of organic solvents, which are often toxic, volatile, and flammable. To improve the sustainability of extraction processes, ionic liquids (ILs) were proposed as extractants.¹⁶¹ Ionic liquids are molten salts that show relatively low melting temperatures, often below 100°C. They are composed solely of ions, and generally comprise of large organic cations combined with organic or inorganic anions.^{65,71} This often results in a negligible vapour pressure and are liquid over a wide temperature range. By varying the type of ions of an IL and e.g. the branching of these ions, physical properties such as hydrophobicity can be tailored.^{72,162,163}

The application of ILs as extractants in bioprocesses depends mainly on whether the ILs are deleterious for the biocatalysts. ILs were firstly considered 'green' alternatives for volatile organic solvents, although later on toxicity and biodegradation studies showed ILs were not all as benign as perceived before.^{163–166} Conventionally the main indices for toxicity are EC₅₀ (effective concentration resulting in 50% change of activity), IC₅₀ (inhibition concentration which leads to 50% inhibition of activity) and LD₅₀ (median lethal dose).¹⁶⁴ However these indices are not sole intrinsic predictors for the possible deleterious effects of the application of specific substances to certain bioprocesses. The nature of the process' microbial community and the process conditions determine the resulting biological activity and the susceptibility and/or toxicity for the compound.¹⁶⁴ To illustrate this variability in microbial response to a specific compound, the toxicity of a widely used IL 1-butyl-3-methylimidazolium bis(trifluoromethyl -sulfonyl)imide varies from 30 µM in *F. candida*¹⁶⁷ to more than 2000 µM in *E. coli*, *S. aureus*, and *Candida sp.*¹⁶⁸

Therefore, we here introduce the term ‘bioprocess compatibility’ in the context of microbial processes for relevant practical industrial applications. The term ‘bioprocess compatible’ is defined as the application of a specific substance within a microbial bioprocess which does not hinder the relevant bioprocess and therefore shows compatibility. The bioprocess may be inhibited to some extent but does not limit the practical use of the substance. To what extent the inhibition really may occur cannot be defined since this will depend on the actual practical case (a real situation will determine the technical and economic feasibility). In addition, we like to stress that a ‘bioprocess compatible’ substance is not intrinsically eco- and cytotoxicological safe to use. The latter will need other studies, like the already mentioned toxicity tests, yet these tests were outside the scope of this paper. Due to the practical relevance, identification of a specific ionic liquid as a bioprocess compatible substance will give further direction to study the working principles of that specific ionic liquid and its potential important role in technological improvements. An important property on the use of IL is its water solubility. In literature, few studies investigated the effects of an IL on methanogenic gas production. Here the ILs were used for biomass pre-treatment to dissolve biomass for anaerobic microbial conversion. The water miscible IL caprolactam-tetrabutyl ammonium bromide (CPL TBAB) was demonstrated to inhibit methane production.¹⁶⁹ Several imidazolium based ILs are studied as solvents for the improved processing of lignocellulosic biomass.¹⁷⁰ The toxicity of imidazolium ILs to subsequent anaerobic digesting methanogenic cultures were later studied, and showed increasing toxicity with increasing IL concentration.¹⁷¹ Both CPL TBAB and the imidazolium ILs reported were water miscible and are therefore not comparable to our experiments because both the concentration of the IL in the water phase and the subsequent effect on the microorganisms differ.

In this paper the first steps towards implementation of ionic liquids for *in situ* extractions in bioprocesses were made. The aim of this study was to evaluate the possible inhibitory effect of two hydrophobic ionic liquids, tetraoctylammonium oleate and trihexyl(tetradecyl)phosphonium oleate (respectively [N₈₈₈₈][oleate] and [P_{666,14}][oleate], for structures see SI), on methanogenic granular sludge. One of the most well-known anaerobic bioprocesses is methanogenesis⁷⁷ and therefore it was chosen in our experiments as model bioprocess. The ILs [N₈₈₈₈][oleate] and [P_{666,14}][oleate] form a biphasic system with aqueous solutions, and thus could be applied as a floating phase on top of fermentation broths.

To study the potential bioprocess compatibility the ILs were temporarily applied to an aqueous phase in which methanogenic granular sludge was present. After 21 days of contact time, the sludge was transferred into fresh medium containing

acetate. Subsequent methane production was followed to study the effects of IL exposure on the sludge. Inhibitory effects of possible contaminants remaining in the ILs, i.e. bromide and oleate, were tested as well in order to evaluate the bioprocess compatibility of the ILs.

Results and Discussion

For ionic liquids to become the envisioned extraction solvents which can be used for *in situ* extraction during bioprocesses, they have to be bioprocess compatible and hydrophobic. Here, two ionic liquids $[N_{8888}][oleate]$ and $[P_{666,14}][oleate]$ were synthesised using water as solvent.

Ionic liquid synthesis

Commonly, these type of ILs are synthesised using organic solvents like toluene and ethanol.^{61,172} Potential toxic effects of remaining trace amounts of synthesis solvent may occur when those traces leak into the water phase where microorganisms are present. To prevent the possible toxic effects, a one-pot synthesis protocol for the ILs was followed using only water as solvent similar to that described by Parmentier, et al.¹⁷³ In order to decrease the potential toxicity of the ILs, an organic and biodegradable anion was selected, i.e. oleate.¹⁷⁴ The cation N_{8888} was demonstrated to be less viscous compared to asymmetrical ammonium branched cations.⁶¹ Furthermore, complete regeneration of $[N_{8888}][oleate]$ was demonstrated in metal extraction,¹⁷⁵ which is a major challenge regarding the use of affinity separation.¹⁷⁶ The $P_{666,14}$ cation was selected because it showed the best performance in previous extraction experiments.⁷⁰

The washing water of the final wash after synthesis contained $0.6 \text{ mg}\cdot\text{L}^{-1}$ and $8.5 \text{ mg}\cdot\text{L}^{-1}$ Br⁻ for $[N_{8888}][oleate]$ and $[P_{666,14}][oleate]$, respectively. Since the ILs were washed with equal volumes of water and bromide is highly hydrophilic, the bromide was considered to be fully exchanged and washed out of the IL. Sodium oleate was added in slight excess and should also be removed during washing with water. The TOC of the final washing water was 28.1 mgC L^{-1} and 25.8 mgC L^{-1} for $[N_{8888}][oleate]$ and $[P_{666,14}][oleate]$, respectively. Hence, extra washing steps would not lead to a significant reduction sodium oleate. The water contents of the ILs were 9.0 wt% and 7.2 wt% for $[N_{8888}][oleate]$ and $[P_{666,14}][oleate]$, respectively. This is similar to the water contents of comparable water-saturated ILs in literature.¹⁷³

The resulting ILs were analysed using ^1H -NMR spectroscopy (400 MHz, CDCl_3 , δ/ppm), see Figure S5.5 and S5.6. For $[N_{8888}][oleate]$ $\delta = 0.88$ (m, 15.6H), 1.28 (m, 62.5H), 1.65 (m, 9.9H), 2.00 (m, 3.8H), 2.18 (t, 2.1H), 3.34 (m, 8.0H), 5.33 (m, 2.0H) and for $[P_{666,14}][oleate]$ $\delta = 0.90$ (m, 16.2H), 1.31 (m, 56.4H), 1.50 (m, 19.0H), 2.00 (m, 4.1H), 2.15 (t, 2.3H), 2.33 (m, 8.0H), 5.34 (m, 2.2H). For $[N_{8888}][oleate]$ the chemical shifts

were similar to those published before¹⁷² and the integrals were in agreement with the theoretical values within the accuracy of the method. Hence, [N₈₈₈][oleate] was synthesized successfully. For [P_{666,14}][oleate], however, the integrals were slightly off, e.g. the CH₃ protons (δ = 0.90) should contribute for 15H and the CH₂ protons of the second peak (δ = 1.31) for 52H. This indicates that there might have been a slight excess of (sodium) oleate present in the IL that was not washed out. Whether sodium oleate would influence the microbial compatibility of [P_{666,14}][oleate] is explored in the sections below.

Ionic liquid inhibition test

After synthesis, the ILs were applied in a biphasic system in which methanogenic sludge was present in the aqueous phase. During an initial contact time of 21 days, the microorganisms were exposed to an IL on top of the aqueous phase (mineral medium) which they were present in. Bottles containing the same medium and same amount of sludge were simultaneously incubated without IL as controls. In this initial contact time no methane was produced in both the IL exposed bottles as well as the controls without IL. The control bottles did not show a pH difference before and after contact time in contrast to the IL contacted water phases. Those showed a pH increase of 1.38 and 1.56 for [P_{666,14}][oleate] and [N₈₈₈][oleate] respectively, see Table S5.4. The medium composition only could not account for this pH increase, however further research is needed to understand what caused the pH increase as this was out of the scope of this experiment.

To investigate whether the presence of the ILs had an inhibitory effect on the microbial activity, the granules were removed from the bottles after 21 days. Special care was taken to prevent the granules from touching the IL phase, as several types of ILs have been reported to disrupt cell membranes.^{177–180} Upon addition of fresh acetate-containing medium the granules were incubated again at 30°C and 110 rpm. All inhibition experiments reported in this paper were executed in triplicate. All data presented report the average of triplicates and the corresponding standard deviation in either percentage of the average or in absolute values. The pressure increase and accompanying methane production in the control bottles started right after the transfer of granules in fresh medium (Figure 5.1) as is known for these granules. The lack of substrate for 21 days did not affect the ability of the sludge to convert the available COD into methane instantly. Approximately 85% available COD was converted into methane (Table 5.1). The granules from the water phase that contacted [N₈₈₈][oleate] also converted 85% of the COD supplied into methane, although the conversion was slower, i.e. 11 days instead of 4 until headspace pressure was stable. The amount of methane produced by the granules exposed to [N₈₈₈][oleate] (511. ± 55.6 mgCOD_{CH₄} gVSS⁻¹) was in the same range as the control

bottles ($471.2 \pm 26.8 \text{ mgCOD}_{\text{CH}_4} \text{ gVSS}^{-1}$). This demonstrates that these granules were still able to convert the supplied substrate, although the rate was slower. Additional experiments will be needed to elucidate whether this observed reduced activity was a permanent impact on the granules or if it was a temporal effect caused by the exposure to [N₈₈₈₈][oleate].

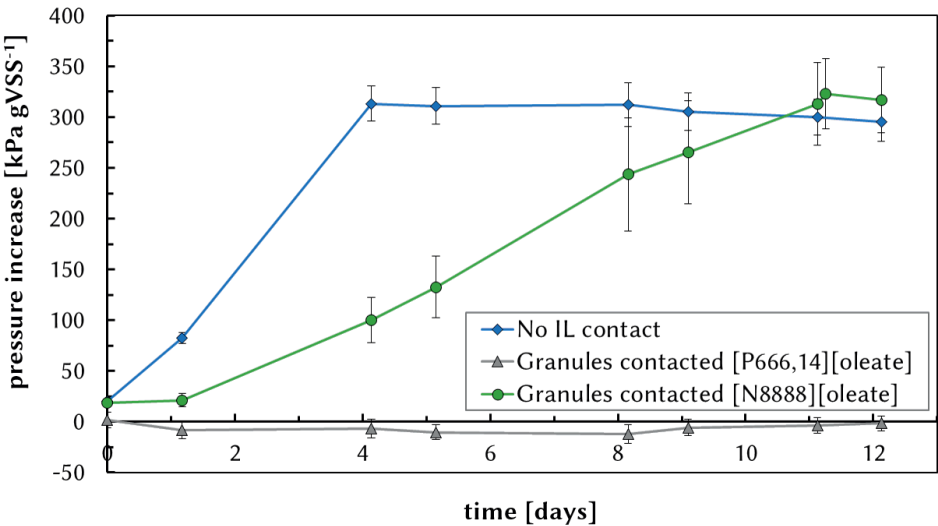


Figure 5.1: ionic liquid inhibition test – Pressure increase over time per gVSS. After contact time of 21 days without carbon source, the methanogenic granules were transferred to fresh medium containing acetate (COD load was approx. 520-600 mgCOD gVSS⁻¹ dependent on how many granules could be transferred).

Table 5.1: ionic liquid inhibition test – methane production and percentage of initial COD converted into methane.

| | Methane produced [mgCOD _{CH₄} gVSS ⁻¹] [a] | COD converted in CH ₄ [%] | pH before | pH end [b] |
|--------------------------------|---|---|--------------|------------|
| Control | 471.2 ± 26.8 | 84.6 ± 1.8 | 7.29 | 7.62 |
| [N ₈₈₈₈][oleate] | 511.3 ± 55.6 | 85.0 ± 3.3 | 7.29 | 7.74 |
| [P _{666,14}][oleate] | 0 | 0 | 7.29 | 7.74 |

[a] assumption: the exposure to the ILs did not change the VSS content of the granular sludge.

[b] standard deviation of all replicates < 0.04

The [P_{666,14}][oleate] exposed granules did not produce any methane and consequently no pressure increase was observed upon acetate addition to the bottles. Negative values in Figure 5.1 were caused by the removal of small amounts of headspace volume by the pressure measurements. Nevertheless it is clear that methanogenic activity of the sludge was fully hampered by the exposure to [P_{666,14}][oleate].

At this stage it was unclear whether the inhibition of the sludge by exposure to [P_{666,14}][oleate] and the moderately reduced activity by [N₈₈₈][oleate] exposure was caused by the IL or by possible residual sodium oleate or bromide still remaining in the IL after synthesis. These ions could have leached into the water phase during contact time and affect the granular sludge. Therefore, to investigate whether the effects observed in the IL inhibition test were caused by either bromide or oleate, separate inhibition tests for these contaminants were performed (next subsections).

Bromide inhibition test

To the best of our knowledge, no study investigated the effect of bromide ions (Br⁻) on methanogenesis by anaerobic granular sludge. The bromide concentration in the last washing water was 0.6 mg L⁻¹ for [N₈₈₈][oleate] and 8.5 mg L⁻¹ for [P_{666,14}][oleate]. Therefore, here the effect of bromide on the production of methane is studied by performing similar acetate conversion experiments in batch bottles as the second part of the ionic liquid inhibition test. Sodium bromide was added in order to achieve bromide concentrations ranging from 5 to 500 ppm. This range was selected because 5 ppm was in the middle of the bromide concentrations in the last washing waters after IL synthesis, and 500 ppm is a factor 100 higher than 5, which could potentially have an impact on the activity of the sludge. The effect of sodium on methanogenic activity in anaerobic digestion is reported to be non-inhibiting up to 5 g Na⁺ L⁻¹,^{181–185} therefore sodium was not considered as inhibiting under all experimental conditions.

For all tested bromide concentrations, the pressure increase was similar to the pressure increase of the positive control (Figure 5.2). The pressure increase of the negative control (no substrate and no bromide added) originates from the amount of methane produced from the organic matter still present in the sludge. The amount of COD converted and the amount of methane produced per gram of VSS was similar to the positive control for all concentrations of bromide, see Table 5.2.

Combining the pressure increase and the produced methane in the presence of bromide, the results demonstrated that bromide had no inhibitory effects on the methanogenic conversion of acetate up to a concentration of 500 ppm. Hence,

bromide leaching from the IL would not have caused the observed inhibition and reduced activity after application of IL on top of the water phase.

Table 5.2: Bromide inhibition test – methane production and percentage of initial COD converted into methane.

| | Methane produced [mgCOD _{CH₄} gVSS ⁻¹] | COD converted in CH ₄ [%] | pH start | pH end |
|------------------|---|--|-------------|-----------|
| Positive Control | 228.2 ± 3.3 | 75.5 ± 0.4 | 7.01 | 7.38 |
| 5 ppm | 226.4 ± 6.7 | 75.0 ± 1.2 | 7.01 | 7.40 |
| 50 ppm | 216.4 ± 8.7 | 71.4 ± 1.2 | 7.00 | 7.39 |
| 100 ppm | 229.6 ± 3.7 | 75.3 ± 1.6 | 7.01 | 7.41 |
| 500 ppm | 213.4 ± 6.5 | 70.3 ± 2.7 | 7.00 | 7.41 |
| Negative Control | 8.3 ± 1.3 | - | 7.04 | 7.09 |

All pH reported have standard deviation $\leq \pm 0.02$.

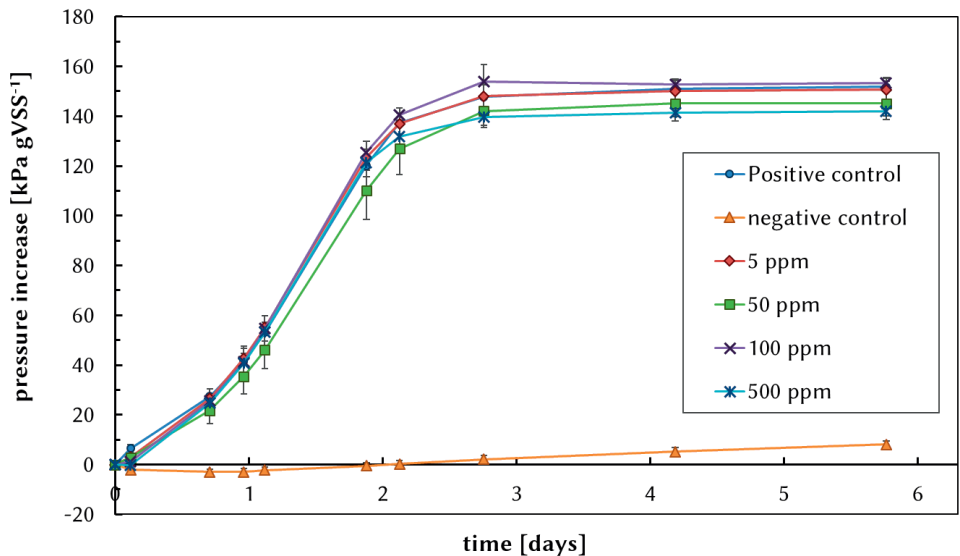


Figure 5.2: Bromide inhibition test - pressure increase over time per gram VSS. All conditions except negative control were loaded with approx. 300 mgCOD gVSS⁻¹.

Oleate inhibition test

In order to investigate whether a sodium oleate excess in the IL and subsequent leaching could have caused the inhibition, identical acetate conversion batch experiments were performed using sodium oleate as toxicant. For [P_{666,14}][oleate] the ¹H-NMR spectrum suggested that there might be a sodium oleate excess present in the IL. The TOC (= total organic carbon) concentration in the last washing water after synthesis can be regarded as an indicative measure for the equilibrium oleate concentration in the water phase. These TOC concentrations were 25.8 mgC L⁻¹ and 28.1 mgC L⁻¹ for [P_{666,14}][oleate] and [N₈₈₈₈][oleate] respectively, and correspond to oleate concentrations of 36.4 mg L⁻¹ (0.13 mM) and 39.6 mg L⁻¹ (0.14 mM). Concentrations of this order of magnitude could be expected in the water phase when ILs were applied. For these reasons concentrations ranging from 10 to 4000 ppm of oleate were selected to study the possible inhibitory effects.

For all the tested oleate concentrations the final pressure increase at the end of the experiment were similar to the positive control (Figure 5.3). Although the final pressure increase was similar for all the tested oleate concentrations compared to the positive control, in the first 3 days the increase was smaller when oleate was added to the medium. The amount of methane produced per gram of VSS (Table 5.3) in 10 ppm, 100 ppm and 1000 ppm was similar to the positive control without oleate. In case of 4000 ppm of oleate, the amount of methane produced was approximately 8% less than the positive control. Interestingly, the percentage of supplied COD (i.e. acetate) converted into methane of the 4000 ppm bottles was similar to the positive control. This difference in amount of methane produced with the same percentage of COD converted could be explained by the approximately 10 % less COD supplied (Table 5.3, loading column).

Early studies on the anaerobic treatment of lipid-rich wastewaters indicated that long-chain fatty acids (LCFAs) had inhibitory effects on biogas formation.^{186–188} More recently, Alves et al. (2009) reviewed the complexity of syntrophic communities of acetogenic bacteria and methanogenic archaea that degrade LCFAs in anaerobic bioreactors.¹⁸⁹ Sensitivity of such microbial communities to alleged inhibitory LCFAs were summarized by Silva et al. (2016) via the toxicity indicator IC₅₀.¹⁹⁰ For granular sludge, reported IC₅₀ values for oleate were 3 to 4 mM, corresponding to 0.84 to 1.13 g L⁻¹; in those studies acetate was the primary substrate for methanogenesis. The oleate concentrations used in our experiments correspond to 0.04 mM (10 ppm), 0.36 mM (100 ppm), 3.55 mM (1000 ppm), and 14.21 mM (4000 ppm). Although based on literature, inhibition could be expected at 1000 ppm and 4000ppm, the present results showed that the employed acetoclastic methanogenic activity of the

granular sludge was not significantly inhibited by the oleate in the medium even up to 4000 ppm.

Although the addition of sodium oleate affected the initial rate of the methanogenesis, all the initial acetate was converted at the end of the experiment. Therefore, this oleate inhibition test demonstrated that it is unlikely that leached sodium oleate caused the observed inhibition of methanogenesis after exposure to the ILs.

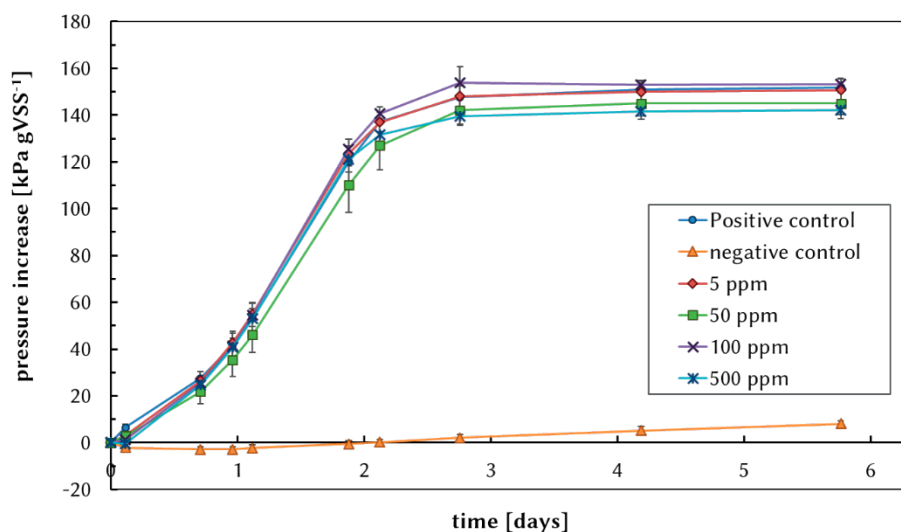


Figure 5.3: Oleate inhibition test - pressure increase over time per gram VSS. The positive control was loaded with approx. 550 mgCOD gVSS⁻¹, 10, 100 and 1000 ppm with approx. 540 mgCOD gVSS⁻¹, and 4000 ppm with approx. 500 mgCOD gVSS⁻¹.

Microbial compatibility of $[N_{8888}][oleate]$ and $[P_{666,14}][oleate]$

The IL exposure test did show that application of $[N_{8888}][oleate]$ did not hinder the bioprocess, hence demonstrating it as microbial compatible. Exposure to $[N_{8888}][oleate]$ affected the rate of the methanogenic conversion, yet the sludge was still active. Exposure to $[P_{666,14}][oleate]$ inhibited fully the conversion of acetate to methane upon transfer of the granules in fresh medium. Possible leaching of excess sodium oleate and/or sodium bromide from the IL into the water phase most probably did not cause the observed inhibition of methanogenesis after IL application. Combining these 3 separate experiments, it can be concluded that the observed inhibition was most likely caused by $[P_{666,14}][oleate]$. Consequently, $[P_{666,14}][oleate]$ was demonstrated to be not microbial compatible. As oleate was the anion in both ILs examined, we state that $[P_{666,14}]$ was the microbial incompatible component.

Table 5.3: Oleate inhibition test – methane production and percentage of initial COD converted into methane.

| | Methane produced [mgCOD _{CH₄} gVSS ⁻¹] | COD converted in CH ₄ [%] | Loading [mgCOD gVSS ⁻¹] | pH before | pH end |
|------------------|---|--|---|--------------|-------------|
| Positive Control | 488.6 ± 12.6 | 88.6 ± 1.1 | 555.1 ± 11.9 | 7.19 ± 0.01 | 7.60 ± 0.01 |
| 10 ppm | 470.1 ± 7.9 | 87.7 ± 2.0 | 536.5 ± 16.5 | 7.18 ± 0.01 | 7.58 ± 0.01 |
| 100 ppm | 479.3 ± 12.3 | 87.7 ± 2.4 | 546.6 ± 10.1 | 7.20 ± 0.01 | 7.51 ± 0.10 |
| 1000 ppm | 495.3 ± 8.3 | 91.9 ± 1.7 | 539.1 ± 3.7 | 7.13 ± 0.05 | 7.51 ± 0.02 |
| 4000 ppm | 450.4 ± 2.9 | 89.9 ± 0.7 | 500.9 ± 7.0 | 7.17 ± 0.04 | 7.47 ± 0.03 |
| Negative Control | 10.6 ± 5.1 | - | - | 7.19 ± 0.01 | 7.05 ± 0.05 |

Microbial compatibility of [N₈₈₈][oleate] and [P_{666,14}][oleate]

The IL exposure test did show that application of [N₈₈₈][oleate] did not hinder the bioprocess, hence demonstrating it as microbial compatible. Exposure to [N₈₈₈][oleate] affected the rate of the methanogenic conversion, yet the sludge was still active. Exposure to [P_{666,14}][oleate] inhibited fully the conversion of acetate to methane upon transfer of the granules in fresh medium. Possible leaching of excess sodium oleate and/or sodium bromide from the IL into the water phase most probably did not cause the observed inhibition of methanogenesis after IL application. Combining these 3 separate experiments, it can be concluded that the observed inhibition was most likely caused by [P_{666,14}][oleate]. Consequently, [P_{666,14}][oleate] was demonstrated to be not microbial compatible. As oleate was the anion in both ILs examined, we state that [P_{666,14}] was the microbial incompatible component.

In case of [N₈₈₈][oleate], the reduced activity after exposure to this IL was not caused by bromide leaching. Yet, it cannot be ruled out that leached oleate attached to the sludge as oleate is amphiphilic (hydrophobic tail and hydrophilic carboxylate head).¹⁸⁹ Even though the TOC concentration of the last washing water after the IL synthesis was considerably low (0.14 mM), absorption of oleate to the sludge could have occurred while concentration in the liquid remained low. Accumulation of LCFAs onto microorganisms causes inhibition or reduced activities due to limited transport over the microbial cell membrane.¹⁹¹ During exposure of the sludge to an IL-contacted water phase, small amounts of oleate could have been absorbed to the

sludge and subsequently upon transfer into fresh medium still have reduced moderately the methanogenic conversion of acetate. If only traces of oleate leached into the aqueous phase or oleate was not absorbed onto the sludge during exposure, the IL itself caused the activity reduction. Albeit from these results it cannot be concluded whether oleate or [N₈₈₈₈][oleate] affected the activity of methanogenic granular sludge, the sludge was still active after exposure to [N₈₈₈₈][oleate]. Still, our results hold promise for future implementation of [N₈₈₈₈][oleate] as microbial compatible extractant in bioprocesses.

Conclusions

The hydrophobic ionic liquids [N₈₈₈₈][oleate] and [P_{666,14}][oleate] were synthesised using no other solvent than water. The advantages of using only water are the simple synthesis method and the improved sustainability (no harmful and/or toxic solvents are used). Possible toxicants remaining in the ILs, bromide (5 to 500 ppm) and oleate (10 to 4000 ppm), were demonstrated to not inhibit conversion of acetoclastic methanogenesis by granular sludge. [P_{666,14}][oleate] was demonstrated not to be microbial compatible as the activity of the sludge was fully inhibited. Either [N₈₈₈₈][oleate] or oleate leaching from the IL did affect the sludge, although microbial activity was sustained. Thus, here [N₈₈₈₈][oleate] was demonstrated as a potential microbial compatible IL with potential use in bioprocesses.

Experimental Section

Ionic liquid materials

Sodium oleate (> 97 %) was obtained from TCI Europe. Tetraoctylammonium bromide (98 %) and trihexyl(tetradecyl)phosphonium bromide (97 %) were purchased from Angene international. Ultrapure water was produced using Milli-Q Integral 5 provided with a Progard TS2 filter, both from Millipore. CAS and lotnumbers of the purchased chemicals can be found in SI.

[N₈₈₈₈][oleate] and [P_{666,14}][oleate] synthesis

The two ionic liquids tetraoctylammonium oleate ([N₈₈₈₈][oleate]) and trihexyl(tetradecyl)phosphonium oleate ([P_{666,14}][oleate]) were synthesised by a one-step water-based procedure, similar to that of Parmentier et al (2015).¹⁷³ Firstly, sodium oleate was dissolved in water (~10 wt%) by stirring for 1.75 h at room temperature. Afterwards the bromide salt was added and stirred for 3 h at 55°C. The obtained organic phase was washed 6 times with ultrapure water to remove NaBr and the excess of sodium oleate. Finally, the water saturated ionic liquid was separated from the aqueous phase using a separation funnel, analysed with ¹H-NMR, and used in the experiments. Detailed synthesis of the ionic liquids can be found in SI.

Ionic liquid inhibition test

In order to investigate whether the presence of the ILs [N₈₈₈][oleate] and [P_{666,14}][oleate] has an inhibitory effect on the viability of methanogenic granular sludge, sludge was first incubated for 21 days without carbon source at 30°C at 110 rpm. During this exposure time, [N₈₈₈][oleate] and [P_{666,14}][oleate] were applied on top of an aqueous phase containing granular sludge, in serum bottles (see experiment schematic in Figure S5.1). Control bottles consisted of granular sludge in aqueous phase, with no contact with any IL. Each experiment and control were run in triplicates. Serum bottles (total volume excluding stopper = 117.6 ml ± 0.77) were filled with 50 ml total volume (controls: 50 ml medium; IL contact bottles: 30 ml medium + 20 ml IL, S/F ratio of 2/3). Medium was prepared as described by Lindeboom et al (2014).¹⁹²

Methanogenic granular sludge originated from an UASB treating paper mill water (Industriewater, Eerbeek, the Netherlands) and was stored at 4°C for several months before use. The sludge was washed several times and approximately 1.5 g wet sludge (0.134 gVSS (g wet sludge)⁻¹; 1.5 g = ~4 gVSS L⁻¹; VSS = volatile suspended solids) was added per bottle. After sludge and medium addition, sequentially a bottle's headspace was flushed with pure N₂ to create anaerobic condition and sealed with a butyl-rubber stopper and aluminium crimp cap. Bottles were placed in 30°C shaker at 110 rpm. Shaking at 110 rpm did not cause the granules to touch the IL. After 21 days the bottles were opened and the granules were transferred to clean bottles. During transfer it was ensured the granules did not touch the IL phase, for more details on transfer method see SI. Fresh medium containing sodium acetate as carbon source was added to the bottles (Table 5.4). pH of the liquid was adapted to 7.3, headspace was flushed with N₂ and sealed again.

Table 5.4: Experimental specifics for ionic liquid inhibitory test.

| Contacted ILs | |
|--|----------------|
| Acetate added [mgCOD bottle ⁻¹] [a] | 109.2 ± 2 % |
| Sludge added [gVSS bottle ⁻¹] [a] | 0.15 – 0.2 [b] |
| pH at start | 7.3 ± 0.1 |

[a] Actual amount of added acetate and sludge are reported as averages for the triplicates and standard deviation is given in percentage the mean.

[b] Granules were transferred from previous bottle to another, therefore value is given as a range.

Bromide and oleate inhibition tests

Batch experiments were performed to evaluate the effect of the potential ionic liquid contaminants bromide (Br⁻) and oleate on methanogenesis. Serum bottles were filled with 50 ml of acetate-containing medium and sludge according to Table 5.5.

Bromide was tested in the concentration range of 5 to 500 ppm Br⁻, by addition of concentrated sodium bromide solution (2.516 g in 25 ml water). Oleate was tested in the concentration range of 10 to 4000 ppm oleate⁻ by addition of concentrated sodium oleate solution (2.5 g in 40 ml water). Sludge and acetate were added in the positive controls of both inhibition tests in the same amount as added to the test bottles. Negative controls with the same amount of sludge and medium but without acetate were tested to evaluate the amount of methane produced from remaining COD in the sludge. pH of the medium was adapted to 7.2 ± 0.2 prior closing the bottles. Headspace was flushed with pure N₂ and sealed. All tests were performed in triplicates.

Analytical methods

For all the inhibition tests the headspace pressure was measured versus time using a digital pressure meter (Greisinger GMH 3151). When headspace pressure did not increase anymore, the headspace composition was analysed using gas chromatography for nitrogen, carbon dioxide, methane and oxygen as reported before.¹²⁷ Thereafter the bottles were opened, the pH was measured, and the aqueous phase was analysed for volatile fatty acids (C2 to C8) and alcohols (methanol to hexanol) as previously reported.¹²⁹

Table 5.5: Experimental specifics for the bromide and oleate inhibition tests.

| Inhibition test | Bromide (Br ⁻) | Oleate |
|--|---|---|
| Acetate added [mgCOD bottle ⁻¹] [a] | 61.7 ± 0.1 % | 108.8 ± 3.6% |
| Sludge added [gVSS bottle ⁻¹] [a] | 0.2 ± 1 % | 0.2 ± 0.7% |
| pH at start | 7.01 ± 0.01 | 7.18 ± 0.03 |
| Toxicant | Br ⁻ 5 – 50 – 100 – 500 ppm | Oleate ⁻ 10 – 100 – 1000 – 4000 ppm |

[a] Actual amount of added acetate and sludge are reported as averages for the triplicates and standard deviation is given in percentage the mean.

In the last washing water after IL synthesis Total organic carbon (TOC) and bromide concentrations were determined. TOC in the aqueous phase was measured using a TOC-L system with ASI-L autosampler (Shimadzu, Benelux). First, a part of the liquid sample is introduced in a furnace (993 K) coated with a platina catalyst and constantly flushed with CO₂-free synthetic air. All the present carbon is converted into CO₂ and is detected by a nondispersive infrared sensor (NDIR) (= total carbon content). Another part of the liquid sample is introduced in a vessel containing 20% phosphoric acid. There all the dissolved inorganic carbon is converted to CO₂. The vessel is then flushed with the same synthetic air and detected by the NDIR sensor (=inorganic carbon content). Total organic carbon is calculated by the difference between total carbon and total inorganic carbon. Bromide concentrations were measured as previously reported.¹⁹³

The water content of the ILs was measured after synthesis using a Mettler-Toledo DL39 coulometric Karl-Fischer titrator without diaphragm. Approximately 20 v/v% of chloroform was added to the titration medium (Hydranal Coulomat AG) in order to improve the solubility of the hydrophobic ILs. The performance of the titrator was evaluated with water standards of 0.01 wt%, 0.1 wt% and 1.0 wt%, both the accuracy and reproducibility were estimated to be ± 1 %. Due to the relatively high water content of the ILs, 1 g of IL was diluted with 4 g of 80/20 v/v% ethanol/chloroform prior to injection (sample size 0.1-0.3 g). The water contents were determined in triplicate and corrected for the water present in the diluent. ¹H-NMR spectra were recorded a Bruker 400 MHz spectrometer equipped with an autosampler carousel. A drop of IL was dissolved in approximately 1 mL CDCl₃ with 3 v/v% tetramethylsilane (TMS) as internal standard. The solution was then transferred to a 5 mm thin-walled economic Wilmad NMR tube. The tube was capped and sealed with Parafilm® to avoid solvent evaporation. The spectra were recorded in 16 scans with a relaxation time of 5 s between the RF pulses and the spectra were auto-shimmed and auto-phased by the Bruker TopSpin® software used to control the equipment. The peaks were integrated using MestReNova 10.0.2, after applying a Withaker Smoother baseline correction and small phase corrections if necessary. Accuracy of integrals is estimated to be within 5%.

Acknowledgements

The financial support from the Netherlands Organisation for Scientific Research (NWO) and the company Paques B.V. (STW-Paques Partnership, project 12999) is gratefully acknowledged. SR acknowledges Katja Grolle for her help in the design of the microbial batch experiments.

Chapter 5 – Supplementary information

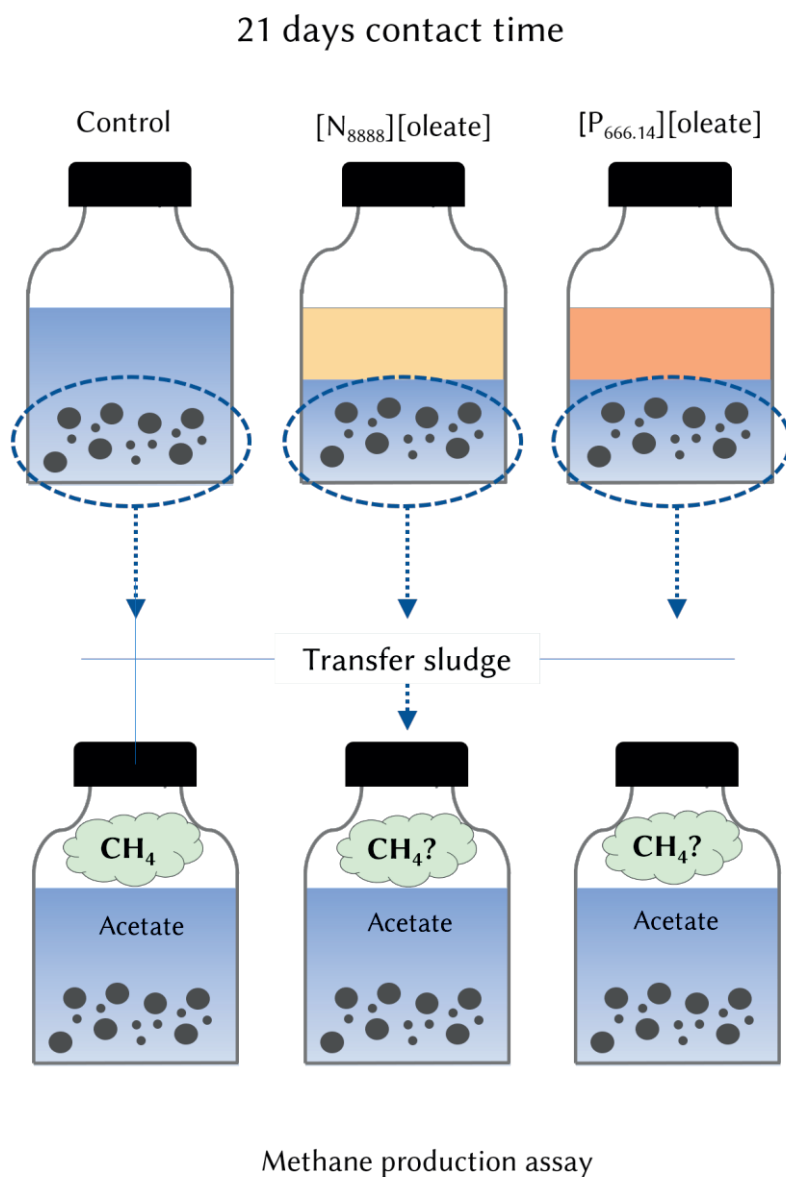


Figure S5.1: schematic of ionic liquid inhibition assay.



Figure S5.2: Structure of tetraoctylammonium oleate ([N₈₈₈][oleate])

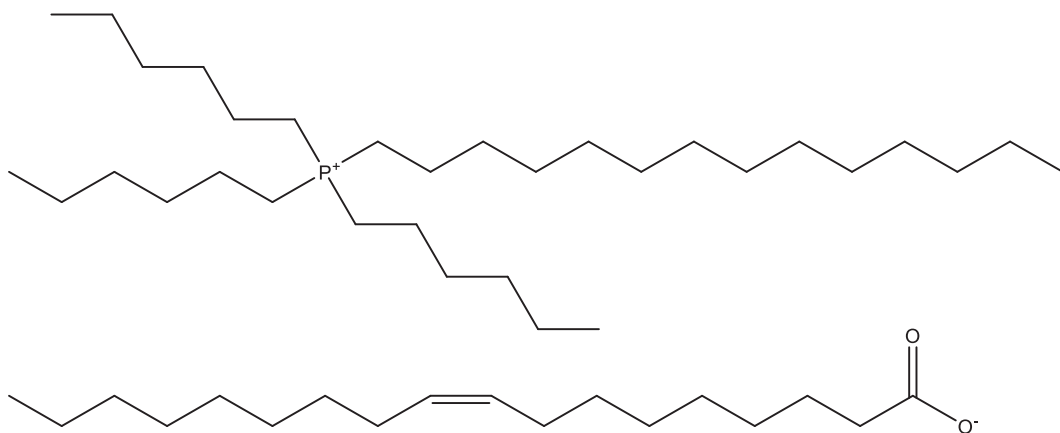


Figure S5.3: Structure of trihexyl(tetradecyl)phosphonium oleate ([P_{66,14}][oleate])

Table S5.1: CAS and lot numbers of the used chemicals

| Chemical | CAS number | Purity | Supplier | Lot number |
|---|-------------|--------|------------------------------|------------------|
| Sodium oleate | 143-19-1 | >97% | TCI Europe N.V. | 3CSSIBI |
| Tetra-octyl-ammonium bromide | 14866-33-2 | 98% | Angene international Limited | AGN2017-9683-001 |
| Trih-exyl-tetradecylphosphonium bromide | 654057-97-3 | 97% | Angene international Limited | AGN2017-9690-001 |

Text S1: Synthesis of tetraoctylammonium oleate [N₈₈₈][oleate]

In three separate erlenmeyers ~45 g of sodium oleate was dissolved in ~450 g water (see Table S5.2) by stirring at room temperature. After 1 h and 45 min the sodium oleate was completely dissolved and a soapy solution was obtained. Tetraoctylammonium bromide was added to the sodium oleate solutions in a stoichiometric ratio +/- 5%. The reaction mixture was stirred for 3 h at 55°C. The content of the three synthesis batches were transferred to one big separation funnel. The organic phase was separated and washed six times with equal volume of ultrapure water in order to remove sodium bromide and sodium oleate residues. The last washing water was analysed for bromide (0.6 mgC L⁻¹) and total organic carbon content (28.1 mgC L⁻¹).

A viscous yellow product was obtained. The water saturated ionic liquid was analysed with ¹H-NMR.

Table S5.2: details of synthesis batches for [N₈₈₈][oleate]. All weights ± 0.1 g.

| | Water [g] | Sodium oleate [g] | [N ₈₈₈][Br] [g] |
|--------------|-----------|-------------------|-----------------------------|
| Erlenmeyer 1 | 491.2 | 44.9 | 82.0 |
| Erlenmeyer 2 | 505.8 | 45.0 | 81.9 |
| Erlenmeyer 3 | 490.3 | 45.0 | 82.0 |

Text S2: Synthesis of trihexyl(tetradecyl)phosphonium [P_{666,14}][oleate]

In three separate erlenmeyers ~45 g of sodium oleate was dissolved in ~450 g water (see Table S5.3) by stirring at room temperature. After 1 h and 45 min the sodium oleate was completely dissolved and a soapy solution was obtained. Trihexyl(tetradecyl)phosphonium bromide was added to the sodium oleate solutions in a stoichiometric ratio +/- 5%. The reaction mixture was stirred for 3 h at 55°C. The content of the three synthesis batches were transferred to one big separation funnel. The organic phase was separated and washed six times with equal volume of ultrapure water in order to remove sodium bromide and sodium oleate residues. The last washing water was analysed for bromide (8.5 mgC L⁻¹) and total organic carbon content (25.8 mgC L⁻¹).

The product was more viscous than the previous one and characterized by a darker colour. Later, the water saturated IL was analysed with ¹H NMR before further use in the extraction experiment.

Table S5.3: details of synthesis batches for [P_{666,14}][oleate]. All weights ± 0.1 g.

| | Water [g] | Sodium oleate [g] | [P _{666,14}][Br] [g] |
|--------------|-----------|-------------------|--------------------------------|
| Erlenmeyer 1 | 450.0 | 45.1 | 79.3 |
| Erlenmeyer 2 | 450.0 | 44.9 | 79.3 |
| Erlenmeyer 3 | 450.0 | 45.1 | 79.9 |

Table S5.4: pH data of water phase at start and after 21 days of contact time with ILs

| | pH start | pH end of contact time |
|--------------------------------|----------|------------------------|
| Control | 7.14 | 7.13 |
| [N ₈₈₈₈][oleate] | 7.17 | 8.73 ± 0.08 |
| [P _{666,14}][oleate] | 7.17 | 8.55 ± 0.03 |

Text S3: Method for removal of aqueous phase and granules from under IL

To separate the aqueous phase including granules from the IL phase floating on top of the water phase, a double valved separation funnel was constructed (named here 'Separation unit'; see Figure S5.4 belowFigure S5.4). For each bottle, the following sequence of actions was taken to prevent the granules from touching the IL:

1. Septum of bottle was removed, bottle opening was cleaned with paper cloth, and separation unit was attached to bottle opening.
2. Both valves of the separation unit were closed.
3. Slowly the bottle was turned upside down in such a way the aqueous phase took along the granules; the result is what is shown in Figure S5.4.
4. Valve 1 was opened. This allows the granules and some of the water phase to fall into the volume between valve 1 and valve 2.
5. Valve 1 was closed again. Now the granules are trapped in between the valves.
6. Bottle was turned straight up again.
7. Separation unit was detached from the bottle opening and the granules plus water phase was released from the separation unit.
8. The remaining of the water phase was removed by further cleaning of bottle opening, closing the bottle with septum, liquid removal using syringe and needle through the septum.

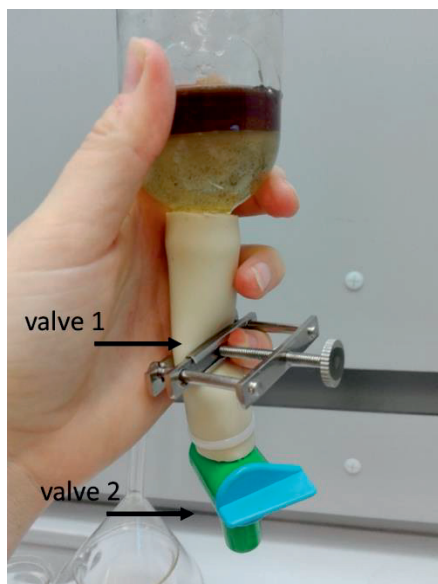
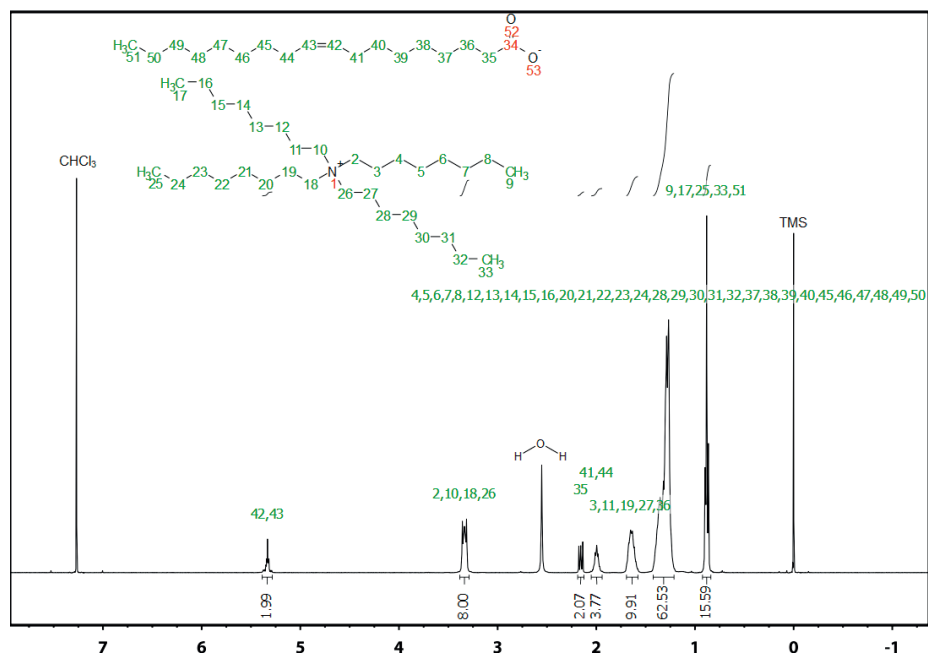
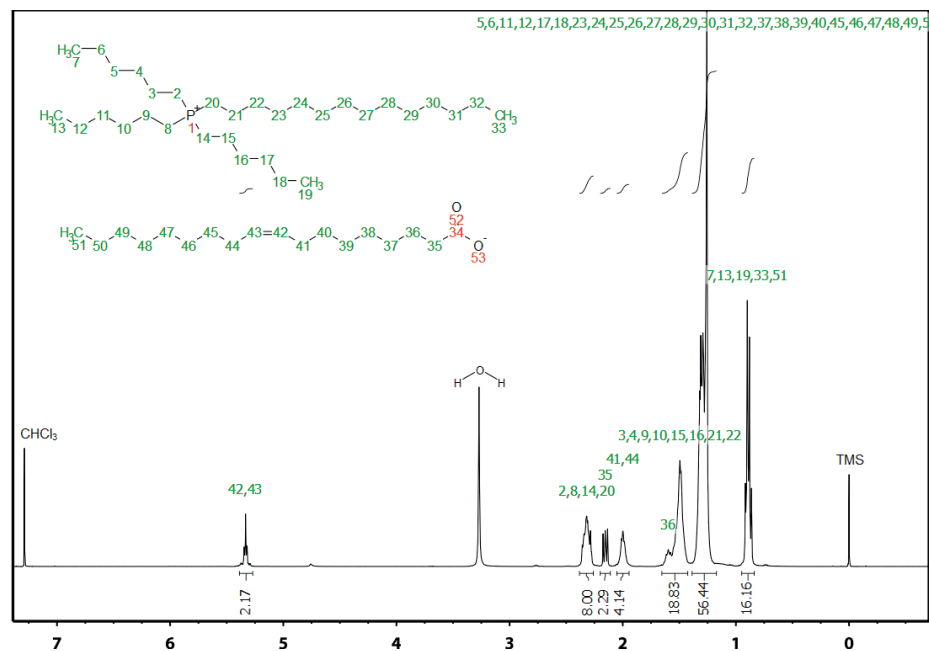
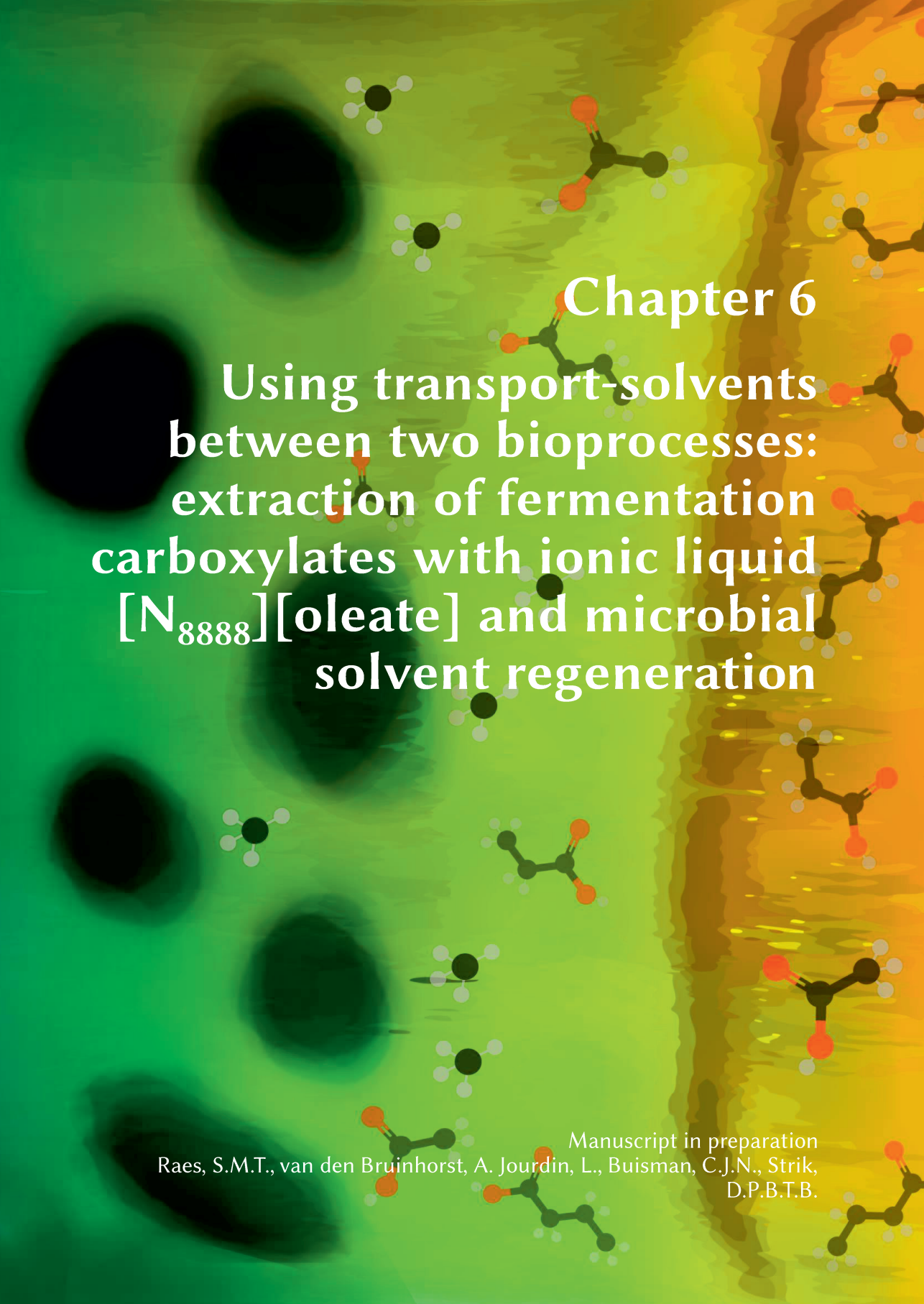


Figure S5.4: Separation unit (= constructed double valved separation funnel) to separate water phase and granules from IL in such a manner that the granules don't touch the IL.

Figure S5.5: ^1H -NMR spectrum of $[\text{N}_{888}][\text{oleate}]$ Figure S5.6: ^1H -NMR spectrum of $[\text{P}_{66,14}][\text{oleate}]$



Chapter 6

Using transport-solvents between two bioprocesses: extraction of fermentation carboxylates with ionic liquid [N₈₈₈₈][oleate] and microbial solvent regeneration

Manuscript in preparation
Raes, S.M.T., van den Bruinhorst, A. Jourdin, L., Buisman, C.J.N., Strik,
D.P.B.T.B.

Abstract

Hydrophobic ionic liquids (ILs) are novel solvents which can be used for the extraction of volatile fatty acids from aqueous streams. Currently, industrial application of such ILs is limited due to their high production costs. Hence, regeneration of ILs is essential. Here, a novel IL regeneration method is demonstrated in which methanogenic granular sludge facilitated the removal of VFAs from [N₈₈₈][oleate]. This microbial assisted regeneration is beneficial as no additional salt is needed for pH control of the bioprocess or recovery of the products from the IL.

The reusability of [N₈₈₈][oleate] was demonstrated in two successive cycles of extraction and microbial regeneration. These experiments present the potential of the novel concept of using hydrophobic ILs as transport liquids between two bioprocesses.

Introduction

Organic residual streams hold great promise as alternative renewable feedstock to replace fossil resources in the production of platform chemicals.^{155,156} Such waste streams can be converted into chemical building blocks, i.e. short volatile fatty acids (VFAs), via fermentative pathways using either soluble electron donors^{36,79,157} or an electrode as electron source.¹²⁷ Due to the low concentrations of VFAs reached in these bioprocesses, effective recovery from dilute aqueous solutions is essential.

Among the recovery methods for carboxylates, liquid-liquid extraction (LLE) is reported to be efficient and economical.¹⁹⁴ However, conventional organic solvents used for LLE are often volatile, flammable, and toxic for the environment. In search for more eco-friendly and sustainable solvents, ionic liquids (ILs) were developed.¹⁶¹ ILs are molten salts (melting temperatures often below 100°C) typically comprised of large organic cations combined with organic or inorganic anions.^{65,71} By choosing the type of ions in an IL (e.g. branching or anion alkyl chain length) the physical characteristics can be tailored.^{72,162,163}

Because the IL properties can be adjusted, ILs can also be tailored for selective extraction of VFAs from dilute aqueous streams. Yet, the current high production costs of ILs prevent their application as extractants in industrial processes.¹⁷⁵ For that reason, ideally an IL is re-used and, in case it cannot be re-used, it is important to regenerate it.^{175,195} Regeneration of ILs after extraction has not been investigated intensively to date. Parmentier et al. evaluated two regeneration methods for the IL [N₈₈₈][oleate] after metal extraction¹⁷⁵ and several other regeneration methods and their potential are reviewed by Fernandez et al.¹⁹⁵

In this study, a novel IL regeneration method is introduced in which microorganisms assist in the extraction of VFAs from a hydrophobic IL. This microbial assisted IL regeneration concept is based on microorganisms consuming the back-extracted VFA from the IL. In that way the equilibrium distribution of the VFA between water and solvent shifts constantly, thereby facilitating the transfer of VFAs from the IL into the water phase. Similar to tailoring an IL for specific product extractions, specific microbiomes or defined cultures could be applied in the regeneration step. Ultimately, the IL would be regenerated simultaneously with VFAs recovery, converting the VFAs into a more valuable product.

In practice, such IL regeneration step does not necessarily need to take place in/at the same physical location, time, and/or medium, as where the extraction of VFAs into the IL occurs. Hence, the loaded IL can be regarded as a transport liquid in which the extracted VFAs are temporarily stored. After VFA extraction, the loaded hydrophobic IL phase can be separated from the water phase based on the density

differences of the immiscible phases. After separation, the loaded IL can be transported to the desired location for regeneration and recovery of the product at any desired moment. For ILs with high VFA affinity, the final VFA concentration in the IL is higher than the initial concentration in the water phase. Hence, less mass has to be transferred and less energy/money has to be spent on the transportation of the loaded IL to the location where the VFAs will be extracted/recovered.

The specific requirements for a hydrophobic IL to be used as transport liquid are i) selective extraction of targeted compound(s), ii) bioprocess compatibility of the IL,¹⁹⁶ iii) the concentration of targeted compound(s) that can be achieved in the IL are significantly higher than the feed concentration, and iv) the regeneration of IL is done in a sustainable way, i.e. performed using minimal energy consumption and without the use of toxic chemicals,¹⁷⁵ e.g. via microbial assisted regeneration.

When the concept of an IL as transport liquid is coupled with the proposed microbial regeneration method, two distinct biological processes can be coupled. For example, in decentral anaerobic digestion short volatile fatty acids are generated during acidification of organic residual streams and are on site extracted into an IL. After separating the IL from the fermentation broth, only the loaded IL is transported to a central regeneration plant. There the VFAs are removed from the IL by microbial assisted regeneration, in which the VFAs serve as feedstock for the production of added-value products (Figure 6.1).

This study demonstrates the proof of principle of the microbial assisted regeneration of an IL, the subsequent reusability of the IL, and the concept of an IL as transport liquid. The IL [N₈₈₈₈][oleate] showed promising results in our previous experiments in terms of bioprocess compatibility,¹⁹⁶ therefore the current research continued with this solvent. To demonstrate the transport liquid concept, two cycles of loading the IL (i.e. extraction of VFAs into the IL) and subsequent microbially assisted regeneration were performed. The two consecutive cycles of loading and regeneration give insight in i) the microbial compatibility of [N₈₈₈₈][oleate], ii) microbially assisted regeneration as a novel IL regeneration method, and iii) the reusability of the IL as transport liquid in the coupling of two biological processes.

Materials & Methods

To assess the microbial compatibility and the reusability of the ionic liquid tetraoctylammonium oleate ([N₈₈₈₈][oleate]) two consecutive cycles were performed. Each cycle comprised a loading (VFA extraction into the IL), and a microbial regeneration step (VFA back-extraction from the IL assisted by microorganisms), see Figure 6.2.

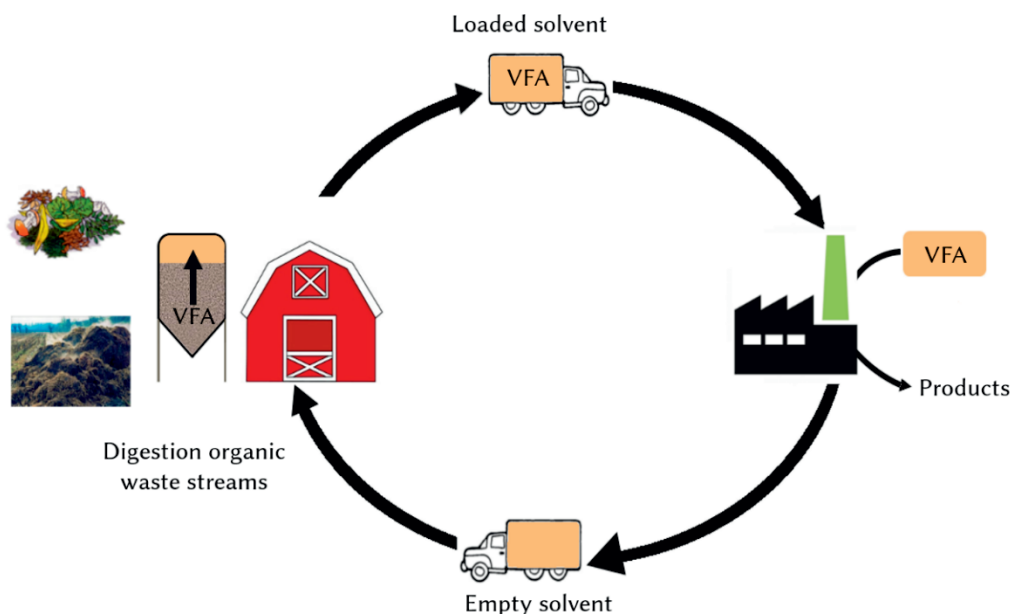


Figure 6.1: Novel concept of an ionic liquid (IL, orange) as transport liquid for the coupling of two distinct biological processes. One possible application could be decentralised anaerobic digestion towards volatile fatty acids (VFAs) and extraction of them into the solvent (orange). The loaded solvent is transported to a central facility where the products are extracted and converted into biobased products. The emptied IL is transported back to the decentral location to be loaded again.

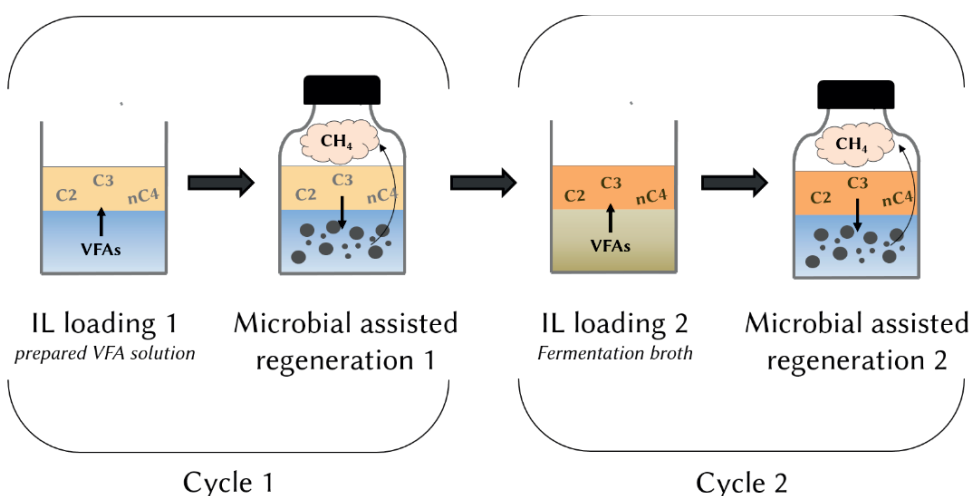


Figure 6.2: Schematic overview of the experimental design in which the reusability and the microbial compatibility of $[N_{888}][oleate]$ were evaluated. Cycle 1 employs unused ionic liquid (yellow top phase). The second cycle continues to re-use the same ionic liquid (orange top phase).

Cycle 1 – VFA extraction into [N₈₈₈][oleate]

The IL [N₈₈₈][oleate] used throughout this research was synthesised as previously reported¹⁹⁶ in a one-step water-based procedure. For loading the IL, an aqueous solution containing acetic acid (C₂; Merck, 99-100%), propionic acid (C₃; Sigma Aldrich, >99.5%) and butyric acid (nC₄; Merck, >99%) was prepared by adding 0.8 ml of each acid into 0.5 L demi water. From here, this VFA mixture is referred to as the VFA-stock solution, and has a concentration of ~1.5 g L⁻¹ of each acid. For loading of the IL, 70 ml of IL (62.33 g) was mixed vigorously with 70 ml of the VFA-stock solution for 10 minutes using a magnetic stirrer (>700 rpm), after which the two phases were separated in a separation funnel overnight. Aqueous phase samples were taken before and after extraction and were analysed for volatile fatty acids by gas chromatography as previously reported.¹²⁹ After separation, the aqueous phase was discharged and the loaded IL was used for successive experiments.

Cycle 1 – microbial assisted regeneration of VFAs from IL

The microbial compatibility of [N₈₈₈][oleate] was studied using anaerobic batch experiments. Serum bottles (total volume excluding stopper 117.6 ml ± 0.77) were filled with 50 ml total volume. For tests involving ILs bottles were filled with 30 ml medium and 20 ml IL (average IL weight added to bottles was 18 ± 0.06 g), resulting in a volumetric solvent to feed ratio (S/F ratio) of 2/3. Mineral medium was prepared as described by Lindeboom et al.,¹⁹² prior to use its pH was adapted to 7.15 using 1 M NaOH. If applicable, 1.5 g wet sludge (0.134 gVSS (g wet sludge)⁻¹) was added to the medium prior to adding the IL, in this manner the sludge did not come into direct contact with the IL. The same anaerobic granular sludge was used as in previous work.¹⁹⁶ After IL was added, the headspace of the bottle was flushed with pure N₂ and sealed with a butyl-rubber stopper and aluminium crimp cap. After filling, the bottle was placed in 30°C shaker at 110 rpm.

Six controls (Figure 6.3 and Table 6.1) were included to i) verify the ability of the sludge to convert the supplied carbon source (positive control 1 with C₂ and positive control 2 (pos2) with C₂, C₃ and nC₄), ii) quantify the amount of methane produced from remaining COD in the sludge (negative control 1), iii) investigate the effect of [N₈₈₈][oleate] on a water phase with and without sludge present (negative control 2 and 3), and iv) estimate the equilibrium concentrations of the VFAs in the medium (negative control 4). Control bottles without IL, positive controls 1 and 2, and negative control, were filled with 50 ml medium and sludge. Sodium acetate was added to the medium of positive control 1 up to a concentration of 2 g L⁻¹ (~2.1 gCOD L⁻¹). For positive control 2 the VFA-stock solution was diluted three times resulting in ~0.5 g L⁻¹ of each acid (~0.5 gCOD L⁻¹ C₂, ~0.8 gCOD L⁻¹ C₃, ~0.9 gCOD L⁻¹ nC₄). Hence, the microorganisms were supplied with a similar

amount of substrate as present in the loaded IL. Bottles of the negative controls 2, 3, and 4 contained 30 ml medium without carbon source, and 20 ml IL).

During the regeneration, the headspace pressure of the bottles was measured versus time using a digital pressure meter (Greisinger GMH 3151). When the pressure did not increase significantly anymore, the headspace composition was analysed for CO_2 , CH_4 , O_2 , and N_2 accordingly Raes et al.¹²⁷ Subsequently, the bottles were opened, the pH was measured, and the aqueous phase was analysed for VFAs (C2 to C8) and alcohols (methanol to hexanol).¹²⁹

The previously loaded and now microbially regenerated IL was separated from the water phase by removing the granules and aqueous phase from the bottles. In this manner the loss of IL was limited to less than 1 wt% of original IL weight for all triplicates, and direct contact of IL and granules could be prevented (for detailed method, see ref ¹⁹⁷).

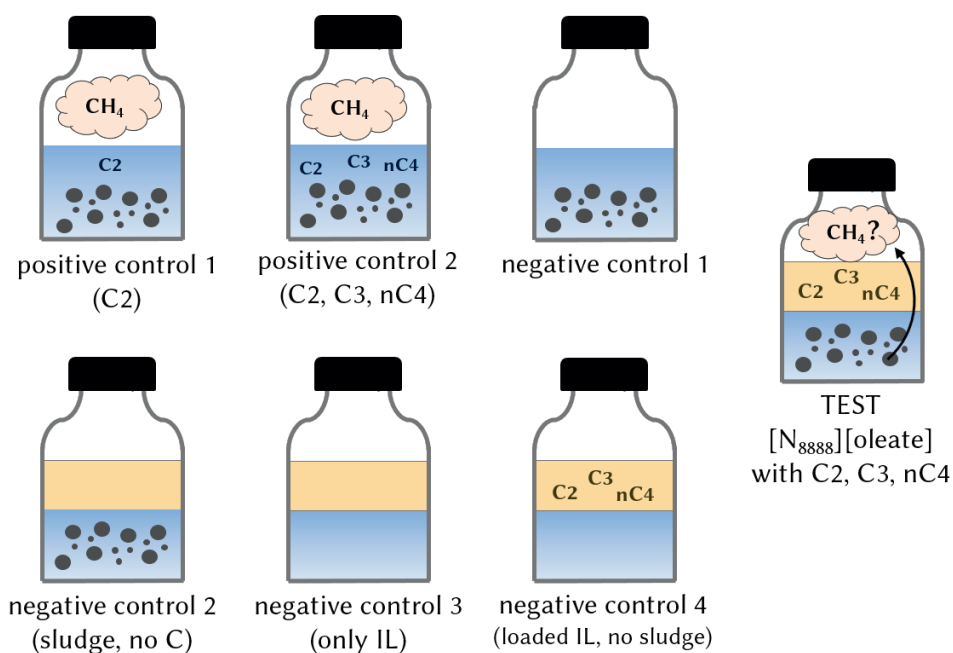


Figure 6.3: Schematic overview of the experimental design of the microbial assisted regeneration of the VFAs acetic acid (C2), propionic acid (C3) and butyric acid (nC4) from the ionic liquid $[N_{888}][oleate]$.

Table 6.1: Overview of the composition of each serum bottles during the microbial assisted regeneration cycle 1.

| | Medium [ml] | IL [ml] | Carbon source | Loading [mgCOD gVSS ⁻¹] | Sludge [gVSS] |
|---|----------------|------------|------------------|--|------------------|
| TEST: [N ₈₈₈][oleate]+ VFAs | 30 | 20 | VFAs in IL | ~ 700 | 0.2 |
| Positive control 1 (C2) | 50 | - | C2 | ~ 500 | 0.2 |
| Positive control 2 (C2, C3, nC4) | 50 | - | C2, C3, nC4 | ~ 550 | 0.2 |
| Negative control 1 | 50 | - | - | - | 0.2 |
| Negative 2 (sludge, no C) | 30 | 20 | - | - | 0.2 |
| Negative 3 (only IL) | 30 | 20 | - | - | - |
| Negative 4 (loaded IL, medium) | 30 | 20 | VFAs in IL | - | - |

Positive control 2 (C₂, C₃, nC₄) was performed in 5 replicates, negative control 4 in duplicate, all other experiments were performed in triplicate.

To verify the role of the microorganisms in the regeneration, loaded [N₈₈₈][oleate] was contacted for 24 days without sludge to examine the VFAs concentration in the water phase after contact time (negative control 4). In order to load the [N₈₈₈][oleate], 20 ml IL was mixed vigorously at 700 rpm with 20 ml VFA stock-solution for 15 minutes. Bottles were placed upside down and after phase separation the water phase was removed using a needles syringe piercing through the septum. 30 ml mineral medium was added to the loaded IL was and placed for 24 days in shaker at 110 rpm and 30°C. After this contact time, the water phase was analysed for VFAs using GC.

Cycle 2 – VFA extraction into [N₈₈₈][oleate] using fermentation broth

A filtered fermentation broth was prepared prior to extraction. In a 1 L bottle, 0.5 L mineral medium, 2.8 g D-glucose, 1.6 g sodium 2-bromoethanesulfonate (Na-2-BES) and 39.3 g wet sludge were added. Na-2-BES was added to prevent produced VFAs to be converted into methane. To release possible gasses produced during fermentation, the headspace of the bottle was connected to a water lock and was incubated for 3 days at 30°C and 110 rpm. After 3 days the broth was vacuum pump filtered using first 20-200 µm filter (Whatman, cat. 4) and subsequently 8 µm filter (Whatman ashless, cat. 40). The filtrate was sampled for VFA analysis using GC.

The VFA concentration in the filtrate was lower than that of the VFA solution prepared for cycle 1. In order to offer the IL as much COD as during cycle 1, the S/F ratio of the extraction needed to be 1:2. Therefore, 40 ml of fermentation broth was added to each bottle with 20 ml regenerated IL. Vigorous stirring for 10 min using a magnetic stirrer resulted in an emulsion. The bottles were left for more than 1 h to separate the two phases, after which the magnetic stirrer was removed. Small loss of IL from the bottles could not be prevented here. The bottles were closed and left for 2 days upside down to advance phase separation. Before continuation of the experiments with the reloaded ILs, the aqueous phase was carefully removed using a needle and syringe via the septum while the bottle was kept upside down.

Cycle 2 - microbial assisted regeneration of VFAs from IL

The microbial regeneration of cycle 2 was similar to cycle 1 (Table 6.2) using anaerobic batch experiments. Positive control 2 (C₂, C₃, nC₄) was included with 5 replicates and a negative control was included in triplicate in this experiment. The initial pH of the aqueous phase at the start of the experiment was 7.14 for the negative control, and the pH of the positive control and the reloaded IL bottles was 4.45 due to no pH adaptation of the medium prior to closing the bottles (manual error). After 2.9 days of incubation methane production was little, even in the positive control. pH was identified as limiting parameter and subsequently adapted by addition of 3 drops of 4 M KOH through the septum. Incubation was stopped after 23.6 days, and headspace and aqueous phase analysis were performed. After analysis the regenerated IL was separated from the aqueous phase.

Table 6.2: Overview of the composition of the serum bottles during the microbial assisted regeneration cycle 2.

| | Medium [ml] | IL [ml] | Carbon source | Loading [mgCOD gVSS ⁻¹] | Sludge [gVSS] |
|--|----------------|------------|---|--|------------------|
| [N8888][oleate]+ VFAs | 30 | ~ 20 | VFAs in IL | ~ 400 | 0.2 |
| Positive control 2 (C ₂ , C ₃ , nC ₄) | 50 | - | C ₂ , C ₃ , nC ₄ | ~ 550 | 0.2 |
| Negative control | 50 | - | - | - | 0.2 |

Positive control was performed in 5 replicates, negative control and regeneration from IL in triplicates.

Extraction experiments after cycle 2

After cycle 2 several small volume extraction experiments were performed in 12 ml crimp cap vials to evaluate i) the extraction capacity of the recycled IL compared to the extraction of VFAs into the IL of cycle 1, ii) the extraction capacity of the IL over a concentration range, and iii) the extraction capacity from a fermentation broth of used IL compared to unused IL. For this purpose, the same S/F ratio of 2/3 was chosen using 3 ml aqueous phase and 2 ml IL (Table 6.3). 0.15 g L⁻¹ VFA solution was prepared by diluting the VFA stock solution 10 times. 15 g L⁻¹ VFA solution (16.7 gCOD L⁻¹ C₂, 25.8 gCOD L⁻¹ C₃, 30.5 gCOD L⁻¹ nC₄) was prepared by addition of 0.8 ml of each acid in 50 ml demi water. The vials were closed with a septum and were stirred vigorously using magnetic stirrer for 15 min resulting in emulsions. After stirring, phases were separated by placing the vial upside down over night. Aqueous liquid samples were taken before and after extraction and analysed for pH, and VFAs and alcohols using GC.

Table 6.3: Small volume extraction experiments performed after cycle 2 to verify reusability of the IL.

| Extraction* | IL | IL [ml] | Aqueous phase | Aqueous phase [ml] |
|-------------|-----------|---------|--|--------------------|
| 1 | Reused ** | 2 | VFA stock solution 1.5 g L ⁻¹ of C ₂ , C ₃ , and nC ₄ | 3 |
| 2 | Unused | 2 | Fermentation broth | 3 |
| 3 | Unused | 2 | 1/10 dilution VFA stock 0.15 g L ⁻¹ of C ₂ , C ₃ , and nC ₄ | 3 |
| 4 | Unused | 2 | 10x VFA stock solution 15 g L ⁻¹ of C ₂ , C ₃ , and nC ₄ | 3 |

* All extractions were performed in duplicate.

** Reused IL: of the three replicates employed in the microbial regeneration experiment, two IL samples were taken.

Extraction evaluation

The extraction performance of loading (extraction into the IL) and microbial regeneration (extraction of VFAs from the IL) was evaluated via i) the distribution coefficient and ii) the extraction efficiency.

The distribution coefficient (β_i) is defined at equilibrium as the fraction of the concentration of VFA in the IL (C_i^{IL}) and the concentration of VFA in the water phase (C_i^{aq}).

$$\beta_i = \frac{C_i^{IL}}{C_i^{aq}}$$

The concentration of VFAs in the IL could not be analysed directly, therefore it was derived using mass balances. During the microbial regeneration an unknown amount of each of the VFAs is converted to CH₄, so the VFAs could not be monitored individually. In order to allow the comparison of distribution coefficients and extraction efficiencies upon loading between cycle 1 and 2, their units should be the same. Hence, the concentration of VFAs in the water phase and the organic IL phase were expressed based on chemical oxygen demand (COD; mgCOD g_{IL}⁻¹ and mgCOD g_{aq}⁻¹).

The extraction efficiency (E) is calculated using the VFA concentration (mgCOD L⁻¹) in the water phase before ($C_{i,start}^{aq}$) and after extraction ($C_{i,end}^{aq}$):

$$E = \frac{C_{i,start}^{aq} - C_{i,end}^{aq}}{C_{i,start}^{aq}} \times 100\%$$

To evaluate the extraction efficiency during the microbial regeneration steps, the concentration of VFAs in the IL. This microbial assisted extraction efficiency is expressed as:

$$E_{\text{microbial assisted}} = \frac{COD_{start}^{IL} - COD_{end}^{IL}}{COD_{start}^{IL}} \times 100\%$$

[N₈₈₈][oleate] was saturated with water after synthesis, prior to the first loading step of cycle 1. The water content of the IL was therefore assumed to be constant. Hence, a change of volume and mass of the IL and water phase due to the transfer of VFAs or water was considered negligible during extraction and regeneration.

Results & Discussion

Cycle 1 - Loading of IL using VFAs in water

In order to assess whether microorganisms are able to assist the extraction of VFAs from [N₈₈₈][oleate], first the VFAs needed to be extracted from a water phase into the IL. The loading of the IL was done using a defined mixture of the three VFAs acetic acid (C2), propionic acid (C3) and n-butyric acid (nC4) in water. Because the pH determines whether the VFA is present in the acid or carboxylate form, here the Cx notation is used to designate either form from now on. The extraction efficiencies

of VFAs into the water-saturated [N₈₈₈₈][oleate] were $\geq 98\%$ for all acids (Table 6.4). The extraction of the VFAs caused the pH of the water phase to increase from initially 3.00 to 5.38 after extraction. The IL loading resulted in 7.9 mgCOD g_{IL}⁻¹ extracted VFAs to serve as feedstock in the subsequent microbial regeneration step.

Table 6.4 shows that [N₈₈₈₈][oleate] selectivity was increased with increasing hydrophobicity; the distribution coefficients increased with the alkyl chain length of the VFAs studied. This is in agreement with previously reported results, as most organic solvents applied as extractants for the LLE of VFAs from (idealised) fermentation broths showed to be more selective to the more hydrophobic VFAs.^{67,70,159}

Table 6.4: Cycle 1 – extraction of acetic acid, propionic acid and butyric acid into [N₈₈₈₈][oleate]. Extraction efficiency and distribution coefficient for each individual acid and total of the acids together.

| | C2 | C3 | nC4 | Total |
|--|------|-------|-------|-------|
| E [%] | 98.1 | 99.1 | 99.6 | 99.0 |
| β_i [g _{aq} g _{IL} ⁻¹] | 57.8 | 124.8 | 254.8 | 112.6 |

The distribution coefficients obtained for [N₈₈₈₈][oleate] were significantly higher than those reported in literature. Marták et al. reported a lactic acid distribution coefficient of just above 40 when using Cyphos IL-104 at similar acid concentration, pH, and solvent-to-feed ratio.⁶⁷ Oliveira et al. reached distribution coefficients ranging from approximately 1.5-5, but it has to be noted that they calculated it differently by taking third phase formation into account, which leads to lower values that are more realistic when a third phase is present.¹⁹⁷ Reyhanitash *et al.* reached an acetic acid distribution coefficient of ca. 14 under comparable conditions using the [P_{666,14}][Phos] IL.⁷⁰ In these studies the distribution coefficient increased with decreasing feed concentration^{67,70,197}, and this trend was observed as well for this initial IL loading step. It has to be noted that the extraction conditions, such as pH,^{70,194,198} acid concentrations,^{67,70,198,199} and the presence of multiple acids affect the extraction performance of a solvent. The applied feed concentration for each VFA in this study was relatively low (approximately 1.5 g L⁻¹ or 17-28 mmol L⁻¹) compared to previous studies

towards the LLE of VFAs using ILs, which might explain the higher distribution coefficients obtained here. Despite the indicative nature of the comparison between literature values and the obtained distribution coefficients, the extraction efficiencies and distribution coefficients showed that the initial loading step was successful.

Cycle 1 - Microbial assisted regeneration of IL

After loading the IL with VFAs, the microbial regeneration was tested using methanogenesis as model bioprocess. Methanogenesis was chosen because it is a well-known bioprocess,⁷⁷ and because in earlier work the IL [N₈₈₈][oleate] showed potential to be used in combination with this bioprocess.¹⁹⁶ In that previous study methanogenic granular sludge was incubated in mineral medium which had a floating [N₈₈₈][oleate] phase on top. After the exposure period, the granules were still viable and could convert acetate to methane, contrary to a similar phosphonium-based IL.

To assess the regeneration of the loaded IL in this study, the headspace pressure increase in the serum bottles was followed over time (Figure 6.4). A pressure increase in the IL-regeneration bottles (hereafter: test bottles) indicates microbial methane production using VFAs recovered from the loaded IL. The methane production of the negative control 1 (neg1) was negligible and related to decaying sludge and residual organic matter still present in the sludge and available for methanogenesis. In negative control 2 (neg2) no methane was detected in the headspace, affirming the IL itself was not degraded by the microorganisms.

The results for positive control 1 (pos1, Figure 6.4) show that the sludge could easily convert acetate into methane, depleting the substrate and reaching the maximal pressure increase within 3 days. Acetate was also easily converted when a mixed VFA feed was applied (pos2 and tests), expressed by the pressure increase in the first four days and a final acetate concentration in the aqueous phase of ≤ 12 mgCOD L⁻¹.

In the test bottles the transport of acetate from the IL to the aqueous phase was not rate limiting since the pressure increased similarly to pos2 during the first 6 days (Figure 6.4). The successive pressure increase from day 6 onwards in pos2 can be assigned to butyrate degradation. After 22 days the butyrate concentration in the water phase decreased to < 5 mgCOD L⁻¹ for pos2, which indicates that the sludge was able to degrade butyrate fully. The pressure increase in the tests did not follow the trend of pos2 after the first 6 days. At the end of the regeneration phase a butyrate concentration of 106 ± 15 mgCOD L⁻¹ was measured in the water phase. The relatively high butyrate concentration indicates that the conversion of butyrate was

impeded or inhibited. However, a lower conversion rate in the presence of IL is in line with our previous results.¹⁹⁶ After 24 days no plateau in pressure increase was reached for the test bottles. Hence, butyrate conversion might have continued beyond 24 days when the bottles would not have been opened. At the end of the regeneration period, the methane content in the headspace of the test bottles was 30.0 ± 0.7 % and in pos2 this was 31.1 ± 0.3 %. This confirms that the pressure increases were indeed caused by methanogenesis.

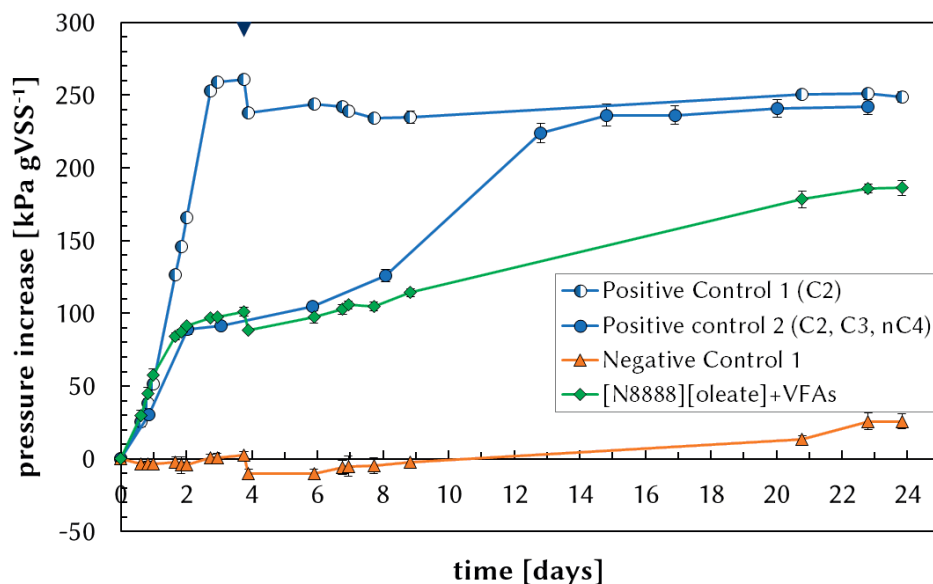


Figure 6.4: Cycle 1 – microbial assisted IL regeneration. Pressure increase in the serum bottles over time per g VSS of biomass. At day 3.8 preliminary headspace samples were taken (inversed blue triangle). Negative controls 2, 3 and 4 were excluded from this graph as the pressure did not change over the time of the experiment.

Verification ‘microbial assisted’ regeneration of IL

In order to verify whether the presence of microorganisms contributed to the regeneration of loaded IL, negative control 4 (neg4) was included. In that control experiment loaded IL was contacted to medium without sludge for 24 days, exploring what the aqueous equilibrium concentrations would be when no VFAs were consumed by microorganisms. After 24 days, 22.5 ± 0.3 % of the total IL-loaded COD was detected in the water phase (Table S6.3). This means that a part of the VFAs were back-extracted from the IL only by changing the water phase from a water-acid mixture to mineral microbial medium. The neg4 distribution coefficients were calculated for the loading step as well as for the regeneration after equilibrium

with mineral medium (Table S6.3), they indeed show a strong decrease for all VFAs when medium is applied.

Several factors can impact the equilibrium distribution of VFAs: the total amount of VFAs in the system, the concentration of components other than VFAs, and the pH of the water phase.^{70,159,198,199} Most likely, the latter two factors contributed to the back-extraction of VFAs upon the medium change. The regeneration medium contained various salts as it is a mineral microbial medium. The addition of salts at low concentrations, results typically in lower distribution coefficients.⁷⁰ Moreover, the pH of the regeneration medium was approximately 7, while that of the VFA solution applied for loading was 3 (increasing to 5.4 after extraction). Typically, mostly protonated acids are extracted, especially because the anion of [N₈₈₈][oleate] has a low water solubility and will not easily participate in an ion exchange with deprotonated VFAs. Other solvents that only extract protonated VFAs exhibit a strong shift in equilibrium between pH 4-7.^{70,159,198,199} Hence, it is rationalised that the loaded VFAs in neg4 were mainly back-extracted from the IL via a pH swing and a higher salt concentration upon changing the aqueous medium.

When sludge was present in the aqueous phase under the loaded IL (i.e. test bottles), the back-extracted VFAs were consumed and converted into methane. Since the VFA concentration in the aqueous phase decreases upon conversion to methane and carbon dioxide, which leave liquid phase, equilibrium was constantly reinstated and VFA transport to the medium was promoted. After 24 days, 55.8 ± 0.6 % of the IL-loaded COD was back-extracted (Table 6.5), which corresponds to the microbial assisted extraction efficiency.

Table 6.5: Microbial assisted regeneration – Comparison of cycle 1 and 2. Table shows conversion parameters, amount of COD present in IL and water phase at the end of the regeneration steps and the microbial assisted extraction efficiency calculated based on the amount of COD extracted from the IL during regeneration. Data represent the averages, and standard deviation of the triplicates. For individual results see supplementary information.

| Cycle | Start in IL [mgCOD _{IL}] | Feed load per biomass [mgCOD gVSS ⁻¹] | Methane produced [mgCOD _{CH₄} gVSS ⁻¹] | End mgCOD _{aq} | End mgCOD _{IL} | Microbial assisted extraction efficiency [%] |
|-------|---------------------------------------|--|---|----------------------------|----------------------------|---|
| 1 | 143.5 ± 2.0 | 708.1 ± 7.7 | 288.7 ± 0.8 | 21.6 ± 0.6 | 63.4 ± 1.4 | 55.8 ± 0.6 |
| 2 | 79.5 ± 2.0 | 388.8 ± 12.6 | 145.4 ± 35.5 | 19.1 ± 6.9 | 30.7 ± 1.6 | 61.4 ± 1.3 |

The extracted COD was the sum of COD detected as methane and the COD of non-converted VFAs in the water phase. The total concentration of non-converted COD was similar for pos2 and the tests (see Table S6.2). The COD remaining in the water was mostly comprised of propionate, for pos2 this was 99.3 % and for the tests 84.3% of the aqueous COD. These results indicate that the employed sludge was not adapted to utilize propionate as substrate for methanogenesis.²⁰⁰ Therefore, it is plausible that utilising more adapted sludge could increase the microbial extraction efficiency.

Theoretically, microbial regeneration continues until the aqueous equilibrium concentration of the VFAs is too low to be converted by the sludge, or until the activity of the sludge has decayed. In the tests, acetate was readily converted and only low concentrations of acetate were measured in the water phase after regeneration. Despite butyrate was not fully converted in the tests, the resulting aqueous concentrations were lower than the equilibrium concentration obtained in neg4 without sludge. Additionally, the microbial assisted extraction efficiency was 55.8 % as compared to 22.5 % for neg4. Hence, it can be concluded that the microorganisms did shift the distribution of the VFAs and thereby aided the regeneration of the IL.

Additional benefits of microbial regeneration of an IL

Microbial assisted regeneration holds promise as regeneration method for economical as well as environmental reasons. Unlike common solvent regeneration processes involving pH swing,¹⁵⁹ microbial assisted regeneration of the IL phase does not require a stoichiometric addition of base salt. Methanogenesis is an acid consuming reaction, therefore the water phase does not acidify when the back-extracted VFAs are converted into methane and carbon dioxide. In this way no base or acid addition is required for pH control during microbial conversion of VFAs. Additionally, the change of pH between the IL loading and the subsequent regeneration step promotes back-extraction. Since both processes are decoupled, the need for salt addition to recover the products is eliminated. It has to be noted that in this study methanogenesis was only selected as a proof-of-principle bioprocess. Other pure or mixed culture microbial processes, e.g. polyhydroxyalkanoates production, that consume the carboxylate and the proton (i.e. acids) are also potentially viable, allowing the production of added-value chemicals other than methane.²⁰¹

Conclusively for cycle 1, the used anaerobic granular sludge was active in the presence of [N₈₈₈₈][oleate], thereby designating [N₈₈₈₈][oleate] as a bioprocess compatible IL – which is in accordance to the potential bioprocess compatibility shown in our preliminary study.¹⁹⁶ Moreover, the microorganisms were able to use

the VFAs from the IL as their substrate and thereby facilitating the extraction of VFAs from the IL, demonstrating that microbial assisted regeneration of [N₈₈₈][oleate] is possible without a stoichiometric addition of base salt.

Cycle 2 – Loading of regenerated IL using fermentation broth

The reusability of [N₈₈₈][oleate] was investigated by applying used IL from cycle 1 in a new extraction cycle. Based on the COD balance, the amount of VFAs in the IL at the end of cycle 1 was 63.4 ± 1.4 mgCOD. This amount of COD remained in the IL until loading in cycle 2. In order to explore the potential reuse of [N₈₈₈][oleate], and to explore a more complex – though more realistic – aqueous matrix, the used IL was exposed to a filtered fermentation broth (composition in Table 6.6)

Table 6.6: Composition of the organic acids and alcohols in the fermentation broth used for loading the IL in cycle 2. All these organics could serve as substrate for methanogenesis. All concentrations in mgCOD L⁻¹.

| C2 | C3 | nC4 | ethanol | propanol | butanol |
|-----|-----|------|---------|----------|---------|
| 584 | 330 | 1732 | 94 | 99 | 87 |

Table SS6.4 shows that used IL could extract VFAs from the fermentation broth, although the extraction was not as efficient as the loading step of cycle 1. The extraction of VFAs from the fermentation broth is graphically depicted for each triplicate in Figure 6.5. The C3-extraction efficiencies were below -100% for all triplicates, signifying that the aqueous C3 concentration was more than two times higher after extraction than before extraction (Figure 6.5). The increase of aqueous C3 originated from the IL, from which C3 was only partly removed during the microbial regeneration in cycle 1. This confirms that the applied anaerobic sludge could not degrade C₃.

Figure 6.5 shows that the aqueous C2 concentration remained fairly constant, while the more hydrophobic nC4 was reduced significantly after loading. The loading using the fermentation broth resulted in 79.5 ± 2 mgCOD present in the IL (including the COD present after cycle 1). This corresponds to a total VFA concentration of 4.4 ± 0.1 mgCOD g_{IL}⁻¹, which served subsequently as feedstock for the regeneration step of cycle 2.

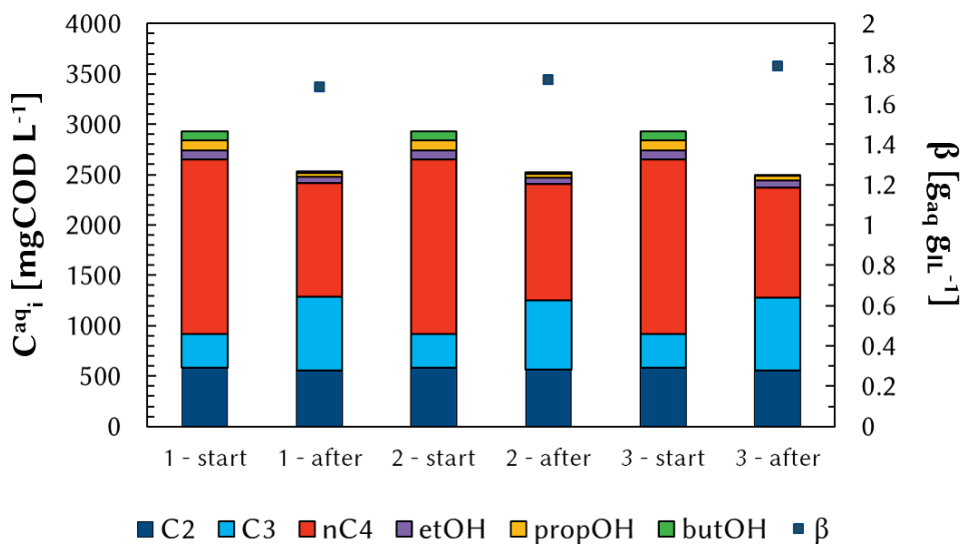


Figure 6.5: Cycle 2 – extraction of VFAs from fermentation broth into the IL $[N_{888}][oleate]$. Concentrations of the extracted compounds in the water phase before and after extraction are depicted for each triplicate of reused IL (1, 2 and 3). For each replicate the total distribution coefficient is presented (black squares).

Cycle 2 - Microbial assisted regeneration of IL

Because the IL loading of cycle 2 resulted in ~45% less COD in the IL as compared to cycle 1, less substrate was available for the microorganisms during regeneration (Table 6.5). Consequently, pos2 of cycle 2 was supplied with 1.4 times as much COD as the tests, ~560 mgCOD gVSS⁻¹ compared to ~400 mgCOD gVSS⁻¹ respectively. At the end of the regeneration of cycle 2, the headspace pressure in pos2 increased 3 times more than the tests with VFAs in the reused IL (Figure 6.6). The methane content of positive control 2 was 28.2 ± 0.7 % compared to 16.0 ± 3.4 % for the tests. Hence, the COD present in the IL was partly converted into methane.

The calculated microbial assisted extraction efficiency of cycle 2 was 61.4 ± 1.3 %, which is comparable to the efficiency obtained in cycle 1 (Table 6.5). The non-converted back-extracted COD present in the water phase consisted of mainly C3 (39.1 %) and nC4 (59.6 %) (Table S6.2). In comparison, in pos2 99.3 % of this non-converted COD in the water phase was C3, similarly as in cycle 1. To further compare the regeneration of cycle 1 to that one in cycle 2, the final pressure increase normalised to the loaded amount of COD was calculated (Table 6.7). This measure represents the capacity of the sludge to convert the available COD into gas for both the tests and pos2. Interestingly, although the loading of the ILs was almost twice as high in cycle 1 compared to cycle 2, the pressure increase per loaded mgCOD was comparable.

The microbial assisted regeneration step of cycle 2 confirmed the ability of the sludge to convert VFAs that were loaded in the IL into methane. The microbial extraction efficiencies were similar for the first and second cycle, and the normalised pressure increase for both cycles were similar, showing that the microbial assisted recovery efficiency is not strongly affected by the loading of VFAs in the IL within these concentration ranges (2-10 mgCOD g_{IL}⁻¹).

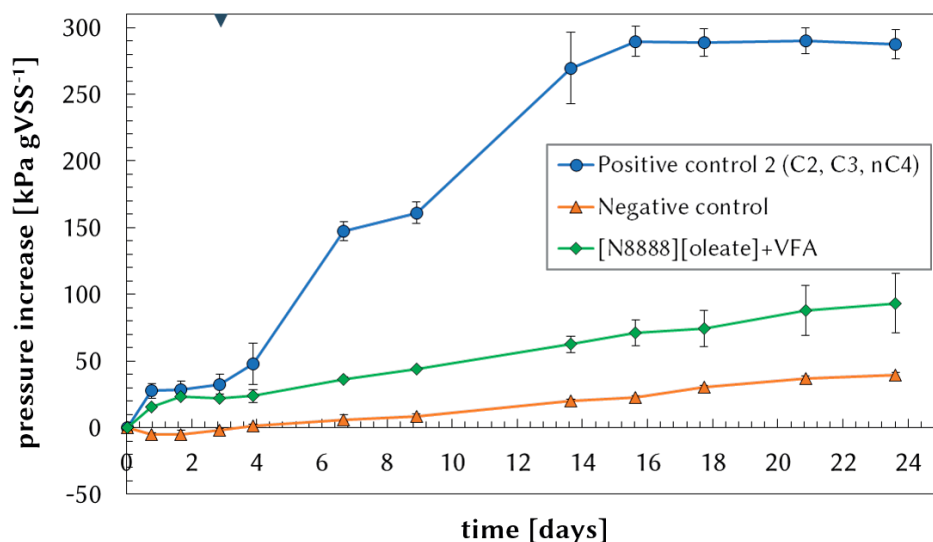


Figure 6.6: Cycle 2 microbial assisted regeneration – Pressure increase over time per g VSS of biomass. The black triangle at day 2.9 represents pH adaptation of the bottles.

Table 6.7: Comparison of microbial regeneration between cycle 1 and 2 based on the headspace pressure increase normalised to loaded COD. The tests were performed in triplicates, and the positive controls in 5 replicates.

| Cycle | Tests [kPa mgCOD ⁻¹] | Positive control 2 [kPa mgCOD ⁻¹] |
|-------|-------------------------------------|--|
| 1 | 0.26 ± 0.003 | 0.44 ± 0.01 |
| 2 | 0.24 ± 0.05 | 0.52 ± 0.02 |

Reusability of ionic liquid [N₈₈₈₈][oleate]

For ILs to become the envisioned transport liquids, they are required to be reused. After cycle 2, small volume extraction experiments were performed with used and fresh [N₈₈₈₈][oleate] to evaluate the reusability of the IL. The used IL of cycle 2 and fresh ILs were loaded using a VFA stock solution and a fermentation broth.

The extraction using the fresh IL was almost as good as with the re-used IL: end concentrations of acids in the water after extraction, and the extraction efficiencies were similar (Figure 6.7 and Table S6.5). When comparing the extraction of VFAs from the VFA stock-solution to the extraction of VFAs from a fermentation broth, several observations can be made. Firstly, overall extraction from the fermentation broth was less efficient. Despite the IL volume and S/F ratio were the same for both feed liquids, the extraction efficiencies were lower when fermentation broth was used. Secondly, the used IL did not perform much differently than the fresh IL, except in case of extraction from the fermentation broth. C₃ was back-extracted from the IL into the water phase, following a similar mechanism as for the loading step of cycle 2.

It is expected that during cycle 1 and/or cycle 2 several ions besides VFAs were transported into the IL, as the microbial medium contained several micronutrients. Salts can have both a negative¹⁷⁶ and a positive effect on the VFA distribution between aqueous phase and IL.^{202,203} The specific influence of aqueous salts on the extraction performance is yet hard to predict due to the many possible synergistic effects of the different compounds encountered in fermentation broths.

These results confirm that the water matrix which the IL needs to extract the VFAs from, heavily influences the extraction. Nonetheless, a reused IL did not show significant differences in extraction performance of the VFA stock-solution compared to a fresh IL. Therefore, these results indicate that ILs might be feasible as reusable transport liquids for extracted products.

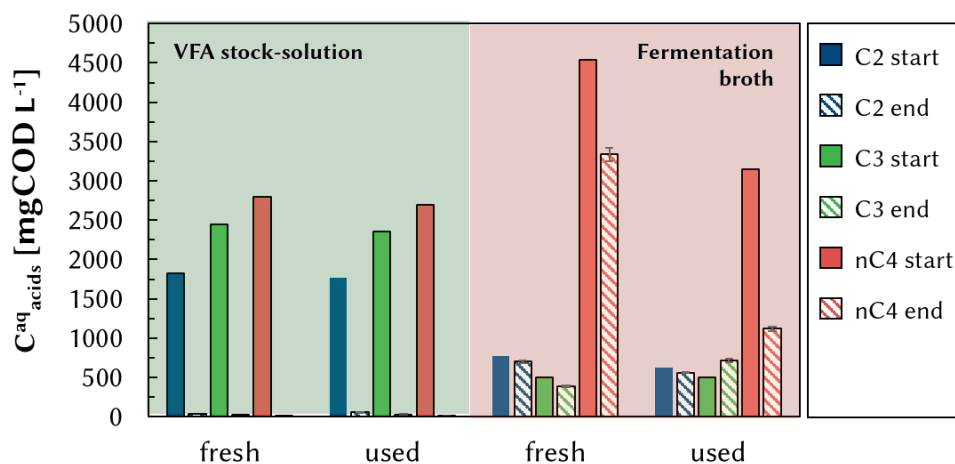


Figure 6.7: Small volume extraction experiments to evaluate the reusability of $[N_{888}][oleate]$. Concentration of acids in water phase before and after extraction using unused $[N_{888}][oleate]$ (fresh) and used $[N_{888}][oleate]$. The extractions were performed with VFA mixture ($\sim 1.5 \text{ g L}^{-1}$ of C2, C3, and nC4) and with fermentation broth, all in duplicate. Standard deviation bars are so small they cannot be observed in this figure.

Conclusions

$[N_{888}][oleate]$ was used to demonstrate the novel concept of an IL as transport liquid for the coupling of two bioprocesses. Firstly, the hydrophobic IL was loaded with VFAs via liquid–liquid extraction from a defined aqueous VFA solution with high efficiencies. The successive microbial regeneration step showed the potential of using microorganisms to facilitate the removal of the products.

To the best of our knowledge, this is the first time such a biological regeneration of a hydrophobic ionic liquid was studied. The advantage of using a biological conversion for IL regeneration is the application of a biological medium which has a nearly neutral pH. The application of a microbial medium caused a pH swing which enhances the acids regeneration from the IL while the microbial conversion consumes the acids resulting in a stable pH. In this way no additional salt is needed for both the pH control of the bioprocess as well for the recovery of the products from the IL.

Reusability of IL as transport liquid was demonstrated by two subsequent cycles of loading and unloading the IL. Our study clearly shows the potential of reusing a regenerated IL as transport liquid. Further research was proposed on the role of salts on the extraction and recovery of VFAs, the tune-ability of the IL on specific VFA extraction, the recovery efficiencies at different VFA concentrations in the IL, and the IL compatibility with different bioprocesses. This all could lead to further

development towards the use of IL-based solvents to transfer or transport VFA or other biochemicals between bioprocesses in various industrial applications.

Acknowledgements

The financial support from the Netherlands Organisation for Scientific Research (NWO) and the company Paques B.V. (STW-Paques Partnership, project 12999) is gratefully acknowledged. Livio Carlucci's support during IL synthesis was greatly valued.

Chapter 6 – supplementary information

Table S6.1: Cycle 1 microbial assisted regeneration – conversion parameters, amount of COD present in IL and water phase at the end of the regeneration step and the microbial assisted extraction efficiency calculated based on the amount of COD extracted from the IL during regeneration.

| | Start mgCOD _{IL} | Loading [mgCOD gVSS ⁻¹] | Methane produced [mgCOD _{CH4} gVSS ⁻¹] | End mgCOD _{aq} | End mgCOD _{IL} | Microbial assisted extraction efficiency [%] |
|---------|------------------------------|---|--|----------------------------|----------------------------|---|
| 1 | 145.2 | 710.8 | 289.7 | 22.2 | 63.8 | 56.0 |
| 2 | 141.3 | 699.4 | 288.4 | 21.2 | 61.8 | 56.2 |
| 3 | 144.1 | 714.0 | 288.1 | 21.3 | 64.6 | 55.1 |
| average | 143.5 ± 2.0 | 708.1 ± 7.7 | 288.7 ± 0.8 | 21.6 ± 0.6 | 63.4 ± 1.4 | 55.8 ± 0.6 |

Table S6.2: VFA concentrations in the water phase at end of cycle 1 and cycle 2 for the tests, pos2 (C2, C3, nC4 as substrate) and neg4 (loaded IL, no sludge after 24 days of contact time). Values shown in the table are averages and standard deviations, all in mgCOD L⁻¹.

| | Experiment | C2 | C3 | nC4 | total |
|---------|------------|--------------|--------------|--------------|---------------|
| | Tests | 11.3 ± 1.1 | 631.8 ± 73.3 | 106.1 ± 15.4 | 749.1 ± 86.3 |
| Cycle 1 | Pos2 | 4.9 ± 0.5 | 742.0 ± 17.8 | < 5* | 747.4 ± 18.0 |
| | Neg4 | 587.5 ± 19.0 | 497.7 ± 12.8 | 272.9 ± 1.9 | 1358.1 ± 21.4 |
| Cycle 2 | Tests | 11.4 ± 7.7 | 265.1 ± 48.4 | 402 ± 0.8 | 678.5 ± 247.9 |
| | Pos2 | 4.7 ± 0.8 | 819.0 ± 12.8 | < 5* | 824.2 ± 11.9 |

* below detection limit.

Table S6.3: Distribution coefficients of negative control 4 (cycle 1) for the extraction of acids into the IL (pure water) and at equilibrium conditions after 24 days of contact time with mineral medium in g_{aq} g_{IL}⁻¹.

| | C2 | C3 | nC4 | total |
|--|------------|------------|------------|------------|
| β_i pure water [g _{aq} g _{IL} ⁻¹] | 11.1 ± 0.4 | 32.6 ± 1.1 | 80.1 ± 2.7 | 27.0 ± 0.9 |
| β_i Medium [g _{aq} g _{IL} ⁻¹] | 0.9 ± 0.03 | 1.5 ± 0.1 | 3.9 ± 0.3 | 1.7 ± 0.1 |

Table S6.4: Cycle 2 – extraction of VFAs from a fermentation broth into reused [N_{ssss}][oleate]. Extraction efficiency for individual VFAs (C2, C3, nC4) as well as the distribution coefficient based on total COD present in organic phase and water phase.

| Replicate no. | E [%] | | | β |
|---------------|-----------|--------------|------------|--|
| | C2 | C3 | nC4 | [g _{aq} g _{IL} ⁻¹] |
| 1 | 4.3 | -118.4 | 35.0 | 1.7 |
| 2 | 3.3 | -106.5 | 33.7 | 1.7 |
| 3 | 4.2 | -115.9 | 36.9 | 1.8 |
| average | 3.9 ± 0.5 | -113.6 ± 6.3 | 35.2 ± 1.6 | 1.7 ± 0.05 |

Table 6.5: Reusability test by small volume extraction experiments - extraction efficiencies and distribution coefficients accompanying Figure 6.7. Extraction efficiency E is expressed as % and the distribution coefficient β is expressed in g_{aq} g_{IL}⁻¹.

| IL | | VFA stock-solution | | | | Fermentation broth | | | |
|---------|-------|--------------------|-------------|--------------|--------------|--------------------|-------------|------------|------------|
| | | C2 | C3 | nC4 | total | C2 | C3 | nC4 | total |
| E | Fresh | 98.1 | 99.1 | 99.6 | 99.0 | 9.4 ± 2.1 | 22.8 ± 1.8 | 26.5 ± 1.9 | 23.9 ± 1.9 |
| | used | 96.6 ± 0.2 | 98.7 ± 0.1 | 99.4 ± 0.1 | 98.4 ± 0.1 | 9.9 ± 0.5 | -41.1 ± 4.1 | 64.4 ± 0.9 | 44 ± 0.5 |
| β | fresh | 57.8 | 124.8 | 254.8 | 112.6 | 0.2 ± 0.04 | 0.5 ± 0.04 | 0.6 ± 0.05 | 0.5 ± 0.04 |
| | used | 45.5 ± 2.6 | 120.5 ± 7.7 | 289.8 ± 42.9 | 233.6 ± 39.0 | n.d. | n.d. | n.d. | 1.7 ± 0.1 |

n.d.: not determined. individual VFA concentration inside the IL could not be determined.

Table S6.6: Cycle 2 microbial assisted regeneration - conversion parameters, amount of COD present in IL and water phase at the end of the regeneration step and the microbial assisted extraction efficiency calculated based on the amount of COD extracted from the IL during regeneration.

| | Start mgCOD _{IL} | Loading [mgCOD gVSS ⁻¹] | Methane produced [mgCOD _{CH₄} gVSS ⁻¹] | End mgCOD _{aq} | End mgCOD _{IL} | Microbial assisted extraction efficiency [%] |
|---------|------------------------------|---|---|----------------------------|----------------------------|---|
| 1 | 78.7 | 381.5 | 116.1 | 27.1 | 27.6 | 35.1 |
| 2 | 78.0 | 381.5 | 135.4 | 21.2 | 29.1 | 37.3 |
| 3 | 81.8 | 403.3 | 184.9 | 14.3 | 30.0 | 36.7 |
| average | 79.5 ± 2.0 | 388.8 ± 12.6 | 145.4 ± 35.5 | 20.9 ± 6.5 | 28.9 ± 1.2 | 36.4 ± 1.2 |



Chapter 7

General Discussion

The conversion of organic waste into valuable products is one of the biggest hurdles to reduce our dependency on fossil resources and achieve a successful bio-based economy. This thesis describes the conversion of short chain fatty acids (SCFAs) into valuable chemicals like precursors of liquid biofuels. Bioelectrochemical chain elongation (BCE) is a secondary fermentation in the carboxylate platform (see Figure 1.3). Electrode-derived electrons drive the chain elongation processes instead of a soluble electron donor such as is the case for fermentative chain elongation (CE).

In the introduction of this thesis the fascinating ability of microorganisms to exchange electrons with a solid-state electrode surface was highlighted. Similarly, the consumption of current for the powering of microbial respiration is a fascinating phenomenon. In chapter 2, 3, and 4 these intriguing capabilities were explored and the potential of a bioelectrochemical system for chain elongation processes was assessed. In order to improve BCE as an organic waste valorisation technology, it is important to understand how the supply of electrons via an electrode can be coupled to microbial metabolism. Therefore, this last chapter focusses on the research question:

How can the electrode serve as electron donor for bioproduct formation in BCE systems?

To answer it, a review on the described electron transfer pathways will be provided. Secondly, it will be discussed how electron transfer can be coupled to bioproduction pathways in BCE systems. Or in other words, how an electrode can serve as electron donor for microbial metabolism. This knowledge is then applied to provide several considerations to be taken into account when developing BCE further as waste valorisation technology.

Part I – On the coupling of microbial metabolism to an electrode as electron donor

Requirements for microbial life: energy and reducing equivalents

To gain energy, electrons are transferred from a substrate (electron donor with relatively low redox potential) towards an electron acceptor (more positive redox potential) in microbial electron transfer chains. These electron transfers take place through carriers, of which NAD(H), FAD(H) and ferredoxin (Fd) are the most common intracellular carriers. Such carriers are also called reducing equivalents. The potential difference between substrate and acceptor determines the quantity of energy that can be conserved. Electron transfer is usually catalysed by membrane-bound compounds, resulting in an ion-gradient across the membrane. This

ion-gradient, either Na^+ or H^+ , can in turn be used for ATP synthesis.²⁰⁴ To sustain microbial life, generation of ATP as well as reducing equivalents is required.

In BCE presumably microbial ET chains exchange electrons with an electrode, i.e. the electrode serves as electron donor for microbial metabolism and thus microbial life. The coupling of electrode-microbial metabolism is for the discussion here divided into two steps: i) the transfer of electrons from electrode to/in the cell, and ii) the synthesis of products by oxidation of the electron(carrier)s (Figure 7.1).

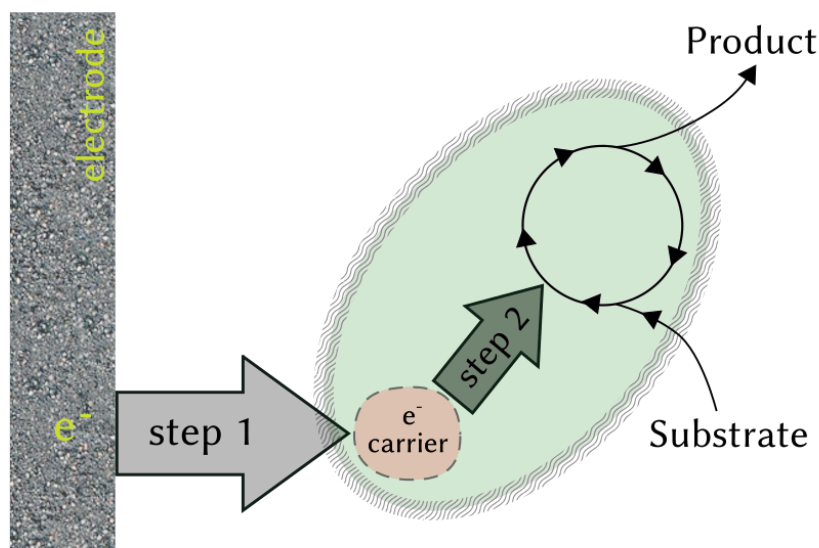


Figure 7.1: Electrode as electron donor for microbial metabolism is divided into two steps. Step 1 is the electron transfer from electrode to/into the microbial cell. There the produced reduced electron carriers are subsequently used to drive metabolic reactions in step 2.

Electron transfer mechanisms from electrode towards microbial cell

The first step to couple metabolism to an electrode is the electron transfer from electrode towards microbial cells (Figure 7.1, step 1). Two types of electron transfer have been described: direct and mediated electron transfer.

Direct electron transfer (DET)

As the name suggests, DET is defined as 'not requiring the diffusion of a mobile component to and from the cell for electron transfer'.³⁹ I.e. in DET a redox active component in the outer membrane exchanges directly electrons with an electrode surface. Several outer membrane enzymes and protein complexes are described

nowadays that can transfer electrons over the membrane. One of the two model microorganism for studying EET *Geobacter sulfurreducens* can form extracellular appendages (named 'pili' or 'nanowires') to physically connect to an electron donor and/or acceptor (Figure 7.3).^{205–207} Nanowires exhibit metal-like conductivity which enables electron transfer over great distances.²⁰⁸ Microorganisms able to form such electrical connections with partners have unique advantages under some environmental conditions.²⁰⁹ In bioelectrochemical systems, these nanowires were the connection of *G. sulfurreducens* to the electrode.^{205,210} Several other species were identified so far also able to produce nanowires, ranging from phototrophic cyanobacterium *Synechocystis*,²⁰⁶ to fermentative bacteria as *Pelotomaculum thermopropionicum*²⁰⁶ and *Clostridium pasteurianum*.²¹¹

Next to conductive nanowires, outer-membrane cytochromes (OMCs) are described to be a direct connection of cell membranes with an electrode. In natural environments these multi-heme enzymes are involved in electron uptake from solid electron donors.²¹² *Geobacter sulfurreducens* and *Shewanella oneidensis* can connect to an electrode via OMC complexes for electron transport over the membrane.^{213,214} In early MES work, Nevin et al. demonstrated that several cytochrome containing acetogens like *Moorella thermoacetica* were able to directly use electrons from an electrode¹⁴³. It was hypothesised that cytochromes were the conduit to the electrode. When electrons are transferred over the membrane via cytochromes, the soluble protein ferredoxin present in the cytoplasm, can be reduced directly (Figure 7.3).

Additionally, cytochromes in the outer membrane can have hydrogenases as redox partner in the inner membrane.²¹² Electron transfer from electrode via these cytochrome-hydrogenase complexes results in intracellularly H₂ production. Subsequently, two things can happen: i) the electrochemical gradient established by the change in intracellular H⁺ concentration can be used for ATP formation, or ii) the produced H₂ can be employed for NADH production via soluble bifurcating hydrogenases (both described later on).

Another membrane bound component identified as possible electrode connection is a reversible NADH-dehydrogenase in *M. thermoacetica*²⁰⁴. Direct ET via this enzyme could yield direct generation of NADH.

Other metal containing proteins such as rusticyanin (Rus) in *Acidithiobacillus ferrooxidans*²¹⁵ are suggested connections to the electrode as well.

Indirect electron transfer

The second electron transfer method, indirect or mediated electron transfer, involves the production of electron shuttles or mediators for electron transport (Figure 7.3, top left).³⁹ Mediators take up electrons at the electrode surface, and 'deliver' them to

the microbial cell by diffusion through the liquid medium. Mediators can be supplied exogenously or produced by the microorganism itself. Examples of self-excreted redox shuttles are azurin, procyanin, phenazines in *Pseudomonas* spp.²¹⁶ or flavins in *S. oneidensis*.²¹⁷

Recently in BESs, it was discovered that microorganisms excrete whole enzymes to facilitate electron flow from a cathode towards their cell^{142,152}. Cytochromes,¹⁵² formate dehydrogenases (FDHs) and hydrogenases¹⁴² were excreted into the cathodic biofilm matrix and catalysed H₂ and formate formation. In the study of Marshall and co-workers, bacteria without cytochromes or other known electron conduits (*Acetobacterium woodii*) were abundant in the cathodic biofilm. Based on analysis of transcriptional activity, they suggested soluble hydrogenases and ferredoxins were excreted and delivered reducing equivalents to the cells.¹⁵²

Another indirect electron transfer mechanism was suggested by Marshall et al., who discovered metals tightly bound on the electrode.¹⁵² Using SEM-EDX it was visualized that extracellular material was deposited on the electrode surface, containing metals such as nickel and iron. These metals were hypothesized to be part of redox active enzymes, but precipitation of nickel and iron as (hydr)oxides, sulfides, carbonates, phosphates, perhaps even as nanoparticles induced by pH or microbially, could not be ruled out.¹⁵² Similarly, copper concentrates on the electrode surface of CO₂ to acetate reducing biocathodes were reported by Jourdin et al.⁹³ After biofilm removal of the electrode, these copper precipitations still catalysed H₂ formation. These reports show that metal precipitation on the electrode play a role in biocathodic electron transfer, yet the exact mechanisms for precipitation and functionality are to be unravelled.

Key components for energy metabolism

Although the production of chemicals using microbial electrosynthesis started about ten years ago, electrodes have been applied for more than thirty years to control and stabilise fermentation processes.²¹⁸ In electrofermentation an electrode is placed in the fermentation broth and there the electrode supplies a (small) part of the reducing equivalents. Thereby it induces a shift in intracellular redox conditions and changes the product spectrum towards more reduced compounds.^{82,211,219,220} From such studies it was learned already some time ago that co-supply of electrode-derived electrons can alter microbial metabolism in fermentations.

In MES and BCE the electrode is not the co-supply of electrons, but the main source of them. In 2017 Koch et al. hypothesised that electrode-derived electrons can “replace” soluble electron donors for the production of ATP and NADH.²²¹ As explained above, electrons entering the microbial cell, either via direct or indirect

electron transfer, need in some way to be used for generation of ATP, NAD(P)H and reduced ferredoxin (Fd^{2-}) to sustain microbial life.

The key components described nowadays which contribute to microbial energy generation are the enzymatic complexes Rnf and Ech (Figure 7.3). Electron transfer via these complexes results in an ion-gradient over the membrane. This ion-gradient can subsequently be harvested by ATP synthases (Figure 7.3). Both Rnf and Ech require reduced ferredoxin to create the ion-gradient. Fd^{2-} can be formed using the soluble hydrogenases Hyd and Nfn (Figure 7.3).

Rnf complex

Acetogens are anaerobic microorganisms employing the Wood-Ljungdahl pathway (or acetyl-CoA pathway) for carbon assimilation. Based on their energy conserving properties, acetogens are often divided into two groups: Na^+ -gradient and H^+ -gradient dependent species. For a long time it remained unknown how acetogens conserve energy for growth using this pathway, because the ATP yield was net zero. Since acetogens are able to grow on only CO_2 and H_2 , the pathway should be a source of net energy conservation. In 2007, studying *Acetobacterium woodii*, an Na^+ dependent acetogen, the mystery was solved: a novel membrane-bound $\text{Fd}:\text{NAD}^+$ oxidoreductase (Rnf complex) was reported to transport Na^+ over the membrane (Figure 7.3).^{222,223} The Rnf complex couples the oxidation of Fd^{2-} to the reduction of NAD^+ to NADH. ²²³ The potential difference between Fd^{2-} ($E'^{\circ}_{\text{Fd}} = -500$ to -420 mV) and NAD^+/NADH ($E'^{\circ} = -320$ mV) is used for the generation of an Na^+ electrochemical gradient. The genes coding for the Rnf complex, the *rnf* (Rhodobacter nitrogen fixation) genes, are widespread in bacteria and some archaea contain them as well.²²⁴ Depending on the host organism, Rnf complexes translocate either Na^+ or H^+ for the generation of the electrochemical gradient.²²⁵

Energy-converting hydrogenase (Ech complex)

In another acetogen model organism, *Moorella thermoacetica*, a different membrane-bound energy converting hydrogenase was identified as main energy conserving mechanism.²²⁶ This Ech complex is widespread in anaerobic bacteria and archaea. Ech complexes couple the exergonic oxidation of Fd^{2-} with H^+ reduction, producing H_2 (Figure 7.3).²²⁶ The potential difference between Fd^{2-} ($E'^{\circ}_{\text{Fd}} = -500$ to -420 mV) and protons ($E'^{\circ}_{\text{H}^+/\text{H}_2} = -414$ mV) is used to translocate Na^+ or H^+ ions over the membrane to establish an electrochemical gradient.²²⁷

ATP synthase

The electrochemical gradients as a result of electron transfer via Rnf or Ech complexes, can be harvested by ATP synthases (Figure 7.3). Although generally ATP generation requires $\sim 3\text{H}^+$ or $\sim 3\text{Na}^+$ per ATP, the actual amount of ATP which can be conserved is dependent on the exact electron chain. Kracke et al. did some

theoretical calculations for some BES conversions using the electrode as electron donor. A major observation they posed was that amount of achievable ATP is dependent on the actual site of electron transfer.²⁰⁴ For example, an electron input in the cellular NADH pool would not yield enough energy to generate ATP. If the electrons yield H_2 production, then via Hyd (see below) reduced ferredoxin and NADH can be produced. Fd^{2-} and NADH can subsequently yield an electrochemical gradient via an Rnf complex in the membrane and ATP can be synthesised.²⁰⁴

Soluble electron bifurcating complexes Nfn and Hyd

Electrochemical potentials and ATP are two ways to fuel endergonic reactions for biomass growth and to sustain life. A third mechanism for drive thermodynamic unfavourable reactions was discovered last decade: electron bifurcation.^{228,229} It's a process in which a soluble enzyme complex splits up the electron pair liberated by oxidation of the electron donor and transfers these electrons towards two electron accepting reactions. One electron goes down the energy gradient and drives the other up (Figure 7.2).²²⁷ Using electron bifurcation reduced ferredoxin (Fd^{2-}) and NADPH can be produced by two soluble enzyme complexes: Hyd and Nfn.

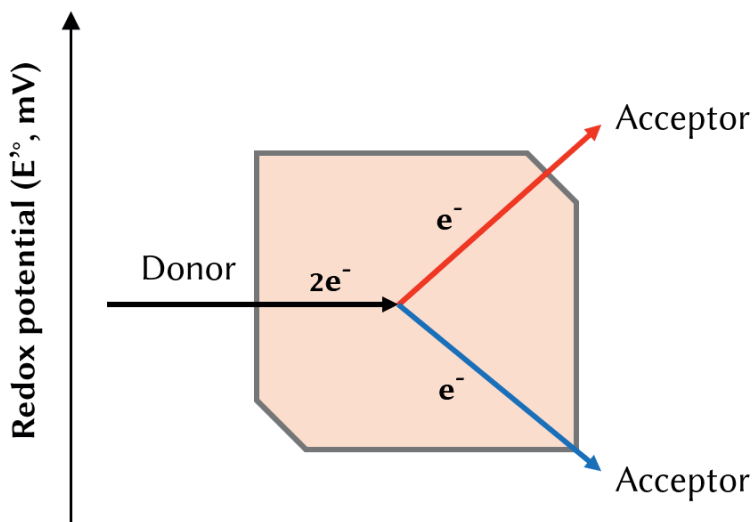
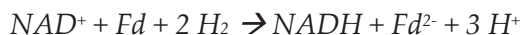


Figure 7.2: Concept of electron bifurcation.

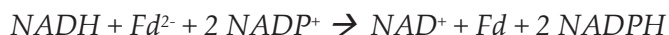
HydABC oxidizes hydrogen with simultaneously reducing NAD^+ and Fd .²³⁰:



The acetogens *M. thermoacetica*²³⁰, *Clostridium pasteurianum* and *C. ljungdahli*²³¹ contain this Hyd-complex. In the microbial electrosynthesis systems reducing CO₂ using electrons of Marshall et al., the *hydABCDE* genes of *Acetobacterium* str. MES-1 were highly expressed¹⁵². The authors suggested that this HydABCDE complex supplied *Acetobacterium* str. MES-1 with ferredoxin and NADH.

To balance the cellular redox pools of NAD⁺/NADH and NADP⁺/NADPH transhydrogenases are essential.^{232,233} Although the redox potential of the NADP⁺/NADPH couple ($E^{\circ} = -324$ mV) is similar to that of NAD⁺/NADH, under physiological conditions the redox potential of both couples is shifted. In the cell > 90% is oxidized, shifting it to $E^{\circ}_{\text{NAD}^+/\text{NADH}} = -280$ mV, while the ratio of NADP⁺/NADPH is 1/40 and that shifts the potential to $E^{\circ}_{\text{NADP}^+/\text{NADPH}} = -380$ mV.²²⁹ This makes NADPH a stronger reductant than NADH.

For some assimilatory reactions not NADH is needed, but the stronger reductant NADPH. For example, elongation of acetate with ethanol in *C. kluyveri*, the reduction step of acetoacetyl-CoA to 3-hydroxybutyryl-CoA is driven by NADPH. To supply for NADPH in *C. kluyveri*, a second soluble hydrogenase complex Nfn (NADH-dependent reduced ferredoxin:NADP oxidoreductase) was identified to catalyse the electron transfer from Fd²⁻ and NADH to generate NADPH²³⁴:



Many *Clostridiaceae* contain *nfn* genes for the generation of NADPH from ferredoxin and NADH.²²⁹

Generation of ATP and reducing equivalents with electrode possible

In the BCE systems in this work, mixed microbial cultures were applied as biocatalysts. Mixed microbial populations enclose great metabolic potential because all the metabolic capabilities of the individual species present can potentially be used.^{107,235,236} Therefore, the assumption is posed that the BCE microbiomes here are a black-box full of metabolic possibilities for electron transfer.

According to the presented theoretical framework (graphically summarised in Figure 7.3), electron transfer in BCE could employ a wide variety of ways for the generation of ATP, NAD(P)H, and reduced ferredoxin using an electrode. In short:

- H₂ – taken up either as H₂ (bio) electrochemically produced at the electrode surface, or formed intracellularly by the cytochrome-hydrogenase membrane bound complexes. Intracellular H₂ induces NADH and Fd²⁻ via Hyd or can together with Fd²⁻ induce an ion-gradient via Ech.

- Fd^{2-} - soluble ferredoxin gets reduced via membrane bound cytochromes or is taken up as redox mediator. Fd^{2-} induces an electrochemical gradient via either Ech or Rnf.
- NADH – cytoplasmic NAD^+ is reduced by membrane-bound NADH-dehydrogenase.
- Established ion-gradients are harvested and ATP is produced by ATP synthases.

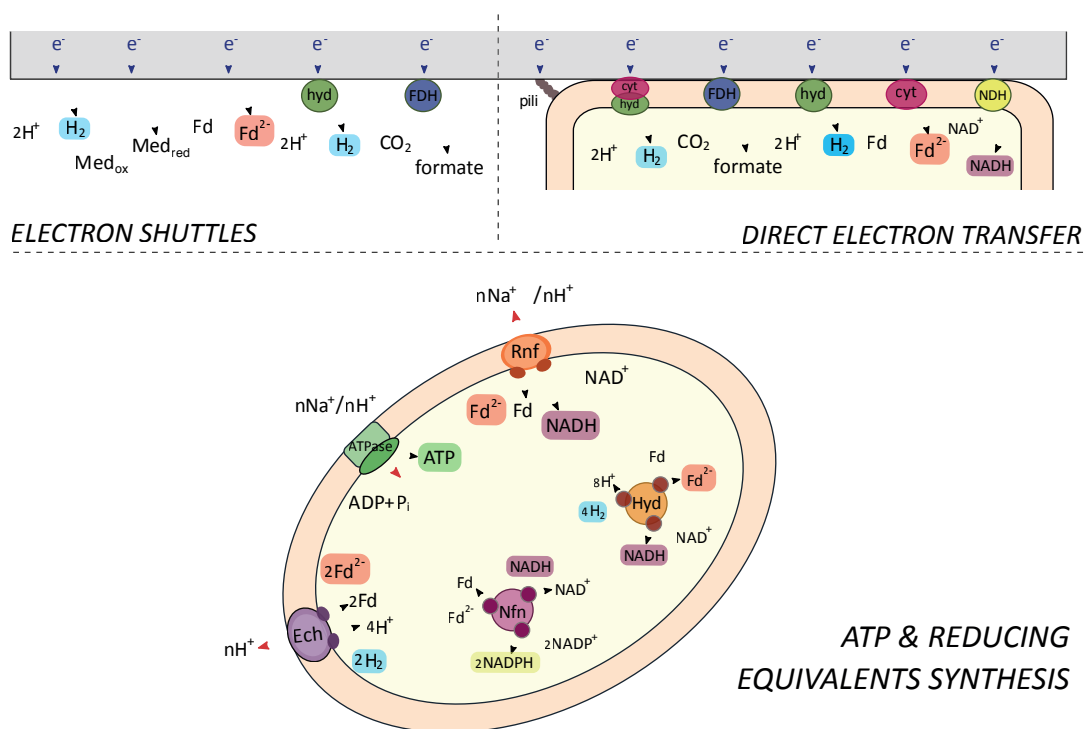


Figure 7.3: Overview of all the described electron transfer pathways (direct or mediated) and the described ways to generate ATP and reducing equivalents. Med: mediator, Fd: ferredoxin, hyd (green): hydrogenase, FDH: formate dehydrogenase, cyt: cytochrome, NDH: NADH dehydrogenase, ATPase: ATP synthase. Rnf, Ech, Nfn, and Hyd (orange) see text for explanation.

Step 2 – Product formation via reverse β -oxidation

Currently, *Clostridium kluyveri* is the most studied model organisms for fermentative chain elongation (CE) via the reverse β -oxidation pathway (RBO, Figure 7.4).^{79,107,237} The acetate elongation to n-butyrate (chapters 2, 3 and 4), the propionate elongation to n-valerate (chapter 4), and n-butyrate elongation to n-caproate (chapter 4) in this thesis, suggest that the main bioproduction route in the BCE systems here is the same. Based on the spiking experiments of chapter 3, it is highly unlikely that soluble electron donors such as ethanol or lactate are formed and used for CE. It gives rise to the question: *what are the consequences of using an electrode instead of a soluble electron donor to fuel the RBO?*

Energetics of RBO pathway

In fermentative CE, ethanol is oxidised and thereby providing for both reducing equivalents, in the form of NADH, and ATP (Figure 7.4 A). Ethanol oxidation produces also acetyl-CoA, the intermediate component which enters the cyclic elongation process (Figure 7.4 C). In the reductive part of the RBO, the produced NADH is used to convert acetoacetyl-CoA into 2-hydroxybutyryl-CoA, the second step of the process. In case of low substrate conditions, NADPH is used as reductant.⁷⁹ Energy is conserved in the reduction step of crotonyl-CoA to butyryl-CoA, which is catalysed by the electron bifurcating complex Bcd-Etf (butyryl-CoA dehydrogenase – electron transferring flavoprotein). This reduction step is NADH dependent, and produces reduced ferredoxin. For more in-depth details of the RBO, the reader is referred to the reviews of Spirito et al.¹⁰⁷ and Angenent et al.⁷⁹

In short, for nC4 to be produced from acetate, NADH and acetyl-CoA required and are produced via ethanol oxidation. NADH drives the reductive cycle and the formation of reduced ferredoxin. Via an Rnf complex the ferredoxin subsequently can produce an ion-gradient and ATP can be harvested to sustain life.

Combining all the ingredients – electrode as electron donor for BCE

Similar to fermentative CE, in BCE systems NADH and acetyl-CoA are required to fuel the RBO pathway. The production of NADH (see Figure 7.3) by an electrode can occur via: i) Hyd fuelled by H₂ (which is abundantly present in our BCE systems or putatively this Hyd could take up electrons from membrane bound complexes), ii) membrane-bound NADH-dehydrogenases which reduce cytoplasmic NAD⁺. In the transcriptomic analysis performed by Marshall et al. of a CO₂ reducing microbiome, *HydABC* was one of the most highly expressed genes,¹⁵² indicating that this soluble hydrogenase is possibly also involved in NADH supply in our BCE systems.

Acetyl-CoA can be formed by activation of acetate by investing ATP (Figure 7.4B). Acetate was supplied continuously in this work, therefore its availability as substrate is presumed. ATP can be produced as a result of an ion-gradient. Ion-gradients can be established by the complexes Rnf and Ech or by change in intracellular concentration of protons by hydrogenase activity (Figure 7.3).

In chapter 2 in an attempt to understand the observed butyrate production, next to the hypothesis of intermediate ethanol formation, a novel bioelectrochemical pathway was postulated. After the analysis in this chapter, the existence of a 'bioelectrochemical butyrate production pathway' is highly unlikely. Instead, here it is suggested to regard the bioelectrochemical pathway as a combination of electron transfer mechanisms and coupling to the RBO as described before. Therefore not a bioelectrochemical pathway exists, but bioelectrochemical production is a result of several combined pathways.

Considerations to an electrode as electron donor

First of all, this chapter discusses the possibility of electrode-derived electrons to serve as the electron donor for microbial metabolism. In a mixed microbial culture, such as the BCE systems of this thesis, multiple options exist for electron entrance of the microbial cell as well as for reducing equivalents and ATP to be generated. In distinguishing the exact electron donor for the production of a specific compound via BCE requires a full understanding of the electron transfer pathways and bioproduction mechanisms. Therefore, it is suggested to not designate the electrode as the electron donor for microbial metabolism but as 'electron source'.

The thermodynamic calculations of chain elongation reactions in chapter 4 (table 4.4) showed it is thermodynamic feasible to reduce acetate to butyrate using electrons or H₂ as electron donor. These calculations contradicted the thermodynamic and kinetic calculation of González-Cabaleiro et al, which ruled out H₂ as electron donor for acetate elongation to n-butyrate.¹⁰⁹ H₂ as electron donor for acetate reduction would not deliver sufficient energy to induce an electrochemical gradient and yield ATP production. This difference in outcomes implies that there is a difference in energy conservation between when a soluble electron donor is supplied and when electrode-derived electrons are supplied. When growing on an electrode, ATP production for growth might be divided from the elongation process. The elongation would then 'only' serve as a way to dispose reducing equivalents. This separation of ATP production and cyclic process actually is quite plausible, given the fact that ATP is required to generate acetyl-CoA from acetate and start the reductive cycle.

The suggestion that electrodes affect metabolism differently than soluble electron donors is supported by the observed preference of our BCE reactors to elongate C3

140 |

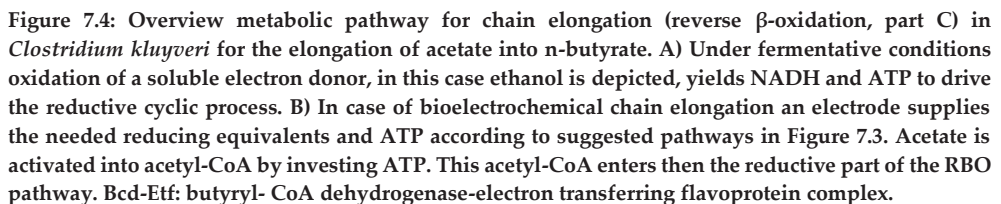


Figure 7.4: Overview metabolic pathway for chain elongation (reverse β -oxidation, part C) in *Clostridium kluyveri* for the elongation of acetate into n-butyrate. A) Under fermentative conditions oxidation of a soluble electron donor, in this case ethanol is depicted, yields NADH and ATP to drive the reductive cyclic process. B) In case of bioelectrochemical chain elongation an electrode supplies the needed reducing equivalents and ATP according to suggested pathways in Figure 7.3. Acetate is activated into acetyl-CoA by investing ATP. This acetyl-CoA enters then the reductive part of the RBO pathway. Bcd-Etf: butyryl- CoA dehydrogenase-electron transferring flavoprotein complex.

Part II – Implications and challenges identified for BCE technology

The electron transfer pathways (and the associated rates) from electrode towards microorganism fundamentally determine the performance of MES –product concentrations, production rates and energy usage will be affected by this.²³⁸ Although the exact pathways are still speculative (see part I of this discussion), to conclude here several implications and challenges are discussed of using an electrode as electron source in bioelectrochemical chain elongation.

Main challenge - improve concentration and production rates

BCE is now developed in the lab as continuous production system. For BCE to be applied as industrial technology, relevant industrial product concentrations and rates need to be reached. The production rates obtained in this thesis cannot yet compete with ethanol based CE, i.e. 57.4 gMCFA L⁻¹ d⁻¹.¹¹⁰ When converting the ethanol supply of Grootscholten et al. (82.4 g L⁻¹ d⁻¹) to current supply, this corresponds to 24 A L⁻¹ reactor volume. The highest obtained production rate of butyrate (0.8 to 1.0 g L⁻¹ d⁻¹, in the triplicate reactor of chapter 4) while 29 mA was applied to a catholyte volume of 50 ml, corresponds to 0.58 A L⁻¹.

From an electron donor energy costs point of view, the sole electron donors ethanol or electricity are comparable. Ethanol from sugar (the cheapest available ethanol) costs about 0.04 to 0.06 € per kWh^{239,240} at €300-450 per ton and a ΔH_c° (heat of combustion of liquid ethanol -1318 kJ mol⁻¹) while renewable electricity from wind also is predicted to cost 0.06 €/kWh.²⁴¹ Still, this comparison neglects the further OPEX/CAPEX involved for BCE and also does not include the different efficiencies on the use of both electron for CE. From this latter perspective BCE with direct electron use could become more effective since no ethanol oxidation is required compared to ethanol based chain elongation. Evenly, with the current developments on renewable electricity technologies, the incentive to convert and store renewable electricity into chemical compounds would make electrification of biotechnological processes more interesting.

To further increase the product concentration in BCE either applied current can be increased, and/or the electrode and cathode compartment design can be optimised to ensure microorganisms to colonise the whole electrode surface. Jourdin et al. optimised the cathode compartment that the liquid flow was forced through the graphite felt which allowed for a thick biofilm to grow when the systems were continuously operated.¹⁴⁶ Most likely because of this highly developed biofilm, the current consumption of that study was as high as -175 A m⁻² projected surface area (E_{cath} was -0.85 V vs SHE) and a volumetric current of already 10 to 14 A L⁻¹ electrode.

The resulting production rates of butyrate and caproate were $3.2 \text{ g L}^{-1} \text{ d}^{-1}$ and $0.95 \text{ g L}^{-1} \text{ d}^{-1}$.¹⁴⁶ Even though this high current density corresponded to relatively low production rates compared to CE, the supplied substrate in the study was CO_2 . To reduce CO_2 to 1 mole of acetate, 8 electrons need to be invested. In case BCE will be operated with acidified organic waste streams, this investment to produce acetate is not necessary. Therefore, applying a higher current density is expected to increase the productivity of BCE systems, also when starting from fatty acids.

To minimize the energy input for BCE systems, ideally the cathode potential should be controlled at a potential close to the thermodynamic potential of the electron transfer pathways enzymes. In that way the least energy (i.e. overpotential) is applied to drive the BCE reactions. Albeit theoretically, the overpotential represents the energy available for the microorganisms to grow. Therefore, if the overpotential is adapted with the purpose of 'least energy input' for the reactors, it will affect the energy metabolism of the microbiome and subsequently as well the productions rates. Oppositely, when a lower cathode potential is applied, it will result in higher currents, which will lead to higher productions rates due to higher overpotentials. So, from a CAPEX (e.g. electrode use)/OPEX (e.g. electricity use) point of view, there is an optimum to be found in applied energy and resulting rates, as shown by e.g. Sleutels et al.²⁴² In chapter 3 more current was applied which doubled the production rates, although that hardly affected the cathode potential. This indicates that the BCE process can likely handle a higher applied current while limited energy input is needed. Which electron transfer pathway(s) is the most effective from a costs (both CAPEX/OPEX) point of view is still to be determined. It probably depends also on the electrode type materials as these have various properties which also can affect biofilm development and as such affect the electron transfer pathways involved.²⁴³ Further systematic studies will be required to study the effect of electrode potential, applied currents and electron transfer pathways involved to further unravel the (efficient) use of electrodes and energy to drive BCE processes.

Implication - more selective odd-MCFA production compared to ethanol-based chain elongation

Supplying a microbiome with electrons appears to have a different effect on the production spectrum. In chapter 4 propionate was co-supplied with acetate as substrate for elongation. In contrast to ethanol-based CE, supply of electrons led to high formation selectivities of nC5 of more than 90 %. Still in this experiment acetate was also present; so future experiments should validate whether sole propionate can be elongated without presence of other electron acceptors. Potentially, this could lead to a product spectrum with even higher selectivities for odd-chain fatty acids. Ethanol oxidation in CE leads to acetate formation, even if propionate is the main

substrate for elongation. In case an electrode supplies reducing equivalents, then no redundant acetate will be formed and it will greatly benefit the product selectivities in odd-chain fatty acid elongation.

Challenge – finding an appropriate waste stream

BCE described in this thesis was intended to convert acidified organic waste into valuable bioproducts. The mentioned high selectivity towards odd-chain fatty acid elongation, gives rise to the question what residual stream contains most propionate? Acidified organic residual streams contain a mixture of SCFAs. Following the results of chapter 6, acetate and nC_4 are more easily consumed than propionate by methanogenic sludge. Methane is not an economical valuable product, plus its greenhouse potential is much bigger than that of CO_2 .⁷⁷ However, if a microbial culture is chosen which consumes acetate and butyrate from the acidified stream, then the remaining propionate can be fed to the BCE reactors to selectively produce odd-chain fatty acids.

Implication – consequences electron donor: water instead of agricultural based ethanol

The choice of electron donor for an industrial process may both depend on the costs (investment and operational) and the environmental impact. For chain elongation of organic waste streams by ethanol-based chain elongation producing nC_6 , a life-cycle assessment showed ethanol was the dominant cause for environmental impact.¹²⁸ The impact of added ethanol to the total life-cycle accounted 20 %. The impact of ethanol could partly be reduced by replacing the fossil-based ethanol by agricultural based ethanol (e.g. bioethanol from fermented sugarcane).¹²⁸ Omitting ethanol and use an electrode (powered by renewable energy) instead, most of the impact of added ethanol can be diminished though not fully eliminated (producing electricity impacts the LCA as well). Whether electrode-derived electrons have indeed a lower impact than ethanol is still to be determined.

Although in BCE systems the electron source for microbial metabolism in the cathode compartment is electrons, these electrons are generated by an oxidation reaction in the anode compartment. The electron source in the laboratory BCE experiments here was water oxidation. Water oxidation as electron source is attractive, because water is abundantly available. The production of valuable bioproducts, using a waste stream as substrate, fuelled by renewable electricity and water oxidation, sounds as a sustainable technology.

Although water is widely available, care should be taken about water containing chloride ions. The standard redox potential at which Cl^- is oxidised to Cl_2 gas is +1.36 V vs SHE. Chloride gas is a well-known disinfectant and therefore the

formation of Cl_2 gas in the anode should be prevented as it may diffuse to the cathode compartment and affect the microbial activity. For that reason, both the electrolytes in this work have been composed to contain few Cl^- ions as possible.

The catalyst for water oxidation of our BCE systems was a platinum/iridium coated titanium plate. Both platinum and iridium belong to the group of rare earth metals, which makes such catalyst fairly expensive and environmentally questionable. Alternatively, an acetate oxidising bioanode could be used. The microbially catalysed oxidation of acetate will supply the electrons in that case. Next to omission of rare metals, using a bioanode will reduce the electrical energy required. A bioanode operates at approximately -0.2V vs SHE²⁴⁴ while the water oxidation potential at actual conditions is 0.805 V vs SHE.²⁴⁵ At a cathode potential of -0.5 V vs SHE (chapters 3 and 4), a bioanode would reduce the cell potential with 77 %. Consequently, assuming the same current, this cell potential reduction would lead to a similar electricity reduction of 77 %. Even though the application of a bioanode in energy or electricity view shows vast reductions, care should be taken with the application of a bioanode. The operational pH of a bioanode is ~ 7 . In the BCE systems in this work, due to water oxidation, the anolyte pH dropped to pH 1.5 - 2. To balance electroneutrality, protons were transported to the cathode and controlled the pH in the cathode. Therefore, the low anodic pH allowed the systems to be operated without external pH control. To combine the bioanodic benefits of electricity reduction as well as the pH controlling benefit of the acid anolyte, it is suggested to apply an (extreme) acidophilic microbial species in the bioanode.

Controlling pH by an acid anolyte goes well as long as the power source applies current. In case of power failure (as seen in chapter 4), backflow of protons from anode to cathode occurs due to the pH gradient between cathode (pH ~ 5.5) and the anode. Due to diffusion of protons the catholyte acidifies and subsequently impedes the biofilm. After restarting power supply and adjusting the pH manually once, the biofilm showed robustness and production of nC4 was restarted after several days.

Challenge – Separation of bioproduct

The second part of this thesis (chapters 5 and 6) focussed on the challenge which arises when bioprocesses are employed for the production of chemicals. Because the production concentrations are relatively low, downstream processing to obtain pure products is costly and energy intensive. The incorporation of *in situ* extraction by a hydrophobic solvent might help to reduce this downstream processing challenge as well as reduce possible toxic effects of high product concentrations. Hydrophobic ionic liquids can be suitable solvents for this purpose, as was demonstrated in chapters 5 and 6. Even though ILs are nowadays expensive, development of easier and thus less expensive synthesis protocols (chapter 5) could reduce costs over the

coming years. Additionally, the numerous ion combinations to make up an IL hold a lot of possibilities to optimise the applied solvent for a specific purpose. For the proposed concept of *in situ* separation of SCFAs from dilute fermentation broths, the IL should both be bioprocess compatible as well as have good extraction capacities for the to be extracted product. Usually, when a solvent has good extraction capacities, then for the recovery of the product from the solvent either a lot of energy is needed (e.g. via distillation) or a big amount of salt is needed (e.g. 'salting out'). Microbial regeneration of the IL (chapter 6) expels these disadvantages and therefore it is an interesting regeneration method for hydrophobic solvents to be explored further in the future.

To conclude, the production of bioproducts using bioelectrochemical systems as presented in this thesis is an appealing concept. Although progress is made in this thesis, a complete system analysis approach is required to elucidate the working of BCE processes, i.e. on the one side the involved microorganisms and the mechanisms of electron transfer and production pathways, and on the other side the techno-economic feasibility of BCE and the proposed *in situ* separation processes for real applications. Such research will give further insights in the current state of applicability and could stimulate further research efforts to the interesting BCE phenomena, and help the development of BCE-technology towards application.

Reference list

1. Potter, M. C. Electrical Effects Accompanying the Decomposition of Organic Compounds. *Proc. R. Soc. B Biol. Sci.* **84**, 260–276 (1911).
2. Sykes, A. H. A D Waller and the electrocardiogram, 1887. *Br. Med. J. (Clin. Res. Ed.)*. **294**, 1396–1398 (1987).
3. Waller, A. D. *Signs of Life in their electrical aspect.* (1903).
4. Clark, W. M. Barnett Cohen, 1891-1952: an appreciation. *Bacteriol. Rev.* **16**, 205–209 (1952).
5. Cohen, B. The bacterial culture as an electrical half-cell. *J. Bacteriol* **21**, 18–19 (1931).
6. Gillespie, R. W. H. & Rettger, L. F. Bacterial oxidation-reduction I. Differentiation of Species of the Spore-Forming Anaerobes by Potentiometric Technique. *J. Bacteriol.* **36**, 605–620 (1938).
7. Gillespie, R. W. H. & Rettger, L. F. Bacterial oxidation-reduction studies II. Differentiation of Lactobaccilli of diverse origin. *J. Bacteriol* **36**, 621–631 (1938).
8. Gillespie, R. W. H. & Porter, J. R. Bacterial oxidation-reduction studies III. Characteristic Potentials of Cultures of Aerobacillus1 Species. *J. Bacteriol* **36**, 633–637 (1938).
9. Hewitt, L. F. *Oxidation-reduction potentials in bacteriology and biochemistry.* (ES Livingstone, 1950).
10. Lewis, K. Symposium on Bioelectrochemistry of Microorganisms. IV. Biochemical Fuel Cells. *Bacteriol Rev.* **30**, 101–113 (1966).
11. Davis, J. B. & Yarbrough, H. F. Preliminary experiments on a Microbial fuel cell. *Science (80-.)*. **137**, 615–616 (1962).
12. Berk, R. S. & Canfield, J. H. Bioelectrochemical Energy Conversion. *Appl. Envir. Microbiol.* **12**, 10–12 (1964).
13. Davis, J. B. Generation of Electricity by Microbial Action. *Adv. Appl. Microbiol.* **5**, 51–64 (1963).
14. van Hees, W. A Bacterial Methane Fuel Cell. *J. Electrochem. Soc.* **112**, 258 (1965).
15. Lovley, D. R. & Phillips, E. J. P. Novel Mode of Microbial Energy Metabolism: Organic Carbon Oxidation Coupled to Dissimilatory Reduction of Iron or Manganese. *Appl. Environ. Microbiol.* **54**, 1472–1480 (1988).
16. Myers, C. R. & Nealson, K. H. Bacterial Manganese Reduction and Growth with Manganese Oxide. *Science (80-.)*. **240**, 1319–1321 (1988).
17. Shi, L. *et al.* Extracellular electron transfer mechanisms between microorganisms and minerals. *Nat. Rev. Microbiol.* **14**, 651–662 (2016).
18. Allen, R. M. & Bennetto, H. P. Microbial fuel-cells. *Appl. Biochem. Biotechnol.* **39**, 27–40 (1993).
19. Park, D. H. O. O. H. & Zeikus, J. G. Electricity Generation in Microbial Fuel Cells Using Neutral Red as an Electronophore. *Appl. Environ. Microbiol.* **66**, 1292–1297 (2000).
20. Bond, D. R., Holmes, D. E., Tender, L. M. & Lovley, D. R. Electrode-Reducing Microorganisms That Harvest Energy from Marine Sediments. *Science (80-.)*. **295**, 483–485 (2010).
21. Kim, B., Kim, H.-J., Hyun, M.-S. & Park, D. H. Direct electrode reaction of Fe(III)-reducing bacterium, *Shewanella putrefaciens*. *Journal of Microbiology and Biotechnology* **9**, (1999).

22. Liu, H., Ramnarayanan, R. & Logan, B. E. Production of Electricity during Wastewater Treatment Using a Single Chamber Microbial Fuel Cell. *Environ. Sci. Technol.* **38**, 2281–2285 (2004).
23. Liu, H., Grot, S. & Logan, B. E. Electrochemically assisted microbial production of hydrogen from acetate. *Environ. Sci. Technol.* **39**, 4317–4320 (2005).
24. Rozendal, R. A., Hamelers, H. V. M., Euverink, G. J. W., Metz, S. J. & Buisman, C. J. N. Principle and perspectives of hydrogen production through biocatalyzed electrolysis. *Int. J. Hydrogen Energy* **31**, 1632–1640 (2006).
25. Kim, Y. & Logan, B. E. Microbial desalination cells for energy production and desalination. *Desalination* **308**, 122–130 (2013).
26. Mohanakrishna, G., Srikanth, S. & Pant, D. Bioelectrochemical Systems (BES) for Microbial Electroremediation: An Advanced Wastewater Treatment Technology BT - Applied Environmental Biotechnology: Present Scenario and Future Trends. in (ed. Kaushik, G.) 145–167 (Springer India, 2015). doi:10.1007/978-81-322-2123-4_10
27. Philp, J. Balancing the bioeconomy: supporting biofuels and bio-based materials in public policy. *Energy Environ. Sci.* **8**, 3063–3068 (2015).
28. Intergovernmental Panel on Climate Change. *Climate Change 2014: Synthesis Report. Contribution of Working Groups I, II and III to the Fifth Assessment Report of the Intergovernmental Panel on Climate Change.* (2014). doi:10.1046/j.1365-2559.2002.1340a.x
29. United Nations, Department of Economic and Social Affairs, P. D. *World population prospects: the 2017 revision, key findings and advanced tables.* (2017).
30. Bloom David Canning et al. Population Health and Economic Growth Commission on Growth and Development. *Commision Growth Dev.* 1–36 (2008).
31. Wynes, S. & Nicholas, K. A. The climate mitigation gap: education and government recommendations miss the most effective individual actions. *Environ. Res. Lett.* **13**, 048001 (2018).
32. European Commission Directorate - General for Research and Innovation. *Bioeconomy: the European way to use our natural resources.* (2018). doi:10.2777/79401
33. European Commission. *Biomass supply and demand for a sustainable bioeconomy - exploring assumptions behind estimates.* (2017). doi:10.2777/39314
34. European Commission. *Towards a Europea knowledge-based bioeconomy. Workshop conclusions on the use of plant biotechnology for the production of industrial biobased products.* EUR 21459. (2004).
35. Sheldon, R. A. Green and sustainable manufacture of chemicals from biomass: state of the art. *Green Chem.* **16**, 950–963 (2014).
36. Agler, M. T., Wrenn, B. A., Zinder, S. H. & Angenent, L. T. Waste to bioproduct conversion with undefined mixed cultures: the carboxylate platform. *Trends Biotechnol.* **29**, 70–78 (2011).
37. Lee, W. S., Chua, A. S. M., Yeoh, H. K. & Ngoh, G. C. A review of the production and applications of waste-derived volatile fatty acids. *Chem. Eng. J.* **235**, 83–99 (2014).
38. Holtzapple, M. T. & Granda, C. B. Carboxylate platform: The MixAlco process part 1: Comparison of three biomass conversion platforms. *Appl. Biochem. Biotechnol.* **156**, 95–106 (2009).
39. Rabaey, K. & Rozendal, R. A. Microbial electrosynthesis - Revisiting the electrical route for microbial production. *Nat. Rev. Microbiol.* **8**, 706–716 (2010).

40. Nevin, K. P., Woodard, T. L., Franks, A. E., Summers, Z. M. & Lovley, D. R. Microbial electrosynthesis: Feeding microbes electricity to convert carbon dioxide and water to multicarbon extracellular organic compounds. *MBio* **1**, (2010).
41. LaBelle, E. V., Marshall, C. W., Gilbert, J. A. & May, H. D. Influence of Acidic pH on Hydrogen and Acetate Production by an Electrosynthetic Microbiome. *PLoS One* **9**, e109935 (2014).
42. Marshall, C. W., Ross, D. E., Fichot, E. B., Norman, R. S. & May, H. D. Electrosynthesis of Commodity Chemicals by an Autotrophic Microbial Community. *Appl. Environ. Microbiol.* **78**, 8412–8420 (2012).
43. Marshall, C. W., Ross, D. E., Fichot, E. B., Norman, R. S. & May, H. D. Long-term Operation of Microbial Electrosynthesis Systems Improves Acetate Production by Autotrophic Microbiomes. (2013).
44. Zhang, T. *et al.* Improved cathode materials for microbial electrosynthesis. *Energy Environ. Sci.* **6**, 217–224 (2013).
45. Nie, H. *et al.* Improved cathode for high efficient microbial-catalyzed reduction in microbial electrosynthesis cells. *Phys. Chem. Chem. Phys.* **15**, 14290–4 (2013).
46. Jourdin, L. *et al.* A novel carbon nanotube modified scaffold as an efficient biocathode material for improved microbial electrosynthesis. *J. Mater. Chem. A* **2**, 13093 (2014).
47. Batlle-Vilanova, P., Puig, S., Gonzalez-Olmos, R., Balaguer, M. D. & Colprim, J. Continuous acetate production through microbial electrosynthesis from CO₂ with microbial mixed culture. *J. Chem. Technol. Biotechnol.* (2015). doi:10.1002/jctb.4657
48. Giddings, C. G. S., Nevin, K., Woodward, T., Lovley, D. R. & Butler, C. S. Simplifying Microbial Electrosynthesis Reactor Design. *Front. Microbiol.* **6**, (2015).
49. Patil, S. A. *et al.* Selective Enrichment Establishes a Stable Performing Community for Microbial Electrosynthesis of Acetate from CO₂. *Environ. Sci. Technol.* **49**, 8833–8843 (2015).
50. Annie Modestra, J., Navaneeth, B. & Venkata Mohan, S. Bio-electrocatalytic reduction of CO₂: Enrichment of homoacetogens and pH optimization towards enhancement of carboxylic acids biosynthesis. *J. CO₂ Util.* **10**, 78–87 (2015).
51. Bajracharya, S. *et al.* Carbon dioxide reduction by mixed and pure cultures in microbial electrosynthesis using an assembly of graphite felt and stainless steel as a cathode. *Bioresour. Technol.* (2015).
doi:http://dx.doi.org/10.1016/j.biortech.2015.05.081
52. Soussan, L., Riess, J., Erable, B., Delia, M. L. & Bergel, A. Electrochemical reduction of CO₂ catalysed by *Geobacter sulfurreducens* grown on polarized stainless steel cathodes. *Electrochem. commun.* **28**, 27–30 (2013).
53. Dennis, P. G., Harnisch, F., Yeoh, Y. K., Tyson, G. W. & Rabaey, K. Dynamics of cathode-associated microbial communities and metabolite profiles in a glycerol-fed bioelectrochemical system. *Appl. Environ. Microbiol.* **79**, 4008–4014 (2013).
54. Sharma, M. *et al.* Bioelectrocatalyzed reduction of acetic and butyric acids via direct electron transfer using a mixed culture of sulfate-reducers drives electrosynthesis of alcohols and acetone. *Chem. Commun.* **49**, 6495–6497 (2013).
55. Cheng, S., Xing, D., Call, D. F. & Logan, B. E. Direct biological conversion of electrical current into methane by electromethanogenesis. *Environ. Sci. Technol.* **43**, 3953–3958 (2009).

56. Van Eerten-Jansen, M. C. A. A., Heijne, A. T., Buisman, C. J. N. & Hamelers, H. V. M. Microbial electrolysis cells for production of methane from CO₂: Long-term performance and perspectives. *Int. J. Energy Res.* **36**, 809–819 (2012).
57. Zaybak, Z., Pisciotta, J. M., Tokash, J. C. & Logan, B. E. Enhanced start-up of anaerobic facultatively autotrophic biocathodes in bioelectrochemical systems. *J. Biotechnol.* **168**, 478–85 (2013).
58. Ganigué, R., Puig, S., Batlle-Vilanova, P., Balaguer, M. D. & Colprim, J. Microbial electrosynthesis of butyrate from carbon dioxide. *Chem. Commun.* **51**, 3235–3238 (2015).
59. Van Eerten-Jansen, M. C. A. A. *et al.* Bioelectrochemical production of caproate and caprylate from acetate by mixed cultures. *ACS Sustain. Chem. Eng.* **1**, 513–518 (2013).
60. Rosenbaum, M. A. & Franks, A. E. Microbial catalysis in bioelectrochemical technologies: Status quo, challenges and perspectives. *Appl. Microbiol. Biotechnol.* **98**, 509–518 (2014).
61. Rocha, M. A. A., van den Bruinhorst, A., Schröer, W., Rathke, B. & Kroon, M. C. Physicochemical properties of fatty acid based ionic liquids. *J. Chem. Thermodyn.* **100**, 156–164 (2016).
62. Osch, D. J. G. P. van, Zubeir, L. F., Bruinhorst, A. van den, Rocha, M. A. A. & Kroon, M. C. Hydrophobic deep eutectic solvents as water-immiscible extractants. *Green Chem.* **17**, 4518–4521 (2015).
63. van den Bruinhorst, A. Deep eutectic solvents : a new generation of designer solvents. (Technische universiteit Eindhoven, 2018).
64. Alkaya, E., Kaptan, S., Ozkan, L., Uludag-Demirer, S. & Demirer, G. N. Recovery of acids from anaerobic acidification broth by liquid-liquid extraction. *Chemosphere* **77**, 1137–1142 (2009).
65. Zhao, H., Xia, S. & Ma, P. Use of ionic liquids as ‘green’ solvents for extractions. *J. Chem. Technol. Biotechnol.* **80**, 1089–1096 (2005).
66. McFarlane, J. *et al.* Room Temperature Ionic Liquids for Separating Organics from Produced Water. *Sep. Sci. Technol.* **40**, 1245–1265 (2005).
67. Marták, J. & Schlosser, Š. Extraction of lactic acid by phosphonium ionic liquids. *Sep. Purif. Technol.* **57**, 483–494 (2007).
68. Blahušiak, M., Schlosser, Š. & Marták, J. Extraction of butyric acid with a solvent containing ammonium ionic liquid. *Sep. Purif. Technol.* **119**, 102–111 (2013).
69. Tonova, K., Svinyarov, I. & Bogdanov, M. G. Hydrophobic 3-alkyl-1-methylimidazolium saccharinates as extractants for l-lactic acid recovery. *Sep. Purif. Technol.* **125**, 239–246 (2014).
70. Reyhanitash, E., Zaalberg, B., Kersten, S. R. A. & Schuur, B. Extraction of volatile fatty acids from fermented wastewater. *Sep. Purif. Technol.* **161**, 61–68 (2016).
71. Wilkes, J. S. A short history of ionic liquids — from molten salts to neoteric solvents. *Green Chem.* **4**, 73–80 (2002).
72. Imperato, G., König, B. & Chiappe, C. Ionic green solvents from renewable resources. *European J. Org. Chem.* 1049–1058 (2007). doi:10.1002/ejoc.200600435
73. Antizar-Ladislao, B. & Turrion-Gomez, J. L. Second-generation biofuels and local bioenergy systems. *Biofuels, Bioprod. Biorefining* **2**, 455 (2008).
74. Langeveld, J. W. A. & Sanders, J. P. M. *The biobased economy biofuels, materials and chemicals in the post-oil era.* (Earthscan, 2012).

75. Lynd, L. R., Cushman, J., Nichols, R. & Wyman, C. Fuel ethanol from cellulosic biomass. *Science* **251**, 1318–1323 (1991).
76. Tilman, D. *et al.* Beneficial Biofuels—The Food, Energy, and Environment Trilemma. *Science* (80-.). **325**, 270–271 (2009).
77. Kleerebezem, R., Joosse, B., Rozendal, R. & Van Loosdrecht, M. C. M. Anaerobic digestion without biogas? *Rev. Environ. Sci. Biotechnol.* **14**, 787–801 (2015).
78. Zaks, D. P. M. *et al.* Contribution of Anaerobic Digesters to Emissions Mitigation and Electricity Generation Under U.S. Climate Policy. *Environ. Sci. Technol.* **45**, 6735–6742 (2011).
79. Angenent, L. T. *et al.* Chain elongation with reactor microbiomes: open-culture biotechnology to produce biochemicals. *Environ. Sci. Technol.* acs.est.5b04847 (2016). doi:10.1021/acs.est.5b04847
80. Schröder, U., Harnisch, F. & Angenent, L. T. Microbial electrochemistry and technology: terminology and classification. *Energy Environ. Sci.* **8**, 513–519 (2015).
81. Hongo, M. & Iwahara, M. Application of Electro-energizing Method to L-glutamic acid fermentation. *Agric. Biol. Chem.* **43**, 2075–2081 (1979).
82. Kim, T. S. & Kim, B. H. Electron flow shift in *Clostridium acetobutylicum* fermentation by electrochemically introduced reducing equivalent. *Biotechnol. Lett.* **10**, 123–128 (1988).
83. Peguin, S., Goma, G., Delorme, P. & Soucaille, P. Metabolic flexibility of *Clostridium acetobutylicum* in response to methyl viologen addition. *Appl. Microbiol. Biotechnol.* **42**, 611–616 (1994).
84. Emde, R. & Schink, B. Enhanced propionate formation by *Propionibacterium freudenreichii* subsp. *freudenreichii* in a three-electrode amperometric culture system. *Appl. Environ. Microbiol.* **56**, 2771–2776 (1990).
85. Choi, O., Um, Y. & Sang, B. I. Butyrate production enhancement by *Clostridium tyrobutyricum* using electron mediators and a cathodic electron donor. *Biotechnol. Bioeng.* **109**, 2494–2502 (2012).
86. Steinbusch, K. J. J., Hamelers, H. V. M., Schaap, J. D., Kampman, C. & Buisman, C. J. N. Bioelectrochemical ethanol production through mediated acetate reduction by mixed cultures. *Environ. Sci. Technol.* **44**, 513–517 (2010).
87. Gildemyn, S. *et al.* Integrated Production, Extraction, and Concentration of Acetic Acid from CO₂ through Microbial Electrosynthesis. *Environ. Sci. Technol. Lett.* (2015). doi:10.1021/acs.estlett.5b00212
88. Molenaar, S. D., Mol, A. R., Sleutels, T. H. J. A. & Heijne, A. Microbial Rechargeable Battery: Energy Storage and Recovery through Acetate. (Wageningen University, 2018). doi:10.1021/acs.estlett.6b00051
89. Harnisch, F. & Schröder, U. Selectivity versus mobility: separation of anode and cathode in microbial bioelectrochemical systems. *ChemSusChem* **2**, 921–926 (2009).
90. Jeremiasse, A. W., Hamelers, H. V. M. & Buisman, C. J. N. Microbial electrolysis cell with a microbial biocathode. *Bioelectrochemistry* **78**, 39–43 (2010).
91. Logan, B. E. *et al.* Microbial fuel cells: Methodology and technology. *Environ. Sci. Technol.* **40**, 5181–5192 (2006).
92. Rozendal, R. A., Jeremiasse, A. W., Hamelers, H. V. M. & Buisman, C. J. N. Hydrogen production with a microbial biocathode. *Environ. Sci. Technol.* **42**, 629–634 (2008).

93. Jourdin, L., Lu, Y., Flexer, V., Keller, J. & Freguia, S. Biologically-induced hydrogen production drives high rate / high efficiency microbial electrosynthesis of acetate from carbon dioxide. *ChemElectroChem* **3**, 581–591 (2016).
94. Stams, A. J. M. Metabolic interactions between anaerobic bacteria in methanogenic environments. *Antonie Van Leeuwenhoek* **66**, 271–294 (1994).
95. Grootsholten, T. I. M., Strik, D. P. B. T. B., Steinbusch, K. J. J., Buisman, C. J. N. & Hamelers, H. V. M. Two-stage medium chain fatty acid (MCFA) production from municipal solid waste and ethanol. *Appl. Energy* **116**, 223–229 (2014).
96. Van Eerten-Jansen, M. C. A. A. *et al.* Microbial community analysis of a methane-producing biocathode in a bioelectrochemical system. *Archaea* **2013**, (2013).
97. Jourdin, L., Freguia, S., Flexer, V. & Keller, J. Bringing High-Rate, CO₂-Based Microbial Electrosynthesis Closer to Practical Implementation through Improved Electrode Design and Operating Conditions. *Environ. Sci. Technol.* **50**, 1982–1989 (2016).
98. Tremblay, P.-L. & Zhang, T. Electrifying microbes for the production of chemicals. *Front. Microbiol.* **6**, 1–10 (2015).
99. Jourdin, L., Freguia, S., Donose, B. C. & Keller, J. Autotrophic hydrogen-producing biofilm growth sustained by a cathode as the sole electron and energy source. *Bioelectrochemistry* **102**, 56–63 (2015).
100. Jourdin, L. *et al.* High Acetic Acid Production Rate Obtained by Microbial Electrosynthesis from Carbon Dioxide. *Environ. Sci. Technol.* **49**, 13566–74 (2015).
101. Ragsdale, S. W. & Pierce, E. Acetogenesis and the Wood-Ljungdahl pathway of CO₂ fixation. *Biochim. Biophys. Acta - Proteins Proteomics* **1784**, 1873–1898 (2008).
102. Daniell, J., Köpke, M. & Simpson, S. D. *Commercial biomass syngas fermentation. Energies* **5**, (2012).
103. Buckel, W. Special clostridial enzymes and fermentation pathways. in *Handbook on Clostridia* (ed. Duerre, P.) 178–212 (CRC Press, 2005).
104. Thauer, R. K., Jungermann, K., Henninger, H., Wenning, J. & Decke, K. The energy metabolism of *Clostridium kluveri*. *Eur. J. Biochem* **4**, 173–180 (1968).
105. Schoberth, S. & Gottschalk, G. Considerations on the energy metabolism of *Clostridium kluveri*. *Arch. Mikrobiol.* **65**, 318–328 (1969).
106. Steinbusch, K. J. J., Hamelers, H. V. M. & Buisman, C. J. N. Alcohol production through volatile fatty acids reduction with hydrogen as electron donor by mixed cultures. *Water Res.* **42**, 4059–4066 (2008).
107. Spirito, C. M., Richter, H., Rabaey, K., Stams, A. J. M. & Angenent, L. T. Chain elongation in anaerobic reactor microbiomes to recover resources from waste. *Curr. Opin. Biotechnol.* **27**, 115–122 (2014).
108. Zhang, F. *et al.* Fatty acids production from hydrogen and carbon dioxide by mixed culture in the membrane biofilm reactor. *Water Res.* **47**, 6122–6129 (2013).
109. González-Cabaleiro, R., Lema, J. M., Rodríguez, J. & Kleerebezem, R. Linking thermodynamics and kinetics to assess pathway reversibility in anaerobic bioprocesses. *Energy Environ. Sci.* **6**, 3780 (2013).
110. Grootsholten, T. I. M., Steinbusch, K. J. J., Hamelers, H. V. M. & Buisman, C. J. N. Improving medium chain fatty acid productivity using chain elongation by reducing the hydraulic retention time in an upflow anaerobic filter. *Bioresour. Technol.* **136**, 735–738 (2013).

111. Agler, M. T., Spirito, C. M., Usack, J. G., Werner, J. J. & Angenent, L. T. Chain elongation with reactor microbiomes: upgrading dilute ethanol to medium-chain carboxylates. *Energy Environ. Sci.* **5**, 8189 (2012).
112. Barker, H. A. & Taha, M. *Clostridium kluverii*, an organism concerned in the formation of caproic acid from ethyl alcohol. *J. Bacteriol.* **43**, 347–363 (1942).
113. Smith, G. M., Kim, B. W., Franke, A. A. & Roberts, J. D. ¹³C NMR studies of butyric fermentation in *Clostridium kluveri*. *J. Biol. Chem.* **260**, 13509–13512 (1985).
114. Bornstein, B. T. & Barker, H. A. The energy metabolism of *Clostridium Kluveri* and the synthesis of fatty acids. *J. Biol. Chem.* **172** (2), 659–669 (1947).
115. Barker, H. A., Kamen, M. D. & Bornstein, B. T. The synthesis of butyric and caproic acids from ethanol and acetic acid by *Clostridium Kluveri*. *Proc. Natl. Acad. Sci. U. S. A.* **31**, 373–381 (1945).
116. ter Heijne, A., Hamelers, H. V. M., Saakes, M. & Buisman, C. J. N. Performance of non-porous graphite and titanium-based anodes in microbial fuel cells. *Electrochim. Acta* **53**, 5697–5703 (2008).
117. Roghair, M. *et al.* Granular Sludge Formation and Characterization in a Chain Elongation Process. *Process Biochem.* (2016). doi:10.1016/j.procbio.2016.06.012
118. Chen, W. S., Ye, Y., Steinbusch, K. J. J., Strik, D. P. B. T. B. & Buisman, C. J. N. Methanol as an alternative electron donor in chain elongation for butyrate and caproate formation. *Biomass and Bioenergy* **93**, 201–208 (2016).
119. Ricci, A. *et al.* Evaluation of the application for a new alternative processing method for animal by-products of Category 3 material (ChainCraft B.V.). *EFSA J.* **16**, (2018).
120. Steinbusch, K. J. J., Hamelers, H. V. M., Plugge, C. M. & Buisman, C. J. N. Biological formation of caproate and caprylate from acetate: Fuel and chemical production from low grade biomass. *Energy Environ. Sci.* **4**, 216–224 (2011).
121. Kucek, L. A., Nguyen, M. & Angenent, L. T. Conversion of L-lactate into n-caproate by a continuously fed reactor microbiome. *Water Res.* **93**, 163–171 (2016).
122. Zhu, X. *et al.* The synthesis of n-caproate from lactate: a new efficient process for medium-chain carboxylates production. *Sci. Rep.* **5**, 14360 (2015).
123. Steinbusch, K. J. J., Arvaniti, E., Hamelers, H. V. M. & Buisman, C. J. N. Selective inhibition of methanogenesis to enhance ethanol and n-butyrate production through acetate reduction in mixed culture fermentation. *Bioresour. Technol.* **100**, 3261–3267 (2009).
124. Ding, H. B., Tan, G. Y. A. & Wang, J. Y. Caproate formation in mixed-culture fermentative hydrogen production. *Bioresour. Technol.* **101**, 9550–9559 (2010).
125. Kenealy, W. R. & Waselefsky, D. M. Studies on the substrate range of *Clostridium kluveri*; the use of propanol and succinate. *Arch. Microbiol.* **141**, 187–194 (1985).
126. Coma, M. *et al.* Product Diversity Linked to Substrate Usage in Chain Elongation by Mixed-Culture Fermentation. *Environ. Sci. Technol.* **50**, 6467–6476 (2016).
127. Raes, S. M. T., Jourdin, L., Buisman, C. J. N. & Strik, D. P. B. T. B. Continuous long-term bioelectrochemical chain elongation to butyrate. *ChemElectroChem* **4**, 386–395 (2017).
128. Chen, W. S., Strik, D. P. B. T. B., Buisman, C. J. N. & Kroeze, C. Production of Caproic Acid from Mixed Organic Waste: An Environmental Life Cycle Perspective. *Environ. Sci. Technol.* **51**, 7159–7168 (2017).

129. Jourdin, L., Raes, S. M. T., Buisman, C. J. N. N. & Strik, D. P. B. T. B. Critical biofilm growth throughout unmodified carbon felts allows continuous bioelectrochemical chain elongation from CO₂ up to caproate at high current density. *Front. Energy Res.* **6**, 7 (2018).
130. Vassilev, I. *et al.* Microbial Electrosynthesis of Isobutyric, Butyric, Caproic Acids, and Corresponding Alcohols from Carbon Dioxide. *ACS Sustain. Chem. Eng.* **6**, 8485–8493 (2018).
131. Batlle-Vilanova, P. *et al.* Microbial electrosynthesis of butyrate from carbon dioxide: production and extraction. *Bioelectrochemistry* **117**, 57–64 (2017).
132. Arends, J. B. A., Patil, S. A., Roume, H. & Rabaey, K. Continuous long-term electricity-driven bioproduction of carboxylates and isopropanol from CO₂ with a mixed microbial community. *J. CO₂ Util.* **20**, 141–149 (2017).
133. Bajracharya, S., Vanbroekhoven, K., Buisman, C., Strik, D. & PANT, D. Bioelectrochemical Conversion of CO₂ to Chemicals: CO₂ as Next Generation Feedstock for the Electricity-driven Bioproduction in Batch and Continuous mode. *Faraday Discuss.* **00**, 1–17 (2017).
134. Wenzel, J. *et al.* Microbial Community Pathways for the Production of Volatile Fatty Acids From CO₂ and Electricity. *Front. Energy Res.* **6**, (2018).
135. LaBelle, E. V. & May, H. D. Energy Efficiency and Productivity Enhancement of Microbial Electrosynthesis of Acetate. *Front. Microbiol.* **8**, 1–9 (2017).
136. Ramió-Pujol, S., Ganigué, R., Bañeras, L. & Colprim, J. How can alcohol production be improved in carboxydutrophic clostridia? *Process Biochem.* **50**, 1047–1055 (2015).
137. Sarkar, O., Butti, S. K. & Venkata Mohan, S. Acidogenesis driven by hydrogen partial pressure towards bioethanol production through fatty acids reduction. *Energy* **118**, 425–434 (2017).
138. Puig, S. *et al.* Tracking H₂-mediated microbial electrosynthesis of commodity chemicals from carbon dioxide. *Bioresour. Technol.* **228**, 201–209 (2017).
139. Blanchet, E. M. *et al.* Importance of the hydrogen route in up-scaling electrosynthesis for microbial CO₂ reduction. *Energy Environ. Sci.* 3731–3744 (2015). doi:10.1039/C5EE03088A
140. Crable, B. R., Plugge, C. M., McInerney, M. J. & Stams, A. J. M. Formate formation and formate conversion in biological fuels production. *Enzyme Res.* **2011**, (2011).
141. Worm, P., Stams, A. J. M., Cheng, X. & Plugge, C. M. Growth- and substrate-dependent transcription of formate dehydrogenase and hydrogenase coding genes in Syntrophobacter fumaroxidans and Methanospirillum hungatei. *Microbiology* **157**, 280–289 (2011).
142. Deutzmann, J. S., Sahin, M. & M., S. A. Extracellular Enzymes Facilitate Electron Uptake in Biocorrosion and bioelectrosynthesis. *MBio* **6**, 1–8 (2015).
143. Nevin, K. P. *et al.* Electrosynthesis of organic compounds from carbon dioxide is catalyzed by a diversity of acetogenic microorganisms. *Appl. Environ. Microbiol.* **77**, 2882–2886 (2011).
144. Lienemann, M., Deutzmann, J. S., Milton, R. D., Sahin, M. & Spormann, A. M. Mediator-free enzymatic electrosynthesis of formate by the Methanococcus maripaludis heterodisulfide reductase supercomplex. *Bioresour. Technol.* **254**, 278–283 (2018).
145. Lentz, K. & Wood, H. G. Synthesis of acetate from formate and carbon dioxide by Clostridium thermoaceticum. *J. Biol. Chem.* **215**, 645–654 (1955).

146. Jourdin, L., Raes, S. M. T., Buisman, C. J. N. & Strik, D. P. B. T. B. Critical biofilm growth throughout unmodified carbon felts allows continuous bioelectrochemical chain elongation from CO₂ up to caproate at high current density. *Front. Energy Res.* **6**, (2018).
147. Elsdén, S. R., Volcani, B. E., Gilchrist, F. M. C. & Lewis, D. Properties of a fatty acid forming organism isolated from the rumen of sheep. *J. Bacteriol.* **72**, 681–689 (1956).
148. Grootsholten, T. I. M., Steinbusch, K. J. J., Hamelers, H. V. M. & Buisman, C. J. N. High rate heptanoate production from propionate and ethanol using chain elongation. *Bioresour. Technol.* **136**, 715–718 (2013).
149. Roghair, M. *et al.* Controlling ethanol use in chain elongation by CO₂ loading rate. *Environ. Sci. Technol.* acs.est.7b04904 (2018). doi:10.1021/acs.est.7b04904
150. Tomlinson, N. & Barker, H. A. Carbon dioxide and acetate utilization by *Clostridium kluyveri* - Influence of nutritional conditions on utilization patterns. *J. Biol. Chem.* **209**, 585–595 (1954).
151. Han, W., He, P., Shao, L. & Lü, F. Metabolic interactions of a chain elongation microbiome. *Appl. Environ. Microbiol.* **84**, 1–16 (2018).
152. Marshall, C. W. *et al.* Metabolic Reconstruction and Modeling Microbial Electrosynthesis. *Sci. Rep.* 8391 (2017). doi:10.1101/059410
153. Candry, P. *et al.* A novel high-throughput method for kinetic characterisation of anaerobic bioproduction strains, applied to *Clostridium kluyveri*. *Sci. Rep.* **8**, 1–13 (2018).
154. Thauer, R. K., Jungermann, K. & Decker, K. Energy Conservation in Chemotrophic Anaerobic Bacteria. *Bacteriol. Rev.* **40**, 100–181 (1977).
155. Eggeman, T. & Verser, D. Recovery of organic acids from fermentation broths. in *Applied biochemistry and biotechnology* (eds. Davison, B. H., Evans, B. R., Finkelstein, M. & McMillan, J. D.) **121–124**, 605–618 (Humana Press, 2005).
156. Cherubini, F. The biorefinery concept: Using biomass instead of oil for producing energy and chemicals. *Energy Convers. Manag.* **51**, 1412–1421 (2010).
157. Arslan, D. *et al.* Selective short chain carboxylates production: a review on control mechanisms to direct mixed culture fermentations. *Crit. Rev. Environ. Sci. Technol.* **3389**, 00–00 (2016).
158. Reyhanitash, E., Zaalberg, B., Ijmker, H., Kersten, S. & Schuur, B. CO₂-enhanced extraction of acetic acid from fermented wastewater. *Green Chem.* **17**, 4393–4400 (2015).
159. López-Garzón, C. S. & Straathof, A. J. J. Recovery of carboxylic acids produced by fermentation. *Biotechnol. Adv.* **32**, 873–904 (2014).
160. Ijmker, H. M., Gramblička, M., Kersten, S. R. A., Van Der Ham, A. G. J. & Schuur, B. Acetic acid extraction from aqueous solutions using fatty acids. *Sep. Purif. Technol.* **125**, 256–263 (2014).
161. Huddleston, J. G. J. G., Willauer, H. D., Swatloski, R. P., Visser, A. E. & Rogers, R. D. R. D. Room temperature ionic liquids as novel media for ‘clean’ liquid – liquid extraction. *Chem. Commun.* 1765–1766 (1998).
162. Thuy Pham, T. P., Cho, C. W. & Yun, Y. S. Environmental fate and toxicity of ionic liquids: A review. *Water Res.* **44**, 352–372 (2010).
163. Coleman, D. & Gathergood, N. Biodegradation studies of ionic liquids. *Chem. Soc. Rev.* **39**, 600 (2010).

164. Egorova, K. S. & Ananikov, V. P. Toxicity of ionic liquids: Eco(cyto)activity as complicated, but unavoidable parameter for task-specific optimization. *ChemSusChem* **7**, 336–360 (2014).
165. Petkovic, M., Seddon, K. R., Rebelo, L. P. N. & Silva Pereira, C. Ionic liquids: a pathway to environmental acceptability. *Chem. Soc. Rev.* **40**, 1383–1403 (2011).
166. Zhao, D., Liao, Y. & Zhang, Z. D. Toxicity of ionic liquids. *Clean - Soil, Air, Water* **35**, 42–48 (2007).
167. Matzke, M. *et al.* The influence of anion species on the toxicity of 1-alkyl-3-methylimidazolium ionic liquids observed in an (eco)toxicological test battery. *Green Chem.* **9**, 1198–1207 (2007).
168. Łuczak, J., Jungnickel, C., Łcka, I., Stolte, S. & Hupka, J. Antimicrobial and surface activity of 1-alkyl-3-methylimidazolium derivatives. *Green Chem.* **12**, 593–601 (2010).
169. Duan, E. *et al.* Anaerobic biodegradability and toxicity of caprolactam-tetrabutyl ammonium bromide ionic liquid to methanogenic gas production. *RSC Adv.* **3**, 18817–18820 (2013).
170. Gao, J., Chen, L., Yuan, K., Huang, H. & Yan, Z. Ionic liquid pretreatment to enhance the anaerobic digestion of lignocellulosic biomass. *Bioresour. Technol.* **150**, 352–358 (2013).
171. Li, W. & Xu, G. Enhancement of anaerobic digestion of grass by pretreatment with imidazolium-based ionic liquids. *Environ. Technol. (United Kingdom)* **38**, 1843–1851 (2017).
172. Parmentier, D., Metz, S. J. & Kroon, M. C. Tetraalkylammonium oleate and linoleate based ionic liquids: promising extractants for metal salts. *Green Chem.* **15**, 205–209 (2013).
173. Parmentier, D., Vander Hoogerstraete, T., Metz, S. J., Binnemans, K. & Kroon, M. C. Selective Extraction of Metals from Chloride Solutions with the Tetraoctylphosphonium Oleate Ionic Liquid. *Ind. Eng. Chem. Res.* **54**, 5149–5158 (2015).
174. Sokolsky-Papkov, M., Shikanov, A., Ezra, A., Vaisman, B. & Domb, A. J. Fatty Acid-Based Biodegradable Polymers: Synthesis and Applications. in *Polymer Degradation and Performance* **1004**, 6–60 (American Chemical Society, 2009).
175. Parmentier, D., Valia, Y. A., Metz, S. J., Burheim, O. S. & Kroon, M. C. Regeneration of the ionic liquid tetraoctylammonium oleate after metal extraction. *Hydrometallurgy* **158**, 56–60 (2015).
176. Reyhanitash, E., Kersten, S. R. A. & Schuur, B. Recovery of Volatile Fatty Acids from Fermented Wastewater by Adsorption. *ACS Sustain. Chem. Eng.* **5**, 9176–9184 (2017).
177. Kontro, I. *et al.* Effects of phosphonium-based ionic liquids on phospholipid membranes studied by small-angle X-ray scattering. *Chem. Phys. Lipids* **201**, 59–66 (2016).
178. Witos, J., Russo, G., Ruokonen, S. K. & Wiedmer, S. K. Unraveling interactions between ionic liquids and phospholipid vesicles using nanoplasmonic sensing. *Langmuir* **33**, 1066–1076 (2017).
179. Ruokonen, S.-K. *et al.* Correlation between ionic liquid cytotoxicity and liposome-ionic liquid interactions. *Chem. - A Eur. J.* **1–13** (2018). doi:10.1002/chem.201704924
180. Cornmell, R. J., Winder, C. L., Tiddy, G. J. T., Goodacre, R. & Stephens, G. Accumulation of ionic liquids in Escherichia coli cells. *Green Chem.* **10**, 836 (2008).

181. Mccarty, P. L. & Mckinney, R. E. Salt toxicity in anaerobic digestion. *J. (Water Pollut. Control Fed.* **33**, 399–415 (1961).
182. Patel, G. B. & Roth, L. a. Effect of sodium chloride on growth and methane production of methanogens. *Can. J. Microbiol.* **23**, 893–7 (1977).
183. Rinzema, A., van Lier, J. & Lettinga, G. Sodium inhibition of acetoclastic methanogens in granular sludge from a UASB reactor. *Enzyme Microb. Technol.* **10**, 24–32 (1988).
184. Liu, Y. & Boone, D. R. Effects of salinity on methanogenic decomposition. *Bioresour. Technol.* **35**, 271–273 (1991).
185. De Vrieze, J. *et al.* Presence does not imply activity: DNA and RNA patterns differ in response to salt perturbation in anaerobic digestion. *Biotechnol. Biofuels* **9**, 244 (2016).
186. Hanaki, K. & Nagase, M. Mechanism of inhibition caused by long chain fatty acids in Anaerobic Digestion Process. *Biotechnol. Bioeng.* **23**, 1591–1610 (1981).
187. Koster, I. W. & Cramer, A. Inhibition of Methanogenesis from Acetate in Granular Sludge by Long-Chain Fatty Acids. *Appl. Environ. Microbiol.* **53**, 403–409 (1987).
188. Rinzema, A., Boone, M., van Knippenberg, K. & Lettinga, G. Bactericidal effect of long chain fatty acids in anaerobic digestion. *Water Environ. Res.* **66**, 40–49 (1994).
189. Alves, M. M. *et al.* Waste lipids to energy: How to optimize methane production from long-chain fatty acids (LCFA). *Microb. Biotechnol.* **2**, 538–550 (2009).
190. Silva, S. A. *et al.* Toxicity of long chain fatty acids towards acetate conversion by *Methanosaeta concilii* and *Methanosarcina mazei*. *Microb. Biotechnol.* **9**, 514–518 (2016).
191. Pereira, M. A., Pires, O. C., Mota, M. & Alves, M. M. Anaerobic biodegradation of oleic and palmitic acids: Evidence of mass transfer limitations caused by long chain fatty acid accumulation onto the anaerobic sludge. *Biotechnol. Bioeng.* **92**, 15–23 (2005).
192. Lindeboom, R. E. F. *Autogenerative high pressure digestion: Anaerobic digestion and biogas upgrading in a single step reactor system.* *Water Science and Technology* **64**, (2014).
193. He, Y., Sutton, N. B., Rijnaarts, H. H. M. & Langenhoff, A. A. M. Pharmaceutical biodegradation under three anaerobic redox conditions evaluated by chemical and toxicological analyses. *Sci. Total Environ.* **618**, 658–664 (2018).
194. Eyal, A. M. & Canari, R. pH Dependence of Carboxylic and Mineral Acid Extraction by Amine-Based Extractants: Effects of pKa, Amine Basicity, and Diluent Properties. *Ind. Eng. Chem. Res.* **34**, 1789–1798 (1995).
195. Fernandez, J. F., Neumann, J., Thoming, J. & Thoeming, J. Regeneration, Recovery and Removal of Ionic Liquids. *Curr. Org. Chem.* **15**, 1992–2014 (2011).
196. Raes, S. M. T. *et al.* Water-Based Synthesis of Hydrophobic Ionic Liquids [N⁸⁸⁸][oleate] and [P^{666,14}][oleate] and their Bioprocess Compatibility. *ChemistryOpen* **7**, 878–884 (2018).
197. Oliveira, F. S., Araújo, J. M. M., Ferreira, R., Rebelo, L. P. N. & Marrucho, I. M. Extraction of l-lactic, l-malic, and succinic acids using phosphonium-based ionic liquids. *Sep. Purif. Technol.* **85**, 137–146 (2012).
198. Kholkin, A. I., Belova, V. V., Zakhodyaeva, Y. A. & Voshkin, A. A. Solvent Extraction of Weak Acids in Binary Extractant Systems. *Sep. Sci. Technol.* **48**, 1417–1425 (2013).
199. Canari, R. & Eyal, A. M. Selectivity in Monocarboxylic Acids Extraction from Their Mixture Solutions Using an Amine-Based Extractant: Effect of pH. *Ind. Eng. Chem. Res.* **42**, 1301–1307 (2003).

200. McMahon, K. D., Zheng, D., Stams, A. J. M., Mackie, R. I. & Raskin, L. Microbial population dynamics during start-up and overload conditions of anaerobic digesters treating municipal solid waste and sewage sludge. *Biotechnol. Bioeng.* **87**, 823–834 (2004).
201. Oehmen, A., Pinto, F. V., Silva, V., Albuquerque, M. G. E. & Reis, M. A. M. The impact of pH control on the volumetric productivity of mixed culture PHA production from fermented molasses. *Eng. Life Sci.* **14**, 143–152 (2013).
202. Müller, A., Schulz, R., Wittmann, J., Kaplanow, I. & Górak, A. Investigation of a phosphate/1-butyl-3-methylimidazolium trifluoromethanesulfonate/water system for the extraction of 1,3-propanediol from fermentation broth. *RSC Adv.* **3**, 148–156 (2013).
203. Dai, J., Wang, H., Li, Y. & Xiu, Z. Imidazolium ionic liquids-based salting-out extraction of 2,3-butanediol from fermentation broths. (2018). doi:10.1016/j.procbio.2018.05.015
204. Kracke, F., Vassilev, I. & Krömer, J. O. Microbial electron transport and energy conservation - The foundation for optimizing bioelectrochemical systems. *Front. Microbiol.* **6**, 1–18 (2015).
205. Reguera, G. *et al.* Biofilm and nanowire production leads to increased current in *Geobacter sulfurreducens* fuel cells. *Appl. Environ. Microbiol.* **72**, 7345–7348 (2006).
206. Gorby, A. *et al.* Electrically conductive bacterial nanowires produced by *Shewanella oneidensis* strain MR-1 and other microorganisms. *Proc. Natl. Acad. Sci.* **103**, 11358–11363 (2006).
207. Malvankar, N. S. & Lovley, D. R. Microbial nanowires for bioenergy applications. *Curr. Opin. Biotechnol.* **27**, 88–95 (2014).
208. Malvankar, N. S. & Lovley, D. R. Microbial nanowires: A new paradigm for biological electron transfer and bioelectronics. *ChemSusChem* **5**, 1039–1046 (2012).
209. Lovley, D. R. Syntrophy Goes Electric: Direct Interspecies Electron Transfer. *Annu. Rev. Microbiol.* **71**, annurev-micro-030117-020420 (2017).
210. Malvankar, N. S. *et al.* Tunable metallic-like conductivity in microbial nanowire networks. *Nat. Nanotechnol.* **6**, 573–579 (2011).
211. Choi, O., Kim, T., Woo, H. M. & Um, Y. Electricity-driven metabolic shift through direct electron uptake by electroactive heterotroph *Clostridium pasteurianum*. *Sci. Rep.* **4**, 6961 (2014).
212. Rosenbaum, M., Aulenta, F., Villano, M. & Angenent, L. T. Cathodes as electron donors for microbial metabolism: Which extracellular electron transfer mechanisms are involved? *Bioresour. Technol.* **102**, 324–333 (2011).
213. Levar, C. E. E., Rollefson, J. B. & Bond, D. R. Energetic and Molecular Constraints on the Mechanism of Environmental Fe(III) Reduction by *Geobacter*. in *Microbial Metal Respiration: From Geochemistry to Potential Applications* (eds. Gescher, J. & Kappler, A.) 29–48 (Springer Berlin Heidelberg, 2012). doi:10.1007/978-3-642-32867-1_2
214. Ross, D. E., Flynn, J. M., Baron, D. B., Gralnick, J. A. & Bond, D. R. Towards electrosynthesis in *Shewanella*: Energetics of reversing the Mtr pathway for reductive metabolism. *PLoS One* **6**, (2011).
215. Liu, W. *et al.* Overexpression of rusticyanin in *acidithiobacillus ferrooxidans* ATCC19859 increased Fe(II) oxidation activity. *Curr. Microbiol.* **62**, 320–324 (2011).
216. Rabaey, K., Boon, N., Höfte, M. & Verstraete, W. Microbial phenazine production enhances electron transfer in biofuel cells. *Environ. Sci. Technol.* **39**, 3401–3408 (2005).

217. Marsili, E. *et al.* Shewanella secretes flavins that mediate extracellular electron transfer. *Proc. Natl. Acad. Sci.* **105**, 3968–3973 (2008).
218. Moscoviz, R., Toledo-Alarcón, J., Trably, E. & Bernet, N. Electro-Fermentation: How To Drive Fermentation Using Electrochemical Systems. *Trends Biotechnol.* (2016). doi:10.1016/j.tibtech.2016.04.009
219. Kracke, F., Virdis, B., Bernhardt, P., Rabaey, K. & Krömer, J. O. Redox dependent metabolic shift in *Clostridium autoethanogenum* by extracellular electron supply. *Biotechnol. Biofuels* 1–12 (2016). doi:10.1186/s13068-016-0663-2
220. Shin, H., Zeikus, J. & Jain, M. Electrically enhanced ethanol fermentation by *Clostridium thermocellum* and *Saccharomyces cerevisiae*. *Appl. Microbiol. Biotechnol.* **58**, 476–481 (2002).
221. Koch, C. *et al.* Predicting and experimental evaluating bio-electrochemical synthesis — A case study with *Clostridium kluyveri*. *Bioelectrochemistry* **118**, 114–122 (2017).
222. Imkamp, F., Biegel, E., Jayamani, E., Buckel, W. & Müller, V. Dissection of the caffeate respiratory chain in the acetogen *Acetobacterium woodii*: Identification of an Rnf-type NADH dehydrogenase as a potential coupling site. *J. Bacteriol.* **189**, 8145–8153 (2007).
223. Müller, V., Imkamp, F., Biegel, E., Schmidt, S. & Dilling, S. Discovery of a ferredoxin:NAD⁺-oxidoreductase (Rnf) in *Acetobacterium woodii*: A novel potential coupling site in acetogens. *Ann. N. Y. Acad. Sci.* **1125**, 137–146 (2008).
224. Biegel, E. & Müller, V. Bacterial Na⁺-translocating ferredoxin:NAD⁺ oxidoreductase. *Proc. Natl. Acad. Sci.* **107**, 18138–18142 (2010).
225. Hess, V. *et al.* Occurrence of ferredoxin:NAD⁺ oxidoreductase activity and its ion specificity in several Gram-positive and Gram-negative bacteria. *PeerJ* **4**, e1515 (2016).
226. Hedderich, R. Energy-Converting [NiFe] Hydrogenases from Archaea and Extremophiles: Ancestors of Complex I. *J. Bioenerg. Biomembr.* **36**, 65–75 (2004).
227. Müller, V., Chowdhury, N. P. & Basen, M. Electron Bifurcation : A Long- Hidden Energy-Coupling Mechanism. *Annu. Rev. Microbiol.* **72**, 31–353 (2018).
228. Herrmann, G., Jayamani, E., Mai, G. & Buckel, W. Energy conservation via electron-transferring flavoprotein in anaerobic bacteria. *J. Bacteriol.* **190**, 784–791 (2008).
229. Buckel, W. & Thauer, R. K. Energy conservation via electron bifurcating ferredoxin reduction and proton/Na⁺ translocating ferredoxin oxidation. *Biochim. Biophys. Acta - Bioenerg.* **1827**, 94–113 (2013).
230. Wang, S., Huang, H., Kahnt, J. & Thauer, R. K. A reversible electron-bifurcating ferredoxin- and NAD-Dependent [FeFe]-Hydrogenase (HydABC) in *Moorella thermoacetica*. *J. Bacteriol.* **195**, 1267–1275 (2013).
231. Schuchmann, K. & Müller, V. Autotrophy at the thermodynamic limit of life: A model for energy conservation in acetogenic bacteria. *Nat. Rev. Microbiol.* **12**, 809–821 (2014).
232. Jungermann, K., Rupprecht, E., Ohrloff, C., Thauer, R. K. & Decker, K. BIOENERGETICS : Regulation of the Reduced Nicotinamide Regulation of the Reduced Nicotinamide Adenine Reductase System in *Clostridium kluyveri* *. *J. Biol. Chem.* **246**, 960–963 (1971).
233. Pedersen, A., Karlsson, G. B. & Rydström, J. Proton-translocating transhydrogenase: An update of unsolved and controversial issues. *J. Bioenerg. Biomembr.* **40**, 463–473 (2008).

234. Wang, S., Huang, H., Moll, J. & Thauer, R. K. NADP⁺ reduction with reduced ferredoxin and NADP⁺ reduction with NADH are coupled via an electron-bifurcating enzyme complex in *Clostridium kluyveri*. *J. Bacteriol.* **192**, 5115–5123 (2010).
235. Koch, C., Müller, S., Harms, H. & Harnisch, F. Microbiomes in bioenergy production: From analysis to management. *Curr. Opin. Biotechnol.* **27**, 65–72 (2014).
236. Marshall, C. W., LaBelle, E. V. & May, H. D. Production of fuels and chemicals from waste by microbiomes. *Curr. Opin. Biotechnol.* **24**, 391–397 (2013).
237. Seedorf, H. *et al.* The genome of *Clostridium kluyveri*, a strict anaerobe with unique metabolic features. *Proc. Natl. Acad. Sci. U. S. A.* **105**, 2128–2133 (2008).
238. Kracke, F., Lai, B., Yu, S. & Krömer, J. O. Balancing cellular redox metabolism in microbial electrosynthesis and electro fermentation – A chance for metabolic engineering. *Metab. Eng.* **45**, 109–120 (2018).
239. Haveren, J. van, Scott, E. L. & Sanders, J. Bulk chemicals from biomass. *Biofuels, Bioprod. Biorefining* **2**, 41–57 (2008).
240. Chen, W. Microbial chain elongation based on methanol. (Wageningen university, 2017).
241. WRR. Klimaatstrategie - tussen ambitie en realisme. *Verkenningen* (2007).
242. Sleutels, T. H. J. A., Ter Heijne, A., Buisman, C. J. N. & Hamelers, H. V. M. Bioelectrochemical Systems: An Outlook for Practical Applications. *ChemSusChem* **5**, 1012–1019 (2012).
243. Jourdin, L. & Strik, D. Electrodes for cathodic microbial electrosynthesis processes : key-developments and criteria for effective research & implementation. in *Functional Electrodes for Enzymatic and Microbial Electrochemical Systems* 429–473 (WORLD SCIENTIFIC (EUROPE), 2017). doi:doi:10.1142/9781786343543_0012
244. Molenaar, S. D. *Optimization of Bioelectrochemical Systems for Sustainable Energy Storage*. (2018).
245. Hamelers, H. V. M. *et al.* New applications and performance of bioelectrochemical systems. *Appl. Microbiol. Biotechnol.* **85**, 1673–1685 (2010).
246. Gildemyn, S. *et al.* Upgrading syngas fermentation effluent using *Clostridium kluyveri* in a continuous fermentation. *Biotechnol. Biofuels* **10**, 83 (2017).
247. Gildemyn, S., Rozendal, R. A. & Rabaey, K. A Gibbs Free Energy-Based Assessment of Microbial Electrocatalysis. *Trends Biotechnol.* **35**, 393–406 (2017).



Summary

To decrease our society's dependence on polluting fossil resources, alternative sources for chemical and fuel production need to be developed. Organic residual streams are a renewable feedstock that can be used to replace these fossil-based fuels and chemicals. In this thesis bioelectrochemical chain elongation (BCE) has been studied to convert short chain fatty acids (SCFAs, model substrates for acidified organic residual streams) into biobased intermediate chemicals. BCE is subtype of a microbial electrosynthesis (MES) system, in which microorganisms catalyse the elongation of SCFAs and/or CO₂ towards medium chain fatty acids in an electrochemical cell.

Part 1 of this thesis studied the formation of valuable products from SCFAs using BCE systems. In **chapter 2** it started with the proof of concept of using an electrode for the sustained chain elongation of CO₂ and acetate in continuous BCE systems. Four BCE reactors were used to study the role of applied current: two were applied with 3.1 A m⁻² (projected surface area of electrode) and the other two with 9.4 A m⁻². n-Butyrate (nC4) was the main identified product in all reactors. The highest applied current led to the highest nC4 production rate of 0.54 g L⁻¹ d⁻¹ (24.5 mMC d⁻¹). The highest concentration of nC4 reached under high current regime was 0.59 g L⁻¹ (26.8 mMC). Trace amounts of propionate and n-caproate were also produced, but no alcohols were detected over the course of the experiments (163 days).

To improve BCE and enhance production, in **chapter 2** as well a literature review is provided to give insights into all the reported pathways to produce nC4 in fermentations. In fermentative chain elongation soluble electron donors, like ethanol or lactate, supply reducing equivalents and drive microbial metabolism. Since such compounds were not detected in the BCE reactors, it was hypothesised that nC4 production was limited by intermediate production and subsequent fast consumption of ethanol or lactate.

This hypothesis of intermediary production of ethanol or lactate limiting BCE performance was verified in **chapter 3**. Both ethanol and lactate were separately introduced in triplicate BCE reactors applied with 9.4 A m⁻². Both compounds did not significantly affect the rates of nC4 production. Next to these compounds, the effect of formate on nC4 production was tested. Formate injection led to acetate production and decreased nC4 production. The results suggested that formate conversion to acetate competed with acetate elongation to nC4 for electrons. This competition subsequently resulted in decreased production of nC4. To investigate role of the electrode as electron donor, the current was increased to 18.1 A m⁻². This increase in applied current doubled the production rates of nC4. Hence, this chapter demonstrates that the nC4 production in our BCE systems was not limited by

intermediate production of well-known electron donors, but was driven by electrode-derived electrons.

For BCE to become a feasible organic waste valorisation technology, the studied substrate range needs to extend beyond acetate reduction. Therefore, in **chapter 4** four different substrate feeding strategies and the subsequent product spectrum were investigated: I) acetate, II) acetate and propionate, III) acetate and n-butyrate, and IV) a mixture of acetate, propionate and n-butyrate. In phase I, nC4 was produced at $0.9 \text{ g L}^{-1} \text{ d}^{-1}$ (39.7 mMC d^{-1}). After introduction of propionate in phase II, n-valerate (nC5) production started and sustained until medium was changed at the start of phase III. The maximum concentration of nC5 reached was 1.2 g L^{-1} (60.6 mMC), and the highest production rate was $1.1 \text{ g L}^{-1} \text{ d}^{-1}$ (57.5 mMC d^{-1}) at a high carbon-based selectivity of 73.8 %. This seems contradictory to ethanol chain elongation studies in which acetate is concurrently formed leading to straight fatty acids as by-products. Upon introduction of acetate and n-butyrate, n-caproate (nC6) production started and reached a maximum concentration of 0.3 g L^{-1} (15.8 mMC). The nC6 formation selectivity was 83.4 % in phase III. When all the three SCFA were supplied as substrate in phase IV, nC5 was the main product (95.4%). The observed preference for propionate elongation over both nC4 formation or nC6 formation is in contrast to fermentative ethanol-based chain elongation studies.

Part 2 of this thesis focusses on the extraction of the bioproducts from dilute aqueous streams using ionic liquids. The conversion of organic waste streams as renewable feedstocks into carboxylic acids (such as SCFAs but as well the medium chain fatty acids (MCFAs)) results in relatively dilute aqueous streams. These relatively low concentrations are a major bottleneck for these bioprocesses to compete with the production of platform chemicals based on fossil resources. A way to overcome this bottleneck is to extract the carboxylates from the fermentation broths using liquid-liquid extraction. Hydrophobic ionic liquids (ILs) are novel extractants which can be used for this purpose. Ionic liquids are salts comprised of ions, with relatively low melting temperatures (often below 100°C). By varying the types of ion and, for example, the branching of the ions, the physical properties of the IL, such as its hydrophobicity, can be tailored. To integrate these ILs as *in situ* extractants in biotechnologies, the ionic liquid should be compatible with the bioprocess.

In **chapter 5** the biocompatibility of the two hydrophobic ILs [N₈₈₈][oleate] and [P_{66,14}][oleate] were investigated in a two-phase system (IL layer on top of water phase). Commonly, ILs are synthesized in organic solvents, such as toluene and ethanol. After synthesis some trace amounts of these solvents can remain in the IL. When that hydrophobic IL is placed on top of a water phase, the trace amounts of synthesis solvent can leak into the water phase. To circumvent possible toxic effects

of the trace amounts of solvent in the IL, water was used as synthesis solvent. After synthesis of the two ILs, their bioprocess compatibility was assessed. Methanogenic granular sludge was placed in medium without carbon source, and on top of that medium the IL phase was placed. After 24 days the sludge was separated from the water phase and placed into fresh medium. Upon transfer of the sludge into fresh medium with acetate as substrate, [P_{666,14}][oleate] exposed granules were completely inhibited. Granules exposed to [N₈₈₈][oleate] sustained anaerobic digestion activity, although moderately reduced. Co-ions of the starting materials of the ILs, bromide and oleate, could have remained in the IL after synthesis. Both bromide (5 to 500 ppm) and oleate (10 to 4000 ppm) were demonstrated to not inhibit methanogenic conversion of acetate. Conclusively, [P_{666,14}] was identified as a bioprocess incompatible component and [N₈₈₈][oleate] as bioprocess compatible.

For an IL to become the envisioned *in situ* extractants for bioprocesses, the IL needs to be regenerated and reused. In **chapter 6** a concept of an IL as transport liquid is presented, in which a product (from a bioprocess) is *in situ* extracted into a hydrophobic IL. The subsequent extraction of the product from the IL (i.e. regeneration) does not necessarily need to take place in/at the same physical location, time and/or medium as where the extraction of product into the IL occurred. Therefore, the IL can be regarded as transport liquid of the product.

To study the feasibility of this concept, the bioprocess compatible hydrophobic IL [N₈₈₈][oleate] was used for two successive cycles of i) extraction of SCFAs into the IL [N₈₈₈][oleate] and ii) regeneration of the IL. For the regeneration of the IL a novel method was described which employs microorganisms to assist in IL regeneration, naming it 'microbial assisted regeneration'. Microbial assisted regeneration is beneficial as no additional salt is needed for both pH control of the bioprocess as well as for recovery of the products from the IL. The experiments in this chapter demonstrate the potential of using hydrophobic ILs as transport liquid between two bioprocesses. When the concept of an IL as transport liquid is coupled with the proposed microbial regeneration method, two distinct biological processes can be coupled.

For BCE to become an industrial waste valorisation technology, the production needs to be improved. Although the electron transfer pathways are not unravelled yet, **chapter 7** gives an overview of all the nowadays described pathways. In this way, the coupling of microbial metabolism with an electrode can be understood more. Based on these insights, several recommendations are provided to improve BCE and to render the technology mature enough to prove its potential using real acidified organic residual streams.



List of Publications

Raes, S.M.T., Jourdin, L., Buisman, C.J.N. & Strik, D.P.B.T.B. Continuous long-term bioelectrochemical chain elongation to butyrate. *ChemElectroChem* **4**, 386–395 (2017).

Jourdin, L., **Raes, S.M.T.**, Buisman, C.J.N. & Strik, D.P.B.T.B. Critical biofilm growth throughout unmodified carbon felts allows continuous bioelectrochemical chain elongation from CO₂ up to caproate at high current density. *Front. Energy Res.* **6**, 7 (2018).

Raes, S.M.T., Jourdin, Carlucci, L., van den Bruinhorst, A., Strik, D.P.B.T.B. & Buisman, C.J.N. Water-Based Synthesis of Hydrophobic Ionic Liquids [N₈₈₈][oleate] and [P_{666,14}][oleate] and their Bioprocess Compatibility. *ChemistryOpen* **7**, 878–884 (2018).

van den Bruinhorst, A, **Raes, S.M.T.**, Maesara, S.A., Kroon, M.C., Esteve, A.C.C. & Meuldijk, J. Hydrophobic eutectic mixtures as volatile fatty acid extractants. *Sep. Purif. Technol.* **216**, 147–157 (2019).



*Netherlands Research School for the
Socio-Economic and Natural Sciences of the Environment*

D I P L O M A

For specialised PhD training

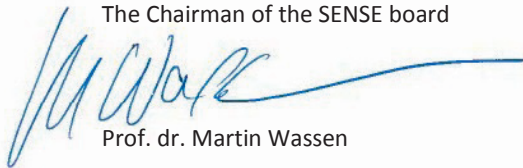
The Netherlands Research School for the
Socio-Economic and Natural Sciences of the Environment
(SENSE) declares that

***Sanne Magdalena Teresa
Raes***

born on 14 April 1989 in Bladel en Netersel, The Netherlands
has successfully fulfilled all requirements of the
Educational Programme of SENSE.

Wageningen, 29 May 2019

The Chairman of the SENSE board


Prof. dr. Martin Wassen

the SENSE Director of Education


Dr. Ad van Dommelen

The SENSE Research School has been accredited by the Royal Netherlands Academy of Arts and Sciences (KNAW)



K O N I N K L I J K E N E D E R L A N D S E
A K A D E M I E V A N W E T E N S C H A P P E N



The SENSE Research School declares that **Sanne Magdalena Teresa Raes** has successfully fulfilled all requirements of the Educational PhD Programme of SENSE with a work load of 32.8 EC, including the following activities:

SENSE PhD Courses

- o Environmental research in context (2014)
- o Research in context activity: 'Co-organizing Alumni Day for the Department of Environmental Technology, 1 May 2015, Wageningen'.

Other PhD and Advanced MSc Courses

- o Competence assessment, Wageningen Graduate School (2014)
- o Efficient Writing Strategies, Wageningen Graduate School (2014)
- o Project and Time Management, Wageningen Graduate School (2014)
- o European Summer School Electrochemical Engineering, Wetsus (2015)
- o Teaching and Supervision thesis students, Wageningen Graduate School (2016)

Management and Didactic Skills Training

- o PhD representative in research meetings of the Environmental Technology chair group (2015-2017)
- o Supervising six MSc students with thesis (2014-2017)
- o Supervising a BSc student with thesis entitled 'To identify and quantify the cause of previously observed large current densities in microbial electrosynthesis cells while no biomass or chemical production was detected' (2015)

Oral and Poster Presentations

- o *Continuous long-term bioelectrochemical chain elongation*. EU-ISMET conference, 28-30 September 2016, Rome, Italy
- o *Microbial Electrosynthesis for the production of carboxylates*. 7th European Summer School Electrochemical Engineering, 22-26 June 2016, Leeuwarden, The Netherlands

SENSE Coordinator PhD Education

Dr. Peter Vermeulen

The research described in this thesis was financially supported by the Netherlands Organisation for Scientific Research (NWO) and the company Paques B.V. (STW-Paques Partnership, project 12999). Their contributions are gratefully acknowledged.

Financial support from the Wageningen University for printing this thesis gratefully acknowledged.

Cover designed with the help of Joeri Willet

Printed by proefschriftmaken, www.proefschriftmaken.nl

This thesis is printed on FSC certified paper

